

Supplementary Information for:
**Palette of Lipophilic Bioconjugatable Bacteriochlorins
for Construction of Biohybrid Light-Harvesting Architectures**

Kanumuri Ramesh Reddy, Jianbing Jiang, Michael Krayner, Michelle A. Harris,
Joseph W. Springer, Eunkyung Yang, Jieying Jiao, Dariusz M. Niedzwiedzki,
Dinesh Pandithavidana, Pamela S. Parkes-Loach, Christine Kirmaier,
Paul A. Loach, David F. Bocian, Dewey Holten, and Jonathan S. Lindsey

Table of Contents

Section	Topic	Page
1.	FTIR spectra of bacteriochlorin–peptide conjugates (for BC1 , BC2)	S1
2.	Spectroscopic data for oligomeric biohybrid complexes of BC2	S2
3.	Preparation and isolation of BC6-P1 (Preps I, II, and III)	S3-S18
4.	Spectroscopic data for BC6-P1 and oligomeric complexes (Prep III)	S18-S20
5.	Spectral data for new compounds	S20-S60

1. FTIR spectra of bacteriochlorin–peptide conjugates.

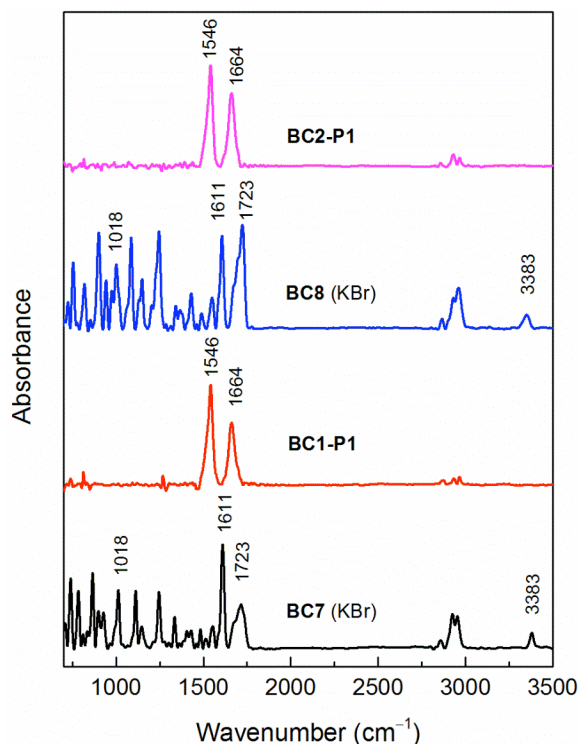


Figure S1. Single-reflection FTIR spectra of bacteriochlorin–peptide conjugates in films on Au substrates (15 h deposition time) and benchmark bacteriochlorins in KBr pellets. The feature at 1723 cm^{-1} is likely a peripheral-group C=O vibration. Other bands are identified in the body of the paper.

2. Spectroscopic data for oligomeric biohybrid complexes of BC2.

Studies analogous to those described for $[(\text{BC6-P1-BChl})_2]_n$ were performed on the oligomeric biohybrid $[(\text{BC2-P1-BChl})_2]_n$, which contains bacteriochlorin **BC2** in place of **BC6**. As noted, the present studies on $[(\text{BC2-P1-BChl})_2]_n$, which were carried out at 9 °C to stabilize the oligomeric complexes, and to complement the prior work on the same constructs carried out at room temperature.¹⁸ The biohybrid complex containing **BC2** exhibits $\geq 90\%$ energy transfer as deduced from steady-state fluorescence data similar to those shown in Fig. 6 and transient absorption data similar to those shown in Fig. 7 and Fig. 8 for the biohybrid complex containing **BC6**. For example, Fig. S2 shows that the energy transfer results in diminished amplitude of the **BC2** emission in the biohybrid complex $[(\text{BC2-P1-BChl})_2]_n$; the amplitude is $\sim 10\%$ of that in the control peptide conjugate **BC2-P1**, which lacks the BChl *a* acceptor array (B850).

Fig. S3 shows that excitation of **BC2** followed by energy transfer to B850 in $[(\text{BC2-P1-BChl})_2]_n$ results in a 1–2 ps rise component in the B850 bleaching and B850* stimulated-emission features. This finding is analogous to the rise phase found after excitation of **BC6** in $[(\text{BC6-P1-BChl})_2]_n$ (Fig. 8). Thus, the transient absorption data for biohybrid complexes containing either bacteriochlorin **BC6** or **BC2** reveal a fast kinetic phase not present in the oligomer control $[(\text{P1-BChl})_2]_n$ that can be attributed to energy transfer from the excited bacteriochlorin to B850. Such findings are in harmony with the results of the steady-state fluorescence quenching and fluorescence excitation versus absorbance spectral analyses for both biohybrid complexes. The collective results show that the appended synthetic bacteriochlorin in the complexes enhances solar coverage and exhibits efficient ($\geq 90\%$) energy transfer to the native-like BChl *a* sites in the biohybrid architectures.

Figure S2. Emission intensity normalized to the absorption value at the excitation wavelength (516 nm) for control peptide **BC2-P1** (magenta) and oligomeric biohybrid complex $[(\text{BC2-P1-BChl})_2]_n$ (black). The inset (an expanded view for the biohybrid assembly) shows residual **BC2** fluorescence (734 nm), fluorescence from the BChl *a* array B850 (850 nm) and possible trace emission from free BChl *a* (780–800 nm).

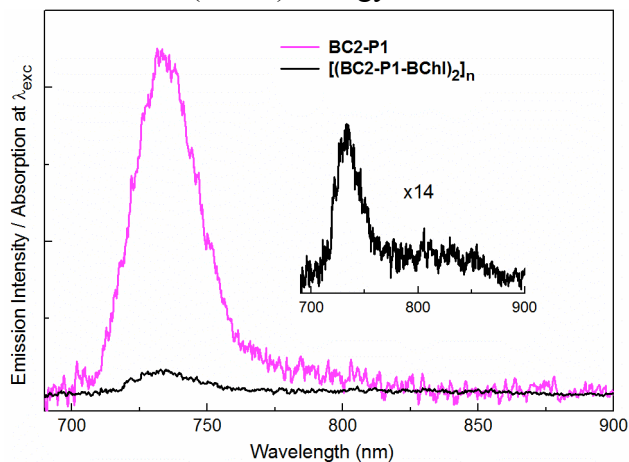
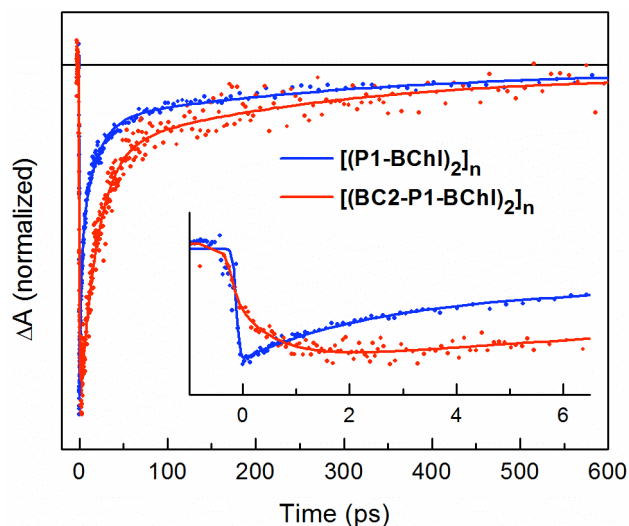


Figure S3. Time-evolution of the bleaching/stimulated-emission for oligomeric biohybrid $[(\text{BC2-P1-BChl})_2]_n$ ($\lambda_{\text{exc}} = 516$ nm, $\lambda_{\text{det}} = 835$ nm) (red) and oligomeric control $[(\text{P1-BChl})_2]_n$ ($\lambda_{\text{exc}} = 590$ nm, $\lambda_{\text{det}} = 855$ nm) (blue) at 9 °C normalized to the same maximum amplitude. The inset shows the 1–2 ps growth of bleaching for the biohybrid complex and the instrument-limited rise for the control. The line through each data set is a fit to a function consisting of three exponentials plus a long-time constant convolved with the instrument response.



3. Preparation and isolation of BC6-P1.

Approximately 15 reactions were carried out for the bioconjugation of peptide **P1** (which contains cysteine at the -14 position) and bacteriochlorin **BC6** (which contains an iodoacetamide group). The conjugations were performed to explore methods for purification, handling, and formation of biohybrid complexes. Here, we present the results for the conjugation reactions, with particular focus on three preps.

- In Prep I, the conjugate was prepared, isolated, and assembled into complexes. The spectral, photophysical and energy-transfer properties are described later in the SI section.
- In Prep II, the conjugate was prepared, isolated, and characterized by HPLC, ESI-MS, MALDI-MS, and stability studies. Somewhat improved methods of purification were developed as part of this prep.
- In Prep III, the new methods of purification were employed to isolate the conjugate, which also was studied with regard to the spectral, photophysical and energy-transfer properties. Such properties were largely identical to the results from Prep I, and are described in the body of the paper.

Prep I. The following describes the initial preparation of bacteriochlorin–peptide conjugate **BC6-P1** and reconstitution to ultimately form oligomeric complexes $[(\mathbf{BC6-P1})_2]_n$.

A. Preparation of BC6-P1. Under dim light, a sample of **P1** (4.5 mg) was dissolved in DMF (0.42 mL), and then 0.08 mL of Tris buffer (0.1 M, pH 7.3) was added with stirring. Oxygen was removed by passing argon over the top of the stirred sample for 10 min. In the same manner, **BC6** (3.0 mg) was dissolved in DMF (0.42 mL) whereupon 0.08 mL of Tris buffer (0.1 M, pH 7.3) was added. The resulting **BC6** solution was added dropwise to the **P1** solution over approximately 2 min with argon flow and stirring. The mixture was further degassed with argon for 10 min, then stoppered and stirred in the dark for 2 h. The reaction mixture was then divided equally into 3 centrifuge tubes and lyophilized overnight.

One-third of the reaction product (i.e., one of the three centrifuge tubes) was extracted with methanol (1 mL) to remove unreacted **BC6**. The sample was suspended using a disposable pipette. The sample was then centrifuged in a tabletop centrifuge for 5 min, and the clear supernatant containing unreacted **BC6** was carefully removed. The procedure was repeated and the resulting pellet was dried on the lyophilizer for 1 h. The residue was dissolved in 30 μ L of hexafluoroacetone trihydrate with sonication for several minutes (color changed to red-brown) and then 30 μ L of 1:1 HPLC A/B solvent added (color changed to green-brown). After sonication for 1 min, the sample was injected onto the HPLC. The HPLC method employed Perkin-Elmer HCOXS C18 columns (150 mm x 4.6 mm) and a solvent system composed of (A) 0.1% trifluoroacetic acid (TFA) in water as the aqueous solvent and (B) 0.1 % TFA in 2:1 (v/v) acetonitrile/2-propanol as the organic solvent using the G3 gradient.³⁰

Several major peaks were obtained upon HPLC analysis (Fig. S4). From the absorption spectra (Figs. S5-S7) and control HPLC experiments, the peaks were identified as free **BC6** (39 min peak), unreacted protein (42 min peak) and the desired **BC6-P1** conjugate containing both bacteriochlorin and protein in the expected ratio for a 1:1 complex (57.5 min and 59 min peaks, respectively). The location of the **BC6-P1** conjugate upon HPLC elution was very similar to that of the analogous **BC2** conjugate in an earlier preparation.¹⁸ A fraction corresponding to each of the 57.5 min and 59 min peaks was collected, and each fraction was dried overnight on the lyophilizer and stored at -20 °C. The two peaks obtained for **BC6-P1** had identical absorption

spectra, reacted the same to form B820- and B850-type biohybrid complexes and are assumed equivalent for the studies reported herein. The overall yield of **BC6-P1** upon HPLC isolation (relative to the starting materials) was estimated to be ~2% on the basis of absorption spectroscopy.

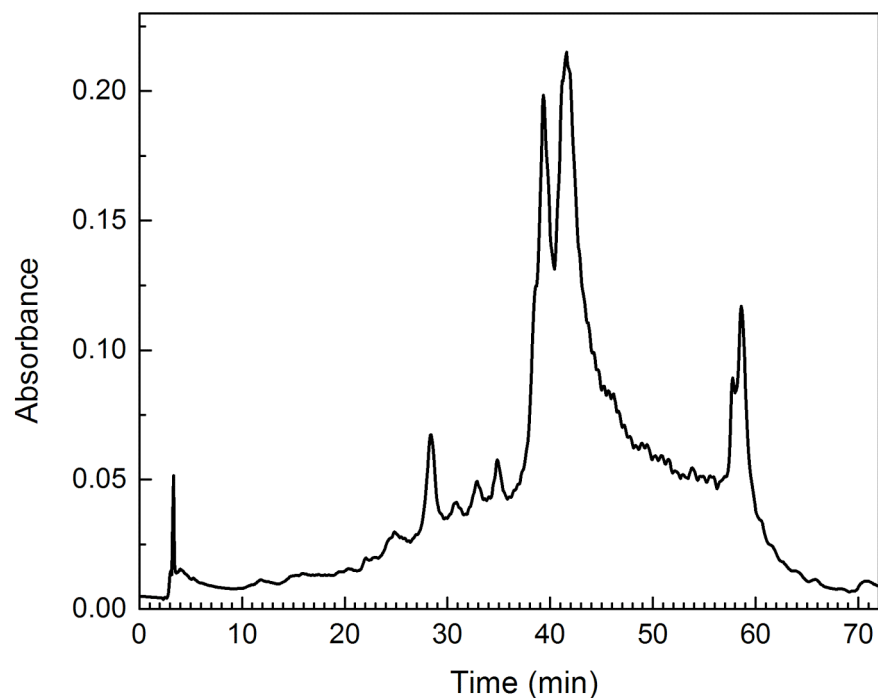


Figure S4. HPLC chromatogram of **BC6-P1**.

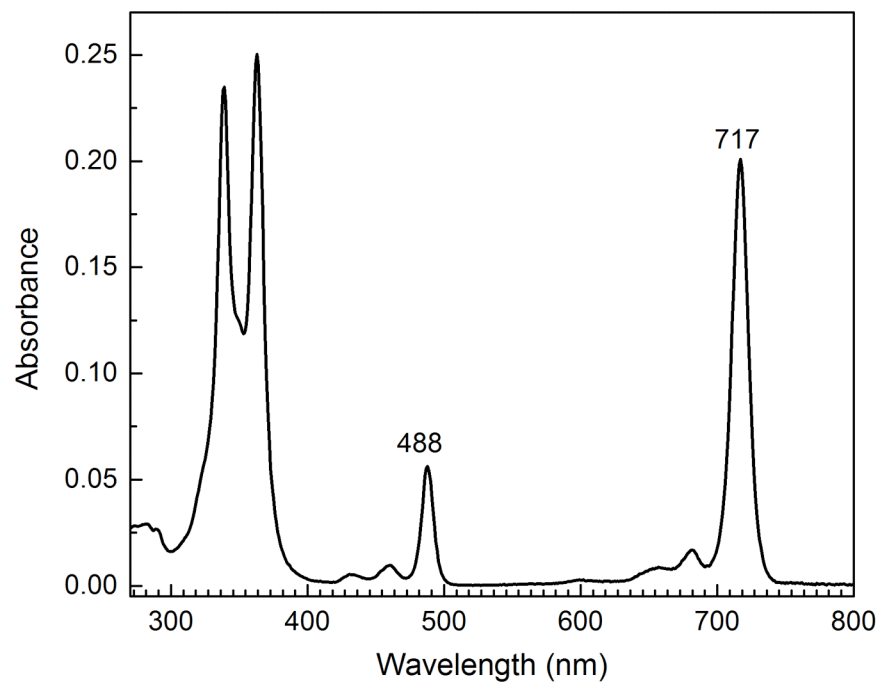


Figure S5. Absorption spectrum of the 39 min peak from the HPLC of Fig. S4. The small peak at 289 nm is characteristic of protein due to contamination from the overlapping protein peak at 42 min.

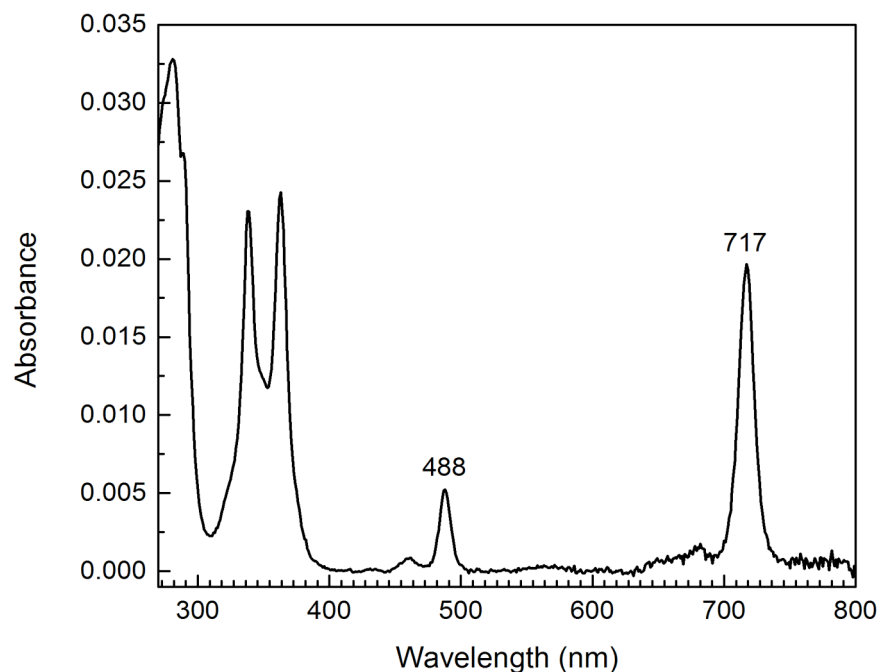


Figure S6. Absorption spectrum of the 42 min peak from the HPLC of Fig. S5. Note the large peak at 289 nm characteristic of protein. The absorbance due to **BC6** stems from the overlap with the pigment peak at 39 min.

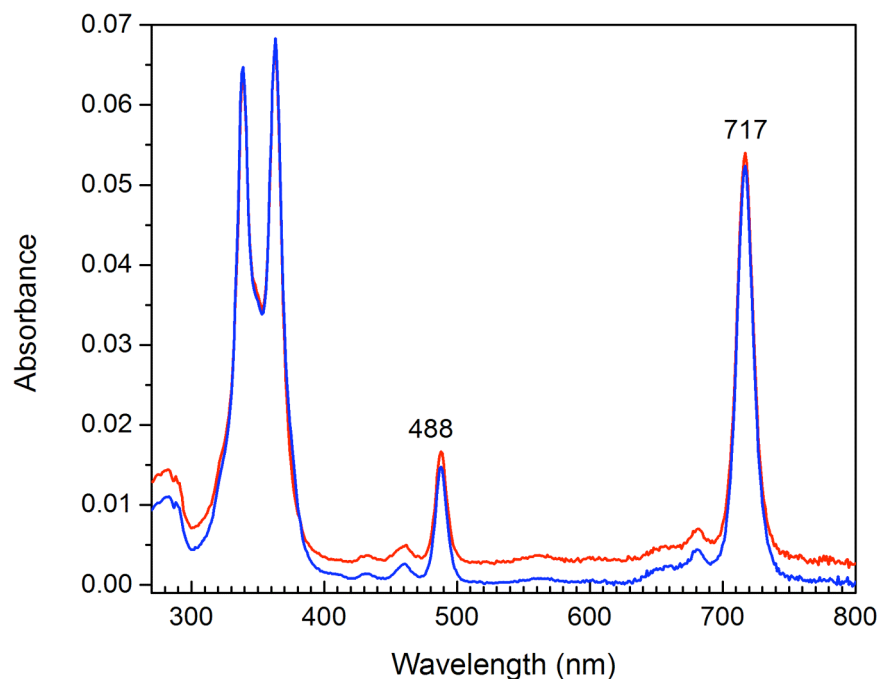
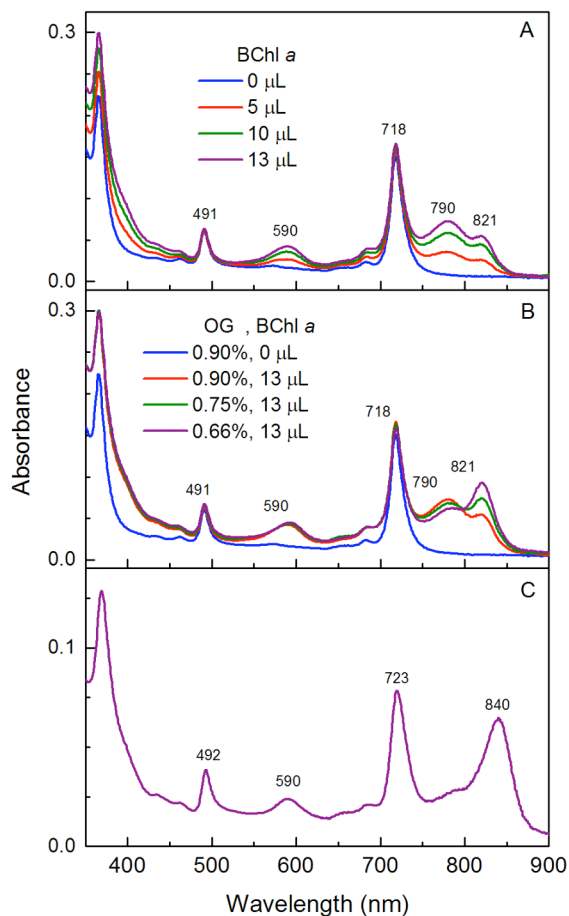


Figure S7. Absorption spectra of the 57 min (red) and 59 min (blue) peaks from the HPLC of Fig. S4. The peak at 289 nm (characteristic of protein) is appropriate for a 1:1 ratio of protein to bacteriochlorin.

B. Reconstitution from BC6-P1. A solution of **BC6-P1** was prepared in potassium phosphate buffer (100 mM, pH 7.5) containing 0.90% *n*-octyl β -D-glucopyranoside (OG). The spectrum of this solution is shown in Fig. S8A (blue). BChl *a* with a geranyl-geraniol esterifying alcohol was isolated from membranes of the G9 carotenoidless mutant of *Rds. rubrum*.³⁰ Increasing amounts of BChl *a* were then added (Fig. S8A: red, green, purple). The resultant sample was then diluted to 0.75% OG and again to 0.66% OG to optimize $\beta\beta$ -subunit formation (Fig. S8B: red, green, purple). The sample was then chilled overnight at 4–8 °C to form the β -oligomeric complex (Fig. S8C). The 820-nm absorption of the $\beta\beta$ -subunit complex was shifted to ~840 nm upon formation of the β -oligomeric complex.

Figure S8. Absorption spectra illustrating the formation of biohybrid complexes. (A) Titration of the **BC6-P1** with BChl *a* at 0.90% OG. Curves are for addition of 0 (blue), 5 (red), 5 (green) and 3 μ L (purple) of a concentrated solution of BChl *a* in acetone (13 μ L total), with the total moles of BChl *a* approaching that of the peptide. (B) Formation of B820 $\beta\beta$ -subunit complex with the **BC6-P1** and BChl *a*. Curves are for 0.90% OG before adding BChl *a* (blue), 0.90% OG after adding 13 μ L of BChl *a* solution (red), 0.75% OG (green) and 0.66% OG (purple). (C) Formation of the oligomeric species upon overnight cooling of the B820 form of **BC6-P1**.



Prep II. The objectives of this preparation were to improve the yield and purification, and to collect chemical characterization data for **BC6-P1**.

A. HPLC conditions. For this prep, two HPLC instruments were employed. Analytical HPLC was performed on a Hewlett-Packard 1100 series instrument using a C4 column (Vydac, 10 μ m, 300 \AA , 150 mm x 4.6 mm) in series with a guard column. Preparative HPLC was performed on a Shimadzu instrument with an APD-10AU Shimadzu UV-Vis detector and a SCL-10A Shimadzu system controller equipped with a C4 column (Vydac, 10 μ m, 300 \AA , 250 mm x 10 mm) in series with a guard column. The flow rate was 0.8 mL/min for the analytical column versus 2.5 mL/min for the preparative column.

For both the analytical and preparative methods, the HPLC solvent system consisted of (A) 0.1% TFA in water as the aqueous solvent and (B) 0.1 % TFA in 1:2 (v/v) acetonitrile/2-propanol as the organic solvent. The original composition of A/B is 50/50 (v/v), and the use of a gradient afforded the final composition of A/B (30/70) at 48 min. In other words, the HPLC solvent was initially H₂O (50%), CH₃CN (16.7%), isopropanol (33.3%), and trifluoroacetic acid (0.1%), which has pH 2.01. The use of a gradient afforded a final composition of H₂O (30%), CH₃CN (23.3%), isopropanol (46.6%), and trifluoroacetic acid (0.1%) at 48 min.

The conjugate was injected (10–40 μ L for the analytical and 60–80 μ L for the preparative column) at a concentration of 0.5–1.0 mM in a solution of hexafluoroacetone trihydrate (25%),

water (37.5%), CH₃CN (12.5%), and isopropanol (25%). The conjugate was first dissolved in neat hexafluoroacetone trihydrate and then the other solvents were added to give the injection sample; the conjugate was soluble in this solvent mixture.

The chromatography conditions (column, solvent system) employed for Prep II were slightly different from those in Prep I. The rationale for the change in conditions stems from the extreme hydrophobicity of the conjugate **BC6-P1**. Three factors were changed:

- (1) Column type. A C4 column was used in place of the C18 column in Prep I so as to lessen possible irreversible adsorption of the hydrophobic starting materials and conjugate with the column matrix.
- (2) Organic eluant. Isopropanol and *n*-butanol have been employed as hydrophobic organic eluants.^{59,60} We adopted a solvent mixture of acetonitrile and isopropanol (1:2, v/v) as organic eluant versus acetonitrile/isopropanol (2:1) in Prep I.
- (3) Retention time. The change in column type and eluant afforded a shortened retention time of the conjugate **BC6-P1** (27 min *versus* 59 min in Prep I).

B. Coupling reaction. DMF and Tris buffer were sonicated for 5 min, followed by bubbling with argon for 30 min to thoroughly remove oxygen. **P1** (1.03 mg, 0.28 μmol) was dissolved in 56 μL of DMF, and 14 μL of Tris buffer (pH 8.6) was then added while the mixture was stirred with an argon flow over the sample. The protein appeared to readily dissolve in DMF and stay in solution when Tris buffer was added. **BC6** (0.2 mg, 0.28 μmol) dissolved in 56 μL of DMF and 14 μL of Tris buffer. The **BC6** solution was then added dropwise to the **P1** solution with argon flow and stirring. A greenish precipitate was observed as the reaction proceeded. The reaction mixture was stirred in the dark at room temperature for 3 h. These conditions were employed followed by the purification and characterization described in section C (*vide infra*).

The above reaction conditions are the consequence of a short study to increase the coupling yield. Selected reactions are shown in Table S1. The following factors were varied:

- (1) Ratio of **P1** to **BC6**. Increasing the amount of **BC6** relative to **P1** did not improve the yield. The best yield was obtained with a ratio of 1:1 of the starting materials.
- (2) Buffer solution. The increase in basicity of the Tris buffer is believed to increase the nucleophilicity of the thiol group, which is beneficial for a better conversion yield.²²
- (3) Concentration of peptide. The concentration of **P1** was increased from 1.1 mM in Prep I to 2.0 mM here, which accelerated the coupling rate.

Table S1. Coupling conditions.

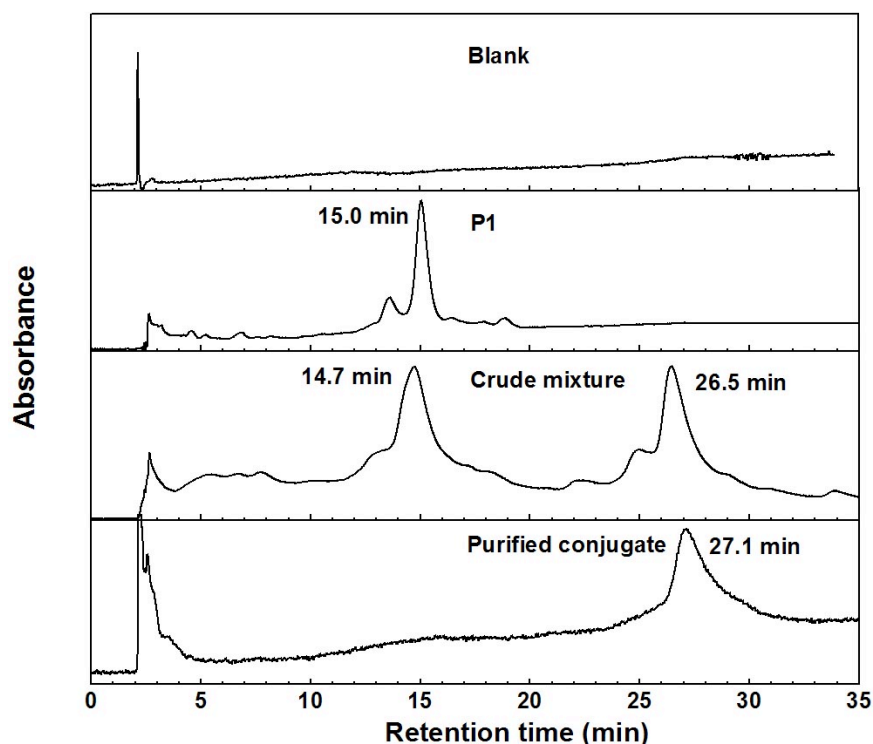
Entry	P1 : BC6 ratio	time (h)	Solvent and buffer	Conc. of [P1]
Batch 1	1:1	3	DMF with 20% Tris buffer (pH 8.6)	2 mM
Batch 2	1:2	3		
Batch 3	1:1	6		
Batch 4	1:1	3	DMSO with 20% Tris buffer (pH 8.6)	
Batch 5	1:1	3	Neat DMF	
Prep I	1:3.6	2	DMF with 16% Tris buffer (pH 7.3)	1.1 mM

The conversion yield was estimated on the basis of the ratio of the peak of the peptide **P1** and the conjugate **BC6-P1**, ignoring any losses of materials on the column. Batches 1–4 gave estimated yields of ~50%. Batch 5 gave no conjugate. The conditions employed in Prep I are provided for comparison (a yield is not known). The conditions of batch 4 were used thereafter.

C. Purification of BC6-P1. The reaction mixture obtained from the protocol described in section B (*vide supra*) was treated with DMF (200 μ L; rather than methanol as in Prep I) and sonicated for 3 min, followed by centrifugation at 4000 rpm for 10 min. The supernatant was carefully decanted and the procedure was repeated twice in an effort to completely remove excess (unreacted) **BC6**. The resulting greenish residue was dried under vacuum for 30 min. Addition of hexafluoroacetone trihydrate (40 μ L) to the greenish solid followed by sonication for 3 min completely dissolved the solid. The color changed from green to pink. Addition of 80 μ L of a solvent mixture [composed of H₂O (50%), isopropanol (33.3%), acetonitrile (17.6%) and TFA (0.1%)] caused a change from pink back to green. This mixture was centrifuged to remove (visibly evident) insoluble particles. The resulting supernatant was analyzed by HPLC. Injection of 10 μ L into the HPLC instrument gave the chromatogram shown in Fig. S9.

The peak eluting at 26.5 min was collected (\pm 1.0 min). The collected fraction (~1.5 mL from the analytical HPLC column) was neutralized by titrating with saturated aqueous NaHCO₃ solution. In so doing, the pH increased from 2.01 to 7.47 (monitored by a pH meter). The resulting neutralized solution containing the conjugate **BC6-P1** was dried under vacuum. Re-injection of the neutralized solution in the same solvent (hexafluoroacetone trihydrate 25%, H₂O 37.5%, isopropanol 25%, acetonitrile 12.5% and TFA less than 0.1%) afforded a major peak, that while not a single peak, was devoid of unreacted bacteriochlorin and unreacted peptide (Fig. S10). Note the impurity in the initial peptide (Fig. S9), and how such leading and tailing peaks appear to afford corresponding peaks in the crude mixture and in the purified conjugate (Fig. S10). Note also that the initial peptide was stated to be >90% pure according to the commercial supplier whereas our HPLC analysis (*vide infra*) indicated a purity of 78%.

Figure S9. Analytical HPLC traces of blank, **P1**, crude mixture and purified **BC6-P1** conjugate (all detected by absorption at 280 nm). The bacteriochlorin **BC6** eluted at 5.9 min (not shown).



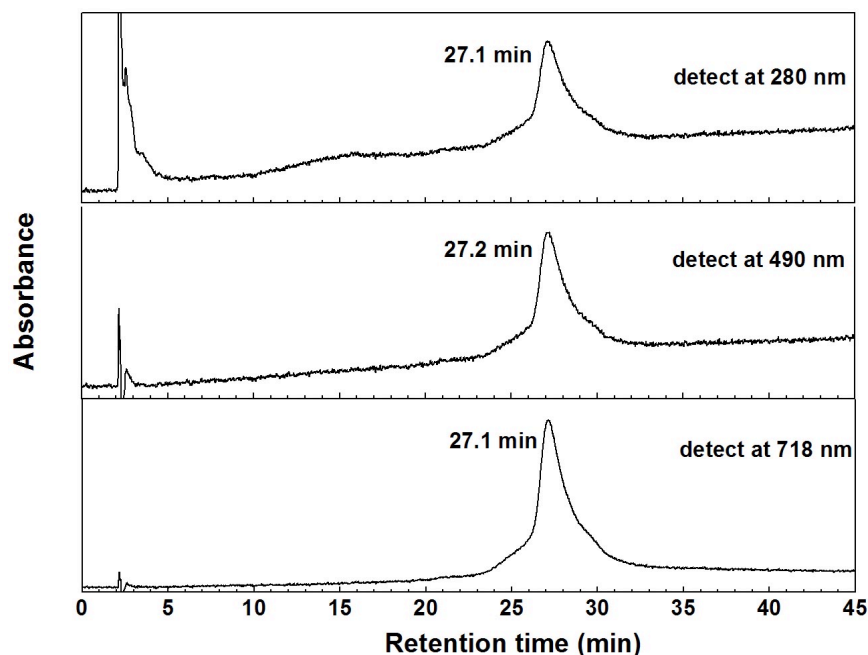


Figure S10. A single re-injection of the analytical HPLC-purified sample of the conjugate **BC6-P1** (absorption detection at 280, 490 and 718 nm).

D. Yield determination of BC6-P1. The total (isolated) yield was determined to be 17% on the basis of absorption spectroscopy of the bacteriochlorin in the starting sample versus the product. The total yield reflects the product of three steps: (1) coupling to form the bacteriochlorin-peptide conjugate, (2) recovery of product upon HPLC (i.e., recovery is 100% if no material is irreversibly bound to or decomposed on the column), and (3) breadth or narrowness in the cutting of the product peak to give a fraction thereof. We estimated the yields as follows.

By integration ($\lambda_{\text{det}} = 718 \text{ nm}$) the percentage of the product peak that was cut in the collected fraction was 70%.

A control experiment was carried out to assess the amount of conjugate **BC6-P1** lost on the column (due to irreversible adsorption or decomposition). After injection (20 μL) of the conjugate solution, fractions from HPLC with the column *versus* without the column* were collected and diluted to the same volume (5 mL). The absorption spectra were then recorded (Fig. S11). Comparison of the Q_y band intensity showed that ~80% of **BC6-P1** was recovered during analytical HPLC purification. Hence, some 20% of the conjugate was lost on the column.

Given the total yield of 17%, and knowledge of the column recovery (80%) and the fraction cutting (70%), the coupling yield is inferred to be 30%. While such values are estimates, the coupling reaction appears to be the most inefficient step.

* “without the column” refers to connection of the injection port to the detector inlet, thereby enabling a control for all HPLC sample handling but eliminating any effect of the chromatography column.

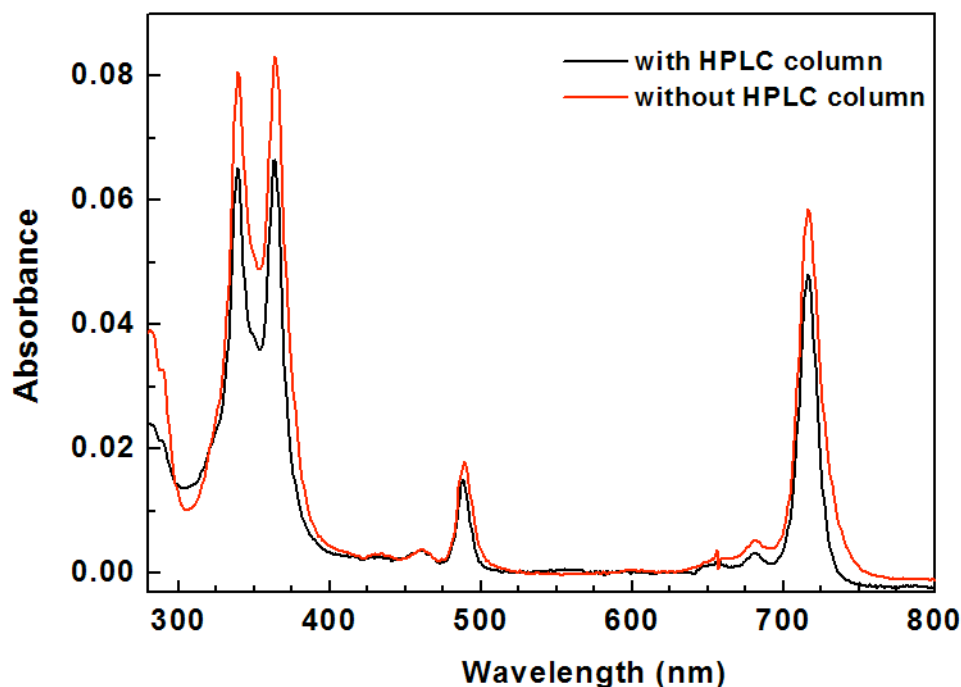


Figure S11. The absorption spectra of fractions from reverse-phase HPLC with the C4 column (black) *versus* without the C4 column (red) in a solvent mixture (isopropanol 40%, H₂O 39.9%, acetonitrile 20% and TFA 0.1%).

E. Characterization of BC6-P1. The fraction from the analytical HPLC was concentrated under vacuum to dryness and subjected to electrospray ionization mass spectrometry. The mass spectrum is shown in Fig. S12. The data are as follows: ESI-MS obsd 2108.6 [M + 2H]²⁺, 1406.1 [M + 3H]³⁺, 1054.8 [M + 4H]⁴⁺, 844.1 [M + 5H]⁵⁺, calcd 4214.2394 [(M + H)⁺, M = C₂₁₄H₂₉₇N₄₇O₄₁S]. Such data can be compared with those for the peptide **P1**, which gave 1818.4540 [M + 2H]²⁺, 1212.6353 [M + 3H]³⁺, and 909.7292 [M + 4H]⁴⁺; calcd 3633.8868 [(M + H)⁺, M = C₁₇₉H₂₅₃N₄₁O₃₉S].

An identical preparation as described via the protocol in section B was performed and the crude product was purified as described in the first paragraph of this section but with use of preparative HPLC rather than analytical HPLC. A fraction was cut corresponding to the fraction of the analytical HPLC that contains the conjugate. The fraction was concentrated under vacuum to dryness and analyzed by MALDI-MS with the matrix α -cyano 4-hydroxycinnamic acid. The data for **BC6-P1** are as follows: obsd 4221.3 (M + H)⁺, 4243.3 (M + Na)⁺. Such data can be compared with those of the peptide **P1**: obsd 3637.8 (M + H)⁺, 3659.5 (M + Na)⁺; calcd 3633.9 [(M + H)⁺, M = C₁₇₉H₂₅₃N₄₁O₃₉S]. In both cases a small, systematic mass displacement error occurred owing to the choice of calibrants. Collection of a sample for MALDI-MS was the only utilization of the preparative HPLC instrument described herein.

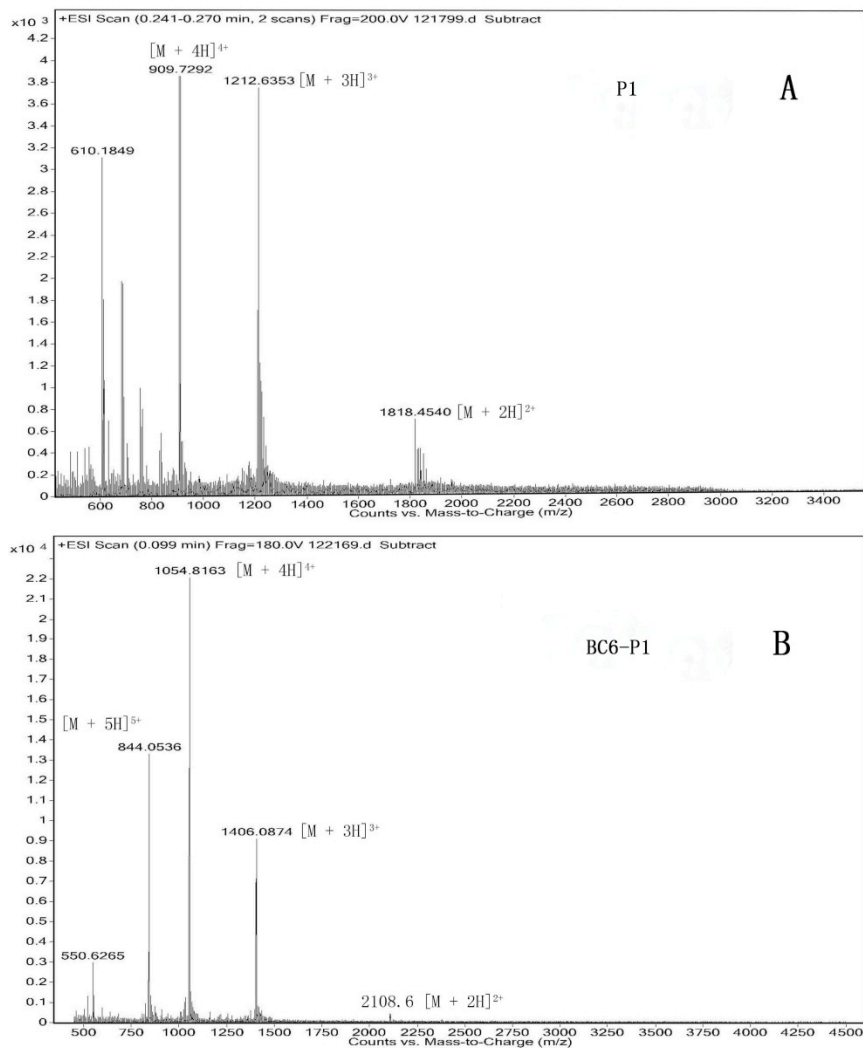


Figure S12. ESI-MS results of **P1** (A) and **BC6-P1** (B).

The absorption spectrum of **BC6-P1** (from the analytical HPLC) is shown in Fig. S13. The peak positions of the purified conjugate are as follows: 282, 339, 364, 489, and 716 nm.

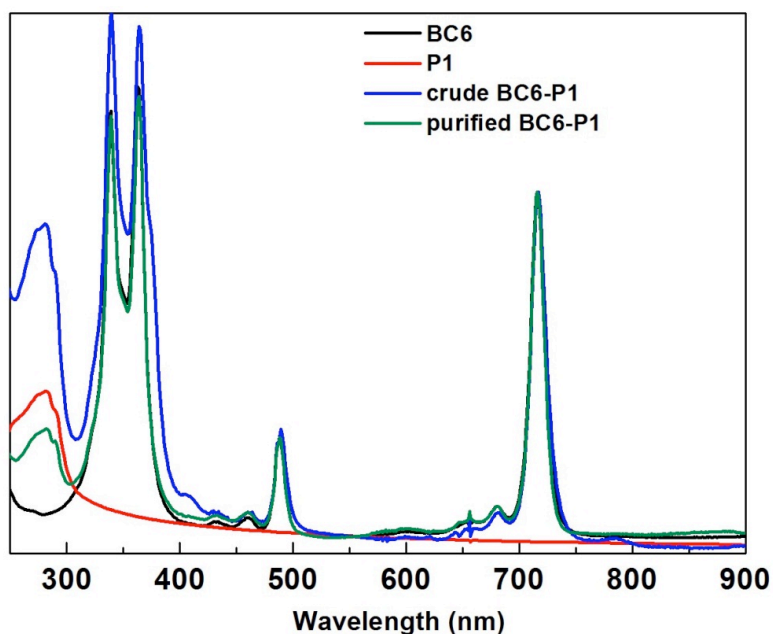


Figure S13. Absorption spectra of **BC6**, **P1**, and the crude mixture of **BC6-P1** in a solvent mixture (isopropanol 40%, H₂O 39.9%, acetonitrile 20% and TFA 0.1%). The absorption spectrum of purified **BC6-P1** is in a slightly different solvent mixture (hexafluoroacetone trihydrate 25%, H₂O 37.5%, isopropanol 25%, acetonitrile 12.5% and TFA less than 0.1%).

F. Stability studies. (i) Stability of P1. The stability of the peptide **P1** alone was studied in the initial HPLC eluant (hexafluoroacetone trihydrate 25%, H₂O 37.5%, isopropanol 25%, acetonitrile 12.5% and TFA less than 0.1%) at both room temperature (rt) and -10 °C by the integration of peaks from analytical HPLC detected by absorption at 280 nm. It turned out that the **P1** was relatively stable at -10 °C (12% decomposed within 5 days), but not stable in solution at room temperature (70% decomposed within 5 days) (Table S2).

Table S2. Stability of the peptide **P1** at room temperature and at -10 °C in the HPLC eluant (hexafluoroacetone trihydrate 25%, H₂O 37.5%, isopropanol 25%, acetonitrile 12.5%, and TFA less than 0.1%) determined by peak integrations detected by absorption at 280 nm.

day	At rt (0.37 mM) (%)	At -10 °C (0.5 mM) (%)
1	100	100
2	66	94
5	30	88

(ii) Stability of the crude mixture of the conjugate BC6-P1. The stability of the crude mixture (after washing by DMF) was studied in the HPLC injection solvent (hexafluoroacetone trihydrate 25%, H₂O 37.5%, isopropanol 25%, acetonitrile 12.5%, and TFA less than 0.1%) at room temperature over a period of 200 min. The sample was analyzed by integration of peaks from analytical HPLC detected by absorption at 718 nm. It turned out that 30% of the product decomposed within 2 h (Fig. S14).

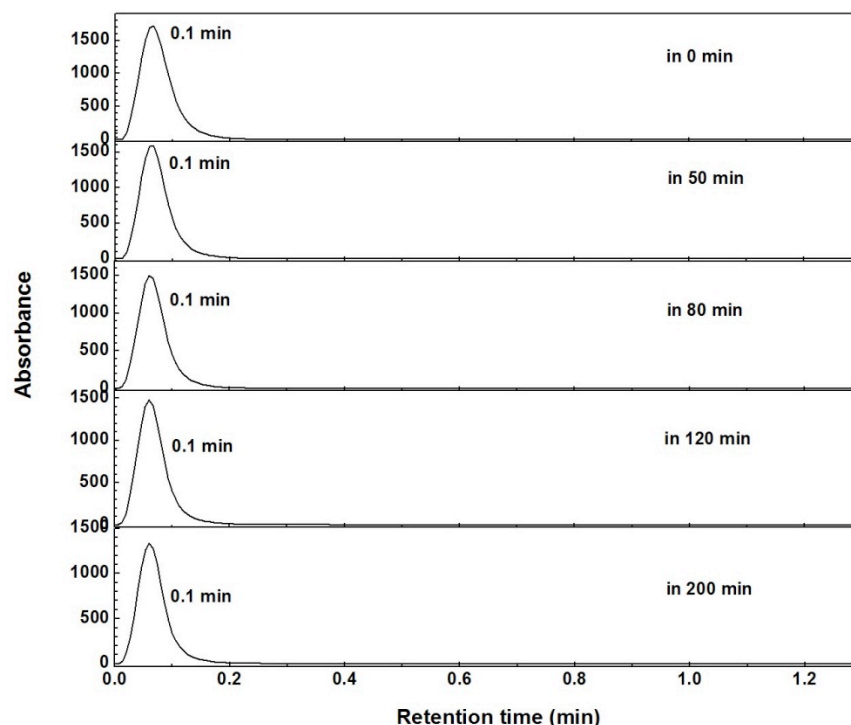


Figure S14. Analytical HPLC traces of crude mixture over time, detected by absorption at 718 nm. The integrations of the peaks from 0 to 200 min are 6815, 5107, 5074, 4763 and 4275.

(iii) Stability of the purified conjugate BC6-P1. The conjugate after analytical HPLC purification was examined in very dilute form in a cuvette where absorption spectral measurements could be performed over time without sample transfers. The absorption of the conjugate solution was studied in the HPLC eluant (pH 2.01) as a function of time (Fig. S15A). A control experiment was conducted at similar concentration but neutralized to pH 7.47 by a saturated aqueous NaHCO_3 solution (Fig. S15B). It turned out that 30% of the conjugate decomposed within 3 h at room temperature at pH 2.01, compared with 15% decomposition at pH 7.47 within 3 h. The conjugate at pH 2.01 completely decomposed after standing overnight at room temperature, while at pH 7.47, 45% remained within the same time frame (Fig. S15). The cuvette samples were not stirred, hence some degree of settling of the sample cannot be ruled out. Regardless, neutralization of the conjugate solution immediately following HPLC is essential for improved stability of the conjugate. The data in Fig. S15 are shown in the kinetic traces of Fig. S16.

If instead of being left in solution at room temperature for such a long time, the conjugate is immediately concentrated to dryness (~10 min) and then immediately used for the reconstitution study (i.e., addition of hexafluoroacetone trihydrate, aqueous phosphate solution containing the detergent OG at 0.66%, and BChl *a*) and stored at 8 °C, a far more stable sample results. Indeed, such samples could be prepared, chilled overnight to induce formation of oligomeric complexes, and shipped overnight in chilled form (from Northwestern University or North Carolina State University) to Washington University or University of California Riverside for ensuing spectroscopic studies of several days duration, a period during which the reconstituted samples maintained a high degree of integrity.

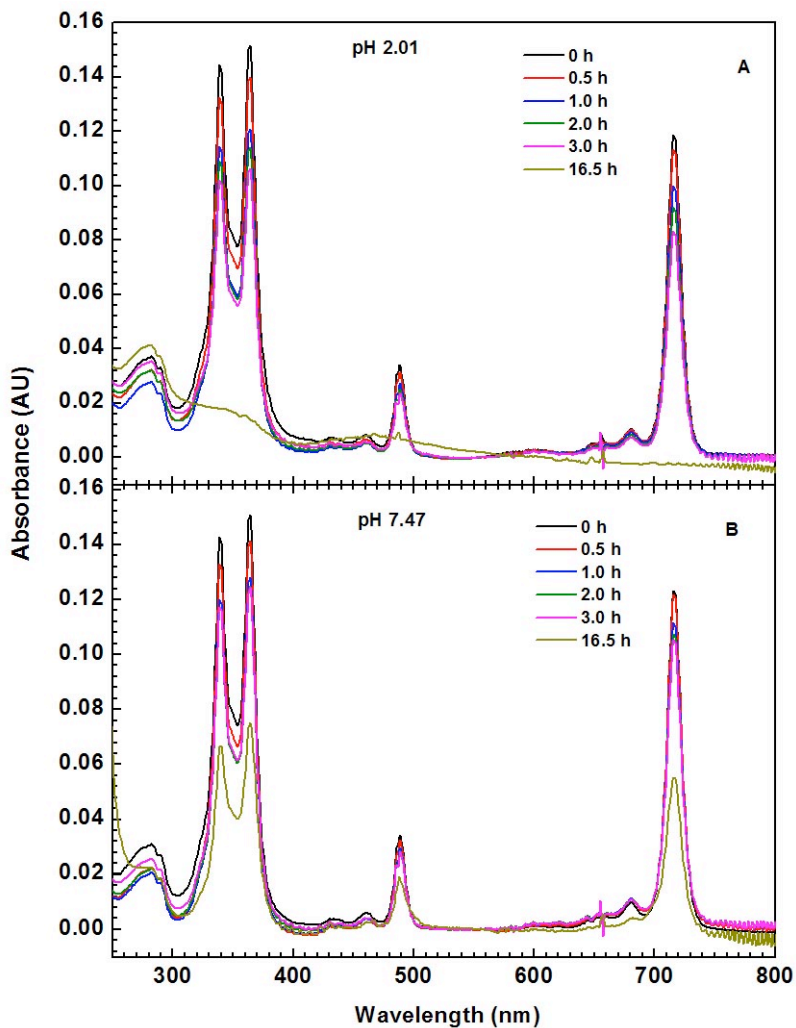


Figure S15. Absorption of conjugate in solution at pH 2.01 (A) and pH 7.47 plus NaHCO₃ (B) in the HPLC eluant (isopropanol 40%, H₂O 39.9%, acetonitrile 20% and TFA 0.1%).

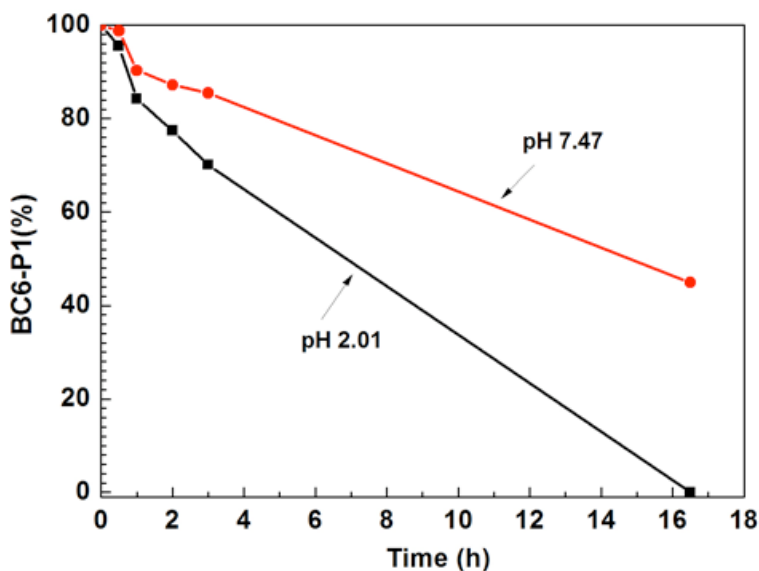


Figure S16. Percentage of conjugate under various conditions *versus* time, determined by the intensity of the Q_y band.

Prep III. The objective of this preparation was to obtain the **BC6-P1** conjugate using the purification conditions described in Prep II, assemble complexes of **BC6-P1** so purified, and examine the spectroscopic properties of such complexes for comparison with those of Prep I.

A. Preparation of BC6-P1. The coupling reaction was done using the same conditions as described in Prep II, but at 1.5-fold larger scale. The purification method in Prep II was also adopted here. A fraction was cut corresponding to the fraction from the analytical HPLC in Prep II that contains the conjugate (Fig. S17). Similar to Prep II, re-injection of the conjugate from the HPLC in Prep III afforded one major peak (Fig. S18). The HPLC-purified conjugate was not characterized by ESI-MS or MALDI-MS but instead was used to prepare biohybrid complexes.

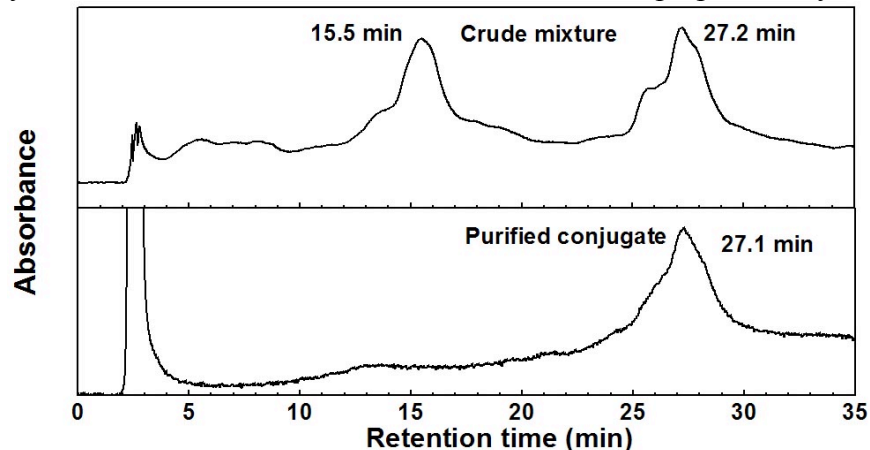


Figure S17. Analytical HPLC traces of the crude mixture and the purified **BC6-P1** conjugate ($\lambda_{\text{det}} = 280$ nm).

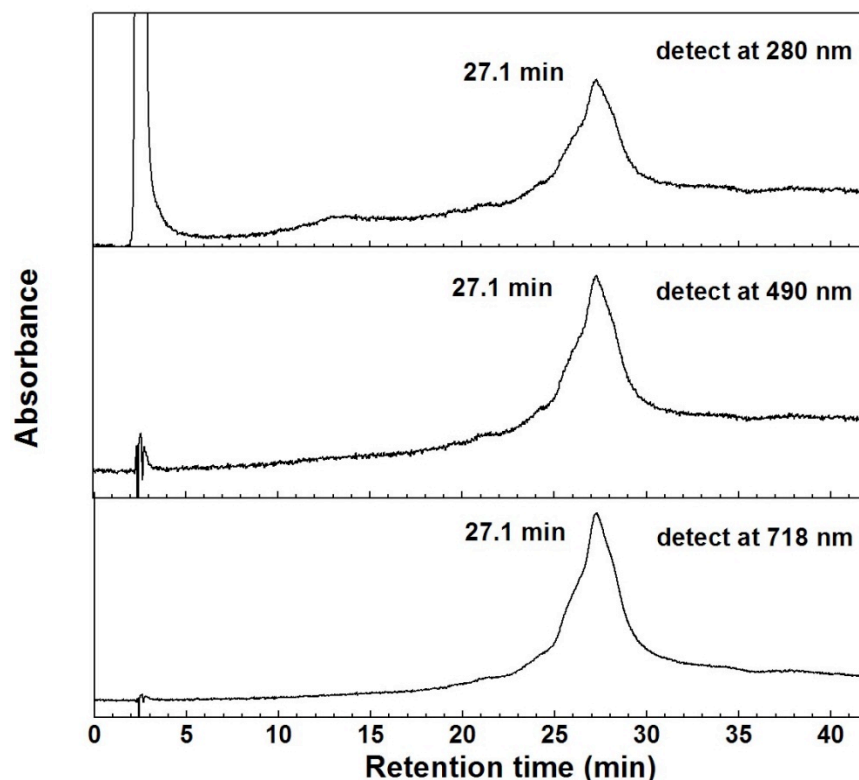


Figure S18. A single re-injection of the analytical HPLC-purified sample of the conjugate **BC6-P1** ($\lambda_{\text{det}} = 280, 490$ and 718 nm).

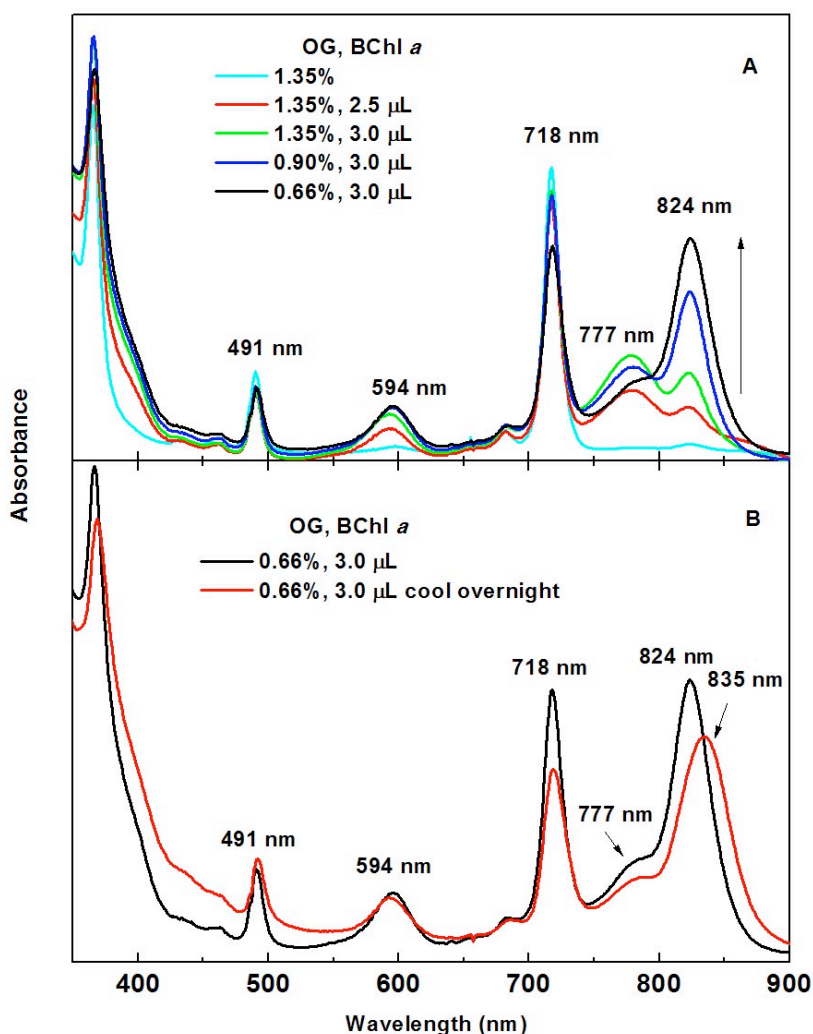
B. Reconstitution. Procedures for formation of dyads and oligomeric complexes were described previously.³¹ The following protocols are essentially identical to that in the body of the paper, and are presented here in detail to provide correspondence with the accompanying spectra in Figs. S19 and S20. The BChl *a* employed in Prep III was isolated from *Rb. sphaeroides* and contains phytol as the esterifying alcohol.

(i) Reconstitution from BC6-P1. Under dim light, a sample of **BC6-P1** (~0.03 mg, from Prep III) was solubilized in 10 μL of hexafluoroacetone trihydrate, diluted with 0.5 mL of 5.4% OG in 100 mM phosphate buffer solution (pH 7.6), and then diluted 3-fold with the same buffer (lacking OG) to bring the OG concentration to 1.35%. This detergent solution containing **BC6-P1** was neutralized by addition of 15 μL of 3 M potassium hydroxide solution. BChl *a* in degassed acetone (~1.5 mM) was then gradually added (2.5 μL first, then 0.5 μL to give 3.0 μL total) to the solution by a microsyringe; the change in absorption upon such additions of BChl *a* is shown in Fig. S19. Formation of dyads and oligomeric species was then induced by (1) addition of 100 mM phosphate buffer solution (pH 7.6, lacking OG) to decrease the OG concentration first to 0.90% and then to 0.66% (1.0 mL, 2.1 mL), followed by (2) chilling the sample at 8 $^{\circ}\text{C}$. The dilution of the OG detergent and the chilling processes change the respective protein and micelle concentrations, which can alter the conditions for complex formation.

Figure S19. Absorption spectra for formation of B820- and oligomeric biohybrid complexes $[(\text{BC6-P1-BChl})_2]_n$.

(A) Titration of the **BC6-P1** at 1.35% OG with no BChl *a* (cyan), 2.5 μL BChl *a* (red), 0.5 μL of BChl *a* (3.0 μL total, green), at 0.90% OG with 3.0 μL total of BChl *a* (blue), and at 0.66% OG with 3.0 μL total of BChl *a* (black).

(B) Complexes at 0.66% OG with 3.0 μL total of BChl *a* before (black) and after (red) overnight chilling at 8 $^{\circ}\text{C}$. The spectra were corrected for dilution, so that each sample would have the same concentration as for the sample with 1.35% OG. The initial sample (1.35% OG) prior to addition of BChl *a* (in panel A) gave an absorbance at 718 nm of 0.46 in a 1-cm cuvette.



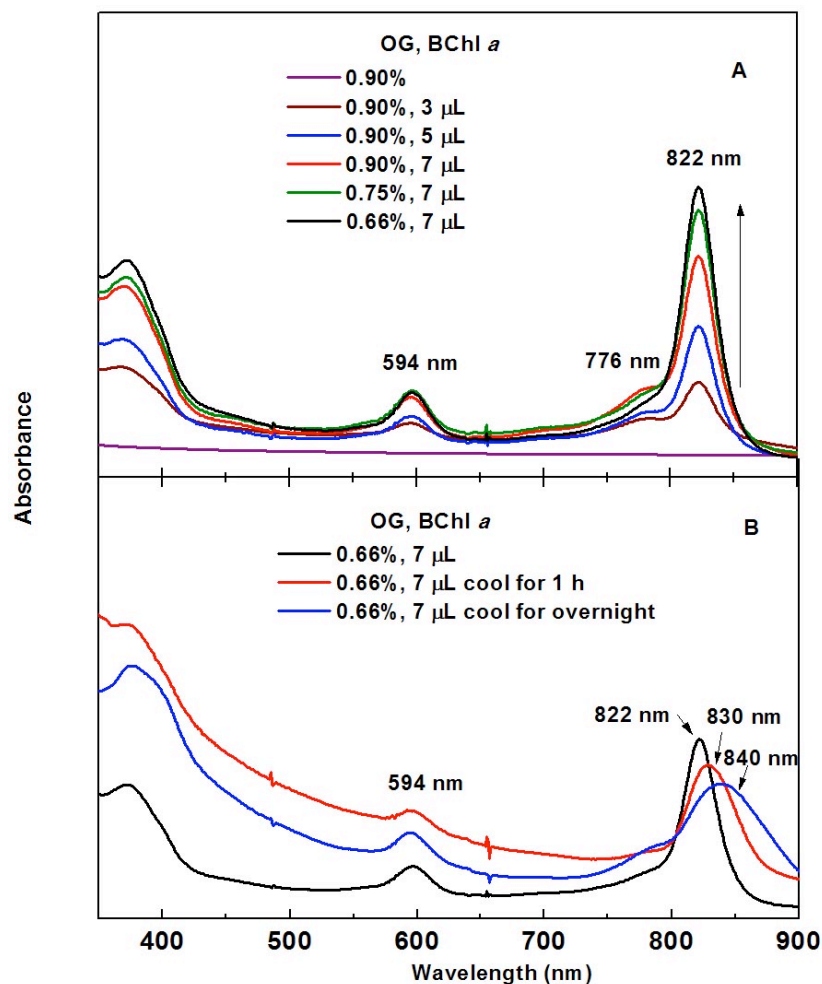
The quantities of BChl *a* added were chosen to give dyad formation (where each peptide dyad contains two BChl *a* molecules) with a minimum amount of free BChl *a*. Hence, the addition of BChl *a* was stopped at the earliest sign of excess “free BChl *a*” as determined by absorption spectroscopy (Fig. S19). A B820-type complex readily formed as the concentration of OG was reduced to 0.66%. Upon overnight storage of the B820 sample at 8 °C, a peak nicely formed at 835 nm (characteristic of oligomeric complexes) with relatively little 777 nm absorbance, indicating the presence of only a minor amount free BChl *a*.

(ii) Reconstitution from P1. A biohybrid complex of free peptide **P1** was reconstituted as a reference for the **BC6-P1** conjugate for energy-transfer studies. Under dim light, a sample of **P1** (~0.03 mg) was solubilized in 10 μL of hexafluoroacetone trihydrate, diluted with 0.25 mL of 100 mM phosphate buffer solution (pH 7.6) containing 5.4% OG, and then diluted 6-fold with the same buffer (no OG) to bring the OG concentration to 0.90%. This detergent solution of **P1** was neutralized by addition of 15 μL of 3 M potassium hydroxide solution. BChl *a* in degassed acetone (~0.8 mM) was then gradually added (3 μL, 2 μL, and 2 μL giving 7 μL total) to the solution by a microsyringe; the change in absorption upon such additions of BChl *a* is shown in Fig. S20. Formation of dyads and oligomer species was induced by (1) addition of 100 mM phosphate buffer solution (pH 7.6, lacking OG) to decrease the OG concentration first to 0.75% and then to 0.66% (0.3 mL, 0.25 mL), followed by (2) chilling the sample at 8 °C.

Figure S20. Absorption spectra for formation of B820- and oligomeric biohybrid control complexes [(P1-BChl)₂]_n.

(A) Titration of the **P1** at 0.90% OG with no BChl *a* (purple), 3.0 μL BChl *a* (wine), 5.0 μL total of BChl *a* (blue), at 0.90% OG with 7.0 μL total of BChl *a* (red), at 0.75% OG with 7.0 μL total of BChl *a* (green), and at 0.66% OG with 7.0 μL total of BChl *a*.

(B) Complexes at 0.66% OG with 7.0 μL total of BChl *a* before (black) and after chilling at 8 °C for 1 h (red) and overnight (blue). The Q_y absorption at 840 nm (blue) further sharpens upon additional chilling as the formation of the oligomer complexes goes to completion. The spectra were corrected for dilution, so that each sample would have the same concentration as for the sample with 0.90% OG.



A B820-type complex readily formed as the concentration of OG was reduced to 0.66%. Upon storage of the B820 sample at 8 °C for 1 h, a peak at 830 nm nicely formed, which represents a mixture of dyad and oligomeric complexes. Chilling the sample overnight at 8 °C gave a peak at 840 nm characteristic of an oligomeric complex (Fig. S20).

4. Spectroscopic data for BC6-P1 (from Prep I).

Highly efficient energy transfer was observed for the β -oligomeric biohybrid complexes containing bacteriochlorin **BC6**. These complexes were obtained from both Prep I and Prep III and studied by the full array of static and time-resolved spectroscopic measurements. Figs. S21–S23 given below for Prep I parallel Figs. 6–8 in the body of the paper. The descriptions of these results for Prep I parallel those given in the body of the paper for Prep III and thus are not reproduced here. Only a few specific comments on the data for Prep I are given.

Energy transfer from **BC6** to the BChl *a* array (denoted B850) in the biohybrid complex $[(\mathbf{BC6-P1-BChl})_2]_n$ to produce excited state B850* was first probed by excitation spectra (Fig. S21A) of the fluorescence from B850 (Fig. S21B). Fluorescence from B850* in this assembly is observed (as expected) at ~850 nm upon direct excitation of B850 in the Q_x band at 590 nm. Fluorescence from $[(\mathbf{BC6-P1-BChl})_2]_n$ is also obtained using excitation in the Q_y band of **BC6** at ~718 nm (Fig. S21B and inset, black). An energy-transfer efficiency (Φ_{ENT}) value of 0.9 ± 0.1 was determined by comparing the amplitudes of the **BC6** features in the fluorescence-excitation versus absorbance spectra (Fig. 6A, blue and magenta, respectively). A similarly high (≥ 0.9) efficiency of energy transfer is also reflected by the observation that the **BC6** fluorescence ($\lambda_{\text{det}} = 720$ nm; $\lambda_{\text{exc}} = 490$ nm) in biohybrid $[(\mathbf{BC6-P1-BChl})_2]_n$ (Fig. S21C, black) is only a few percent of that in the control peptide conjugate (magenta). Similar quenching is observed upon excitation of **BC6** in the Q_y band (718 nm) for biohybrid $[(\mathbf{BC6-P1-BChl})_2]_n$ versus peptide control **BC6-P1**, where in this case the scan cannot reveal the $Q_y(0,0)$ fluorescence peak but only the vibronic features to longer wavelengths (Fig. S21B, black versus magenta).

Fig. 5B and inset reveal that excitation of **BC6** gives rise to not only B850* fluorescence at ~850 nm, but also fluorescence at shorter wavelengths extending to <800 nm due in part to energy transfer to species present in small amounts relative to the biohybrid complex. Such contributions include (i) a tail of emission from free **BC6** ($\lambda_{\text{max}} \sim 720$ nm) or **BC6-P1** from which BChl *a* has dissociated, (ii) free BChl *a* ($\lambda_{\text{max}} \sim 780$ nm) that has dissociated from the complex, (iii) a small fraction of $\beta\beta$ -subunit subunit complexes or less extended oligomers ($\lambda_{\text{max}} \sim 830$ nm). The fluorescence yields (Φ_f) are on the order of 0.1 for monomeric synthetic bacteriochlorins (bioconjugatable and benchmarks) and BChl *a* (Table 1), on the order of 0.01 for the BChl *a* dimer (B820) in $\beta\beta$ -subunits, and on the order of 0.001 for the BChl *a* array (B850) in oligomeric complexes (with or without conjugated bacteriochlorin), as found here for **BC6** complexes and previously¹⁸ for **BC1** and **BC2** complexes. Thus, very small amounts of monomeric chromophores or subunits will give rise to detectable fluorescence (780–840 nm) in addition to that for B850 (~850 nm) in the biohybrid complexes even if the latter is the overwhelmingly dominant species present. An additional preparation of $[(\mathbf{BC6-P1-BChl})_2]_n$ is largely free of such emission at shorter wavelength (Fig. 6 in the body of the paper). The latter sample also gives a high (≥ 0.9) yield of energy transfer from **BC6** to B850. This comparison shows that the presence of a small amount of relatively highly emitting species such as free BChl *a* or synthetic chromophore (or bacteriochlorin–peptide conjugate) does not compromise the photophysical measurements on or the functionality of the oligomeric assembly.

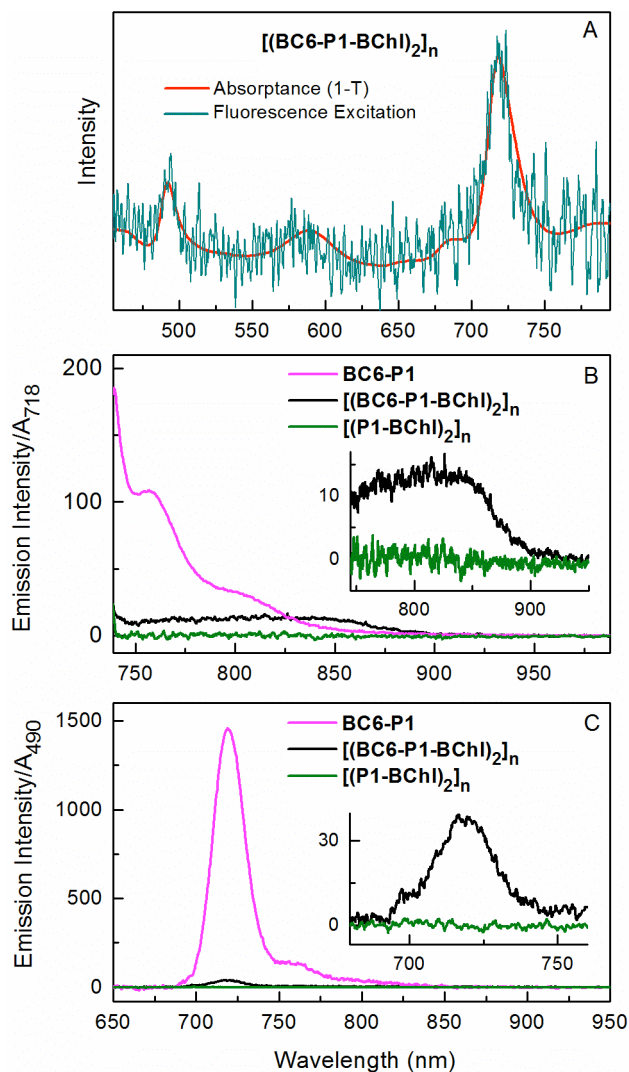


Figure S21. Steady-state fluorescence data for oligomeric biohybrid $[(\text{BC6-P1-BChl})_2]_n$, oligomer control $[(\text{P1-BChl})_2]_n$, and control peptide BC6-P1 at 9 °C. (A) Absorbance (1-T) and fluorescence excitation spectra ($\lambda_{\text{det}} = 850$ nm) for the biohybrid complex normalized at the 590-nm BChl Q_x maximum. The absorbance spectrum was corrected for light scattering and the excitation spectrum for instrument parameters. (B) Fluorescence spectra of the biohybrid complex (black), control peptide (magenta) and oligomer control (green), with the intensities divided by the absorbance at $\lambda_{\text{exc}} = 718$ nm. (C) Fluorescence spectra of the biohybrid complex, (black), control peptide (magenta) and control oligomer (green) with the intensities divided by the absorbance at $\lambda_{\text{exc}} = 490$ nm.

Biohybrid complex $[(\text{BC6-P1-BChl})_2]_n$ and oligomer control $[(\text{P1-BChl})_2]_n$ were also studied using ultrafast transient absorption spectroscopy. The data shown in Figs. S22 and S23 are similar to those shown for Prep I in Figs. 7 and 8 of the body of the paper, with a few small differences in spectra/kinetic detail. For Prep III, B850* shows decay time constants of ~ 4 , ~ 30 and ~ 600 ps for oligomeric control $[(\text{P1-BChl})_2]_n$ and ~ 40 and ~ 300 ps for biohybrid $[(\text{BC6-P1-BChl})_2]_n$. The main finding is that B850 bleaching and B850* stimulated emission show an instantaneous (<300 fs) overall rise for the oligomeric control but comparatively slow growth (1–2 ps) as are shown in Fig. S23. These rise-time data are the same as those found for the complexes from Prep I shown in Fig. 8 of the body of the paper. The 1–2 ps lag in the formation

of B850* reflects energy transfer from BC6* to the BChl *a* array (B850) in the biohybrid complex. The B850* rise-time constant, which reflects the BC6* lifetime in the biohybrid complex, is significantly shorter than the lifetime of BC6* in the control peptide conjugate or organic media and the benchmark bacteriochlorin (Table 1 in the body of the paper). This comparison again reflects the near-quantitative yield of energy transfer from excited BC6 to the BChl *a* array (B850) in the biohybrid complex.

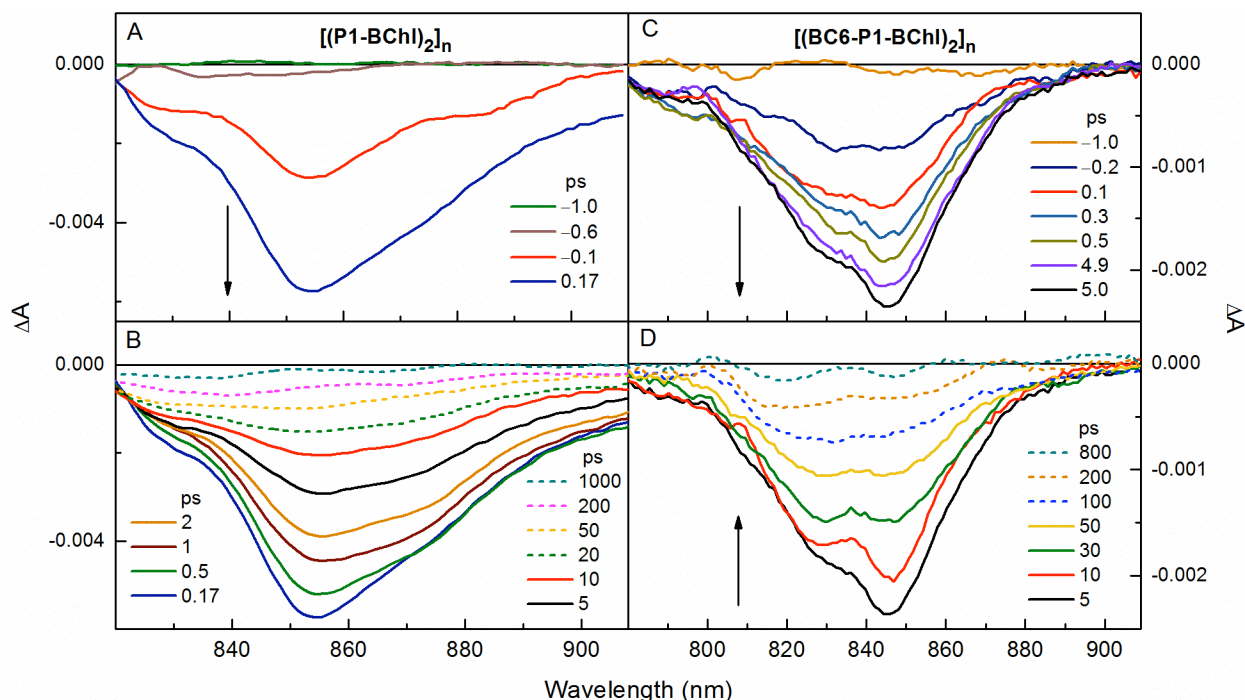
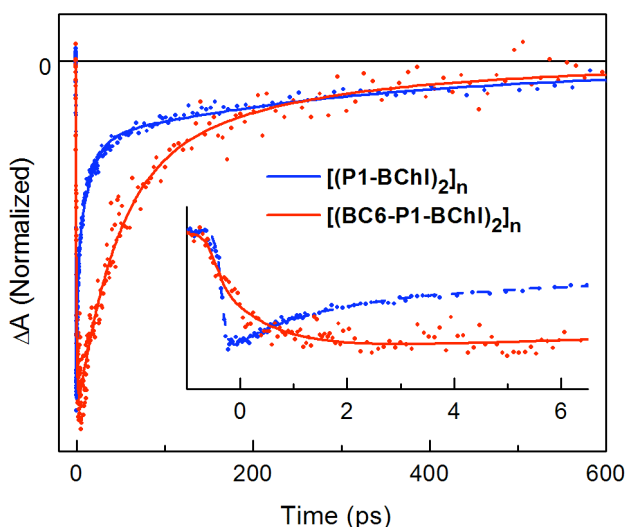
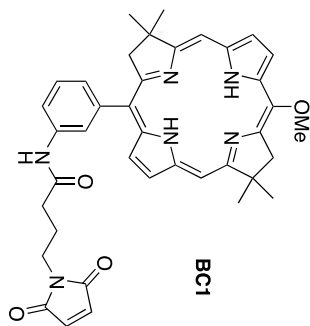
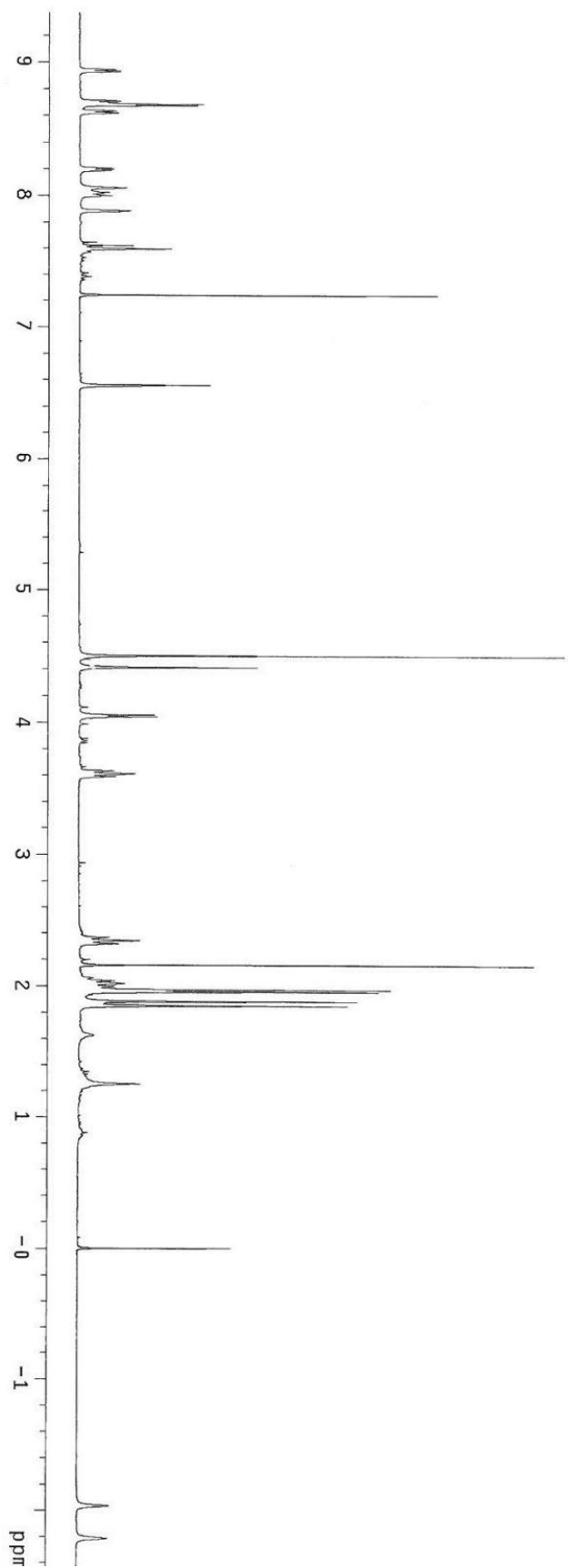


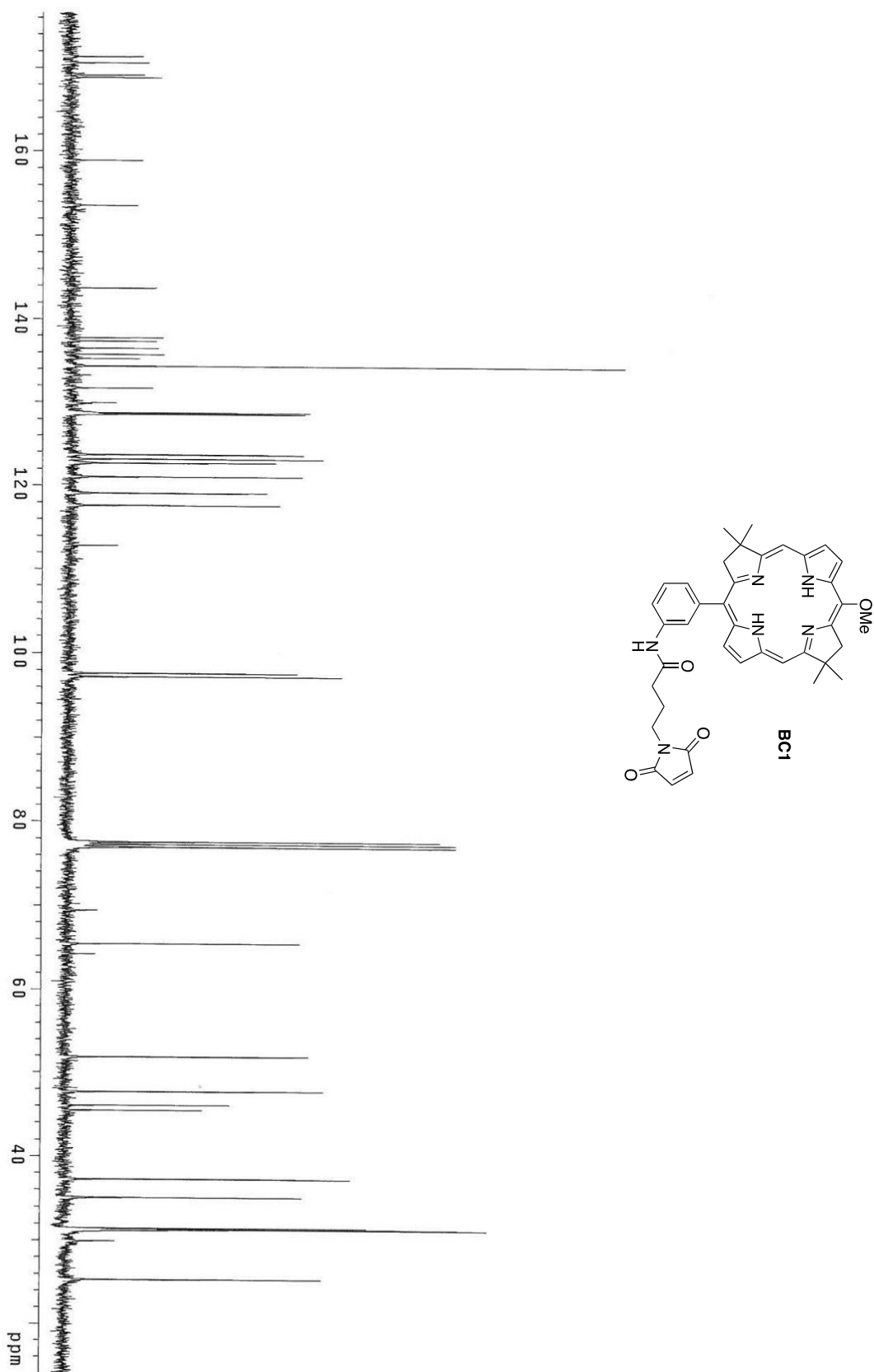
Figure S22. NIR transient absorption spectra at 9 °C of the BChl complex in oligomeric control $[(P1-BChl)_2]_n$ using excitation at 590 nm (left panels) and oligomeric biohybrid $[(BC6-P1-BChl)_2]_n$ using excitation of BC6 at 718 nm (right panels). Panel (A) shows the instrument-limited rise and panel (B) the decay of the combined B850 bleaching B850* stimulated emission for the oligomeric control. Panel (C) shows non-instrument-limited growth and panel (D) decay of the features for the biohybrid complex.

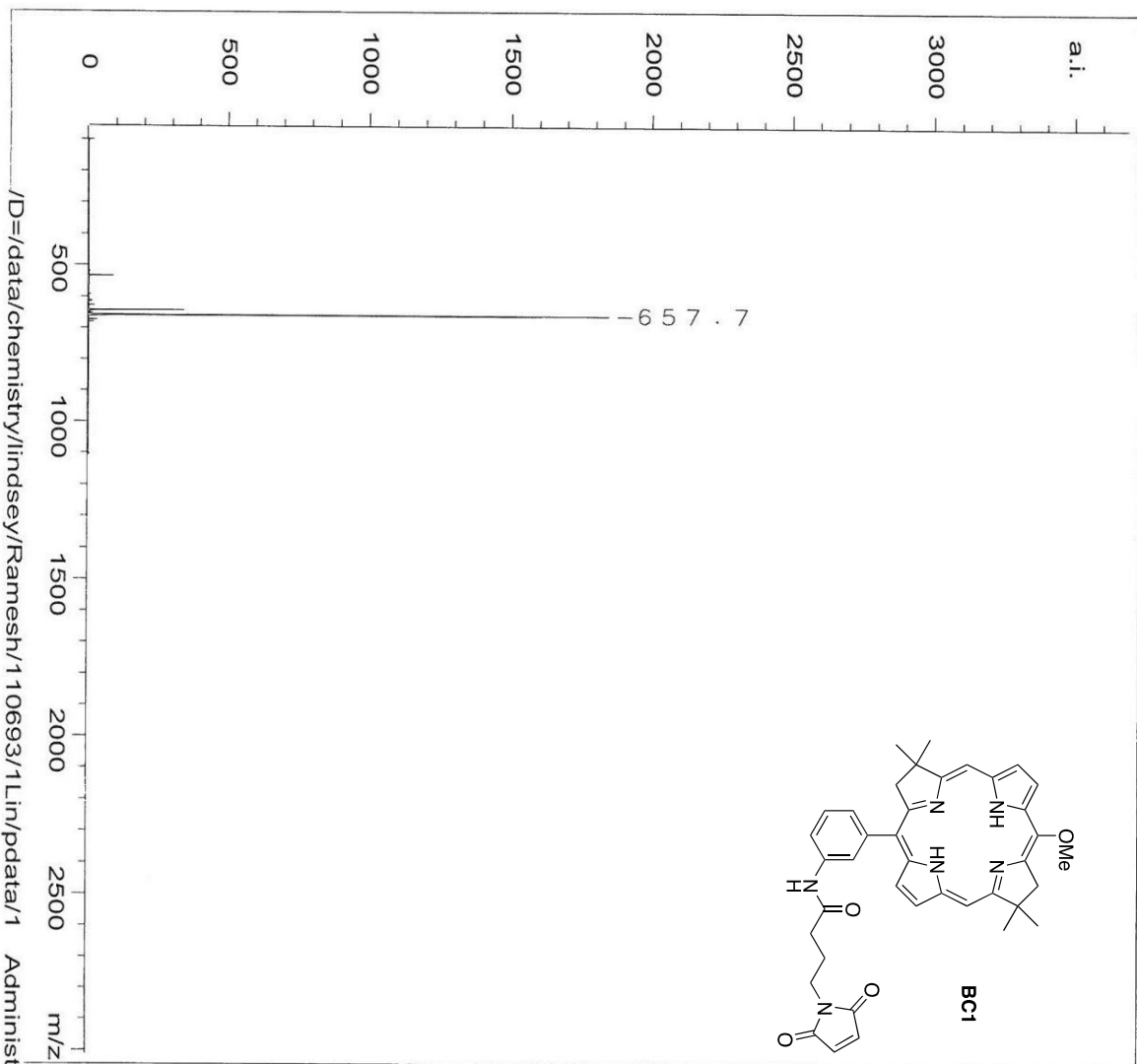
Figure S23. Time-evolution of the bleaching/stimulated-emission (845 nm) for oligomeric biohybrid $[(BC6-P1-BChl)_2]_n$ and oligomeric control $[(P1-BChl)_2]_n$ at 9 °C. The inset shows the 1–2 ps growth of bleaching for the biohybrid complex and the instrument-limited rise for the control. The line through each data set is a fit to a function consisting of three exponentials plus a long-time constant convolved with the instrument response.



5. Spectral data for new compounds.

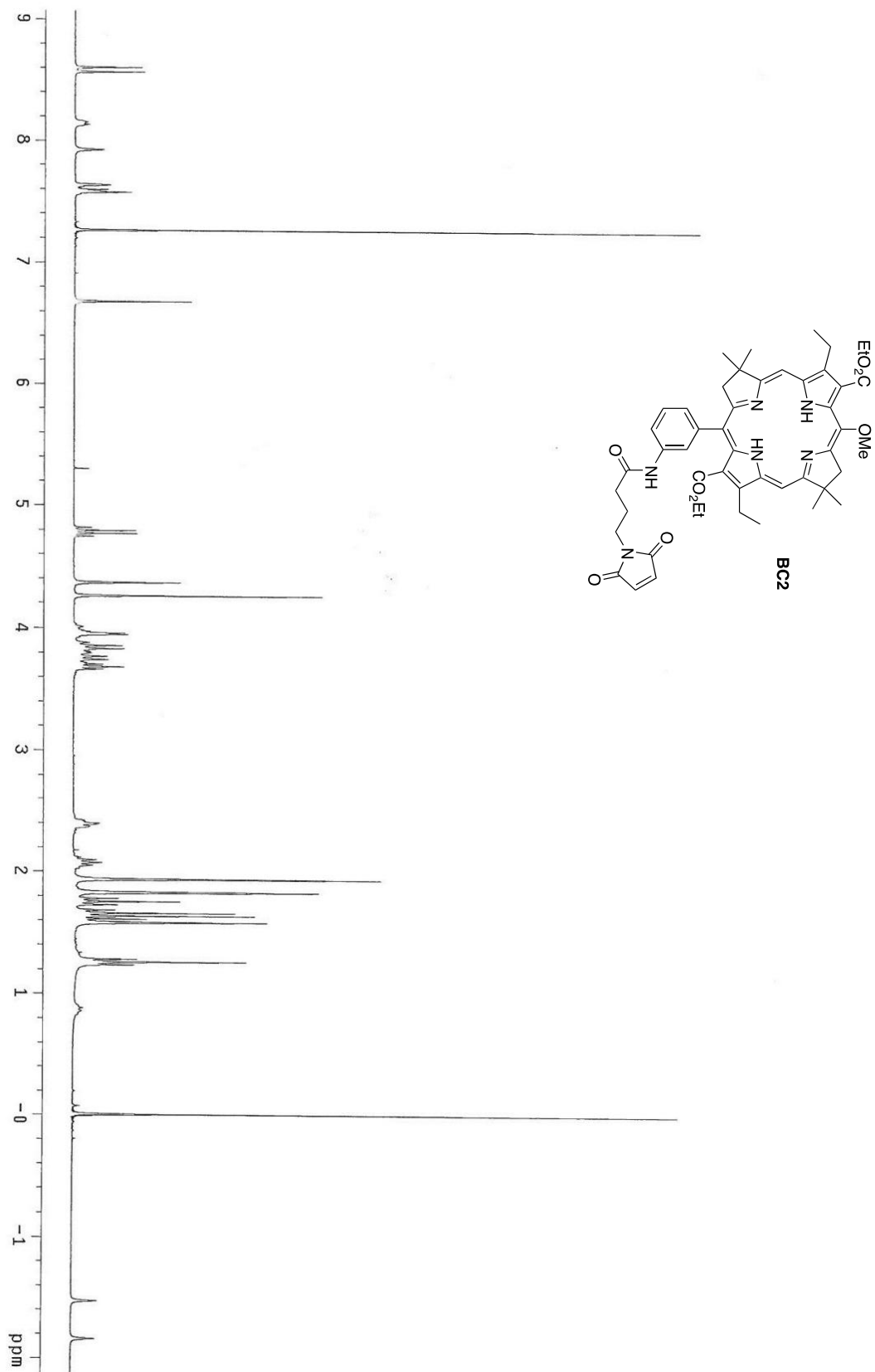


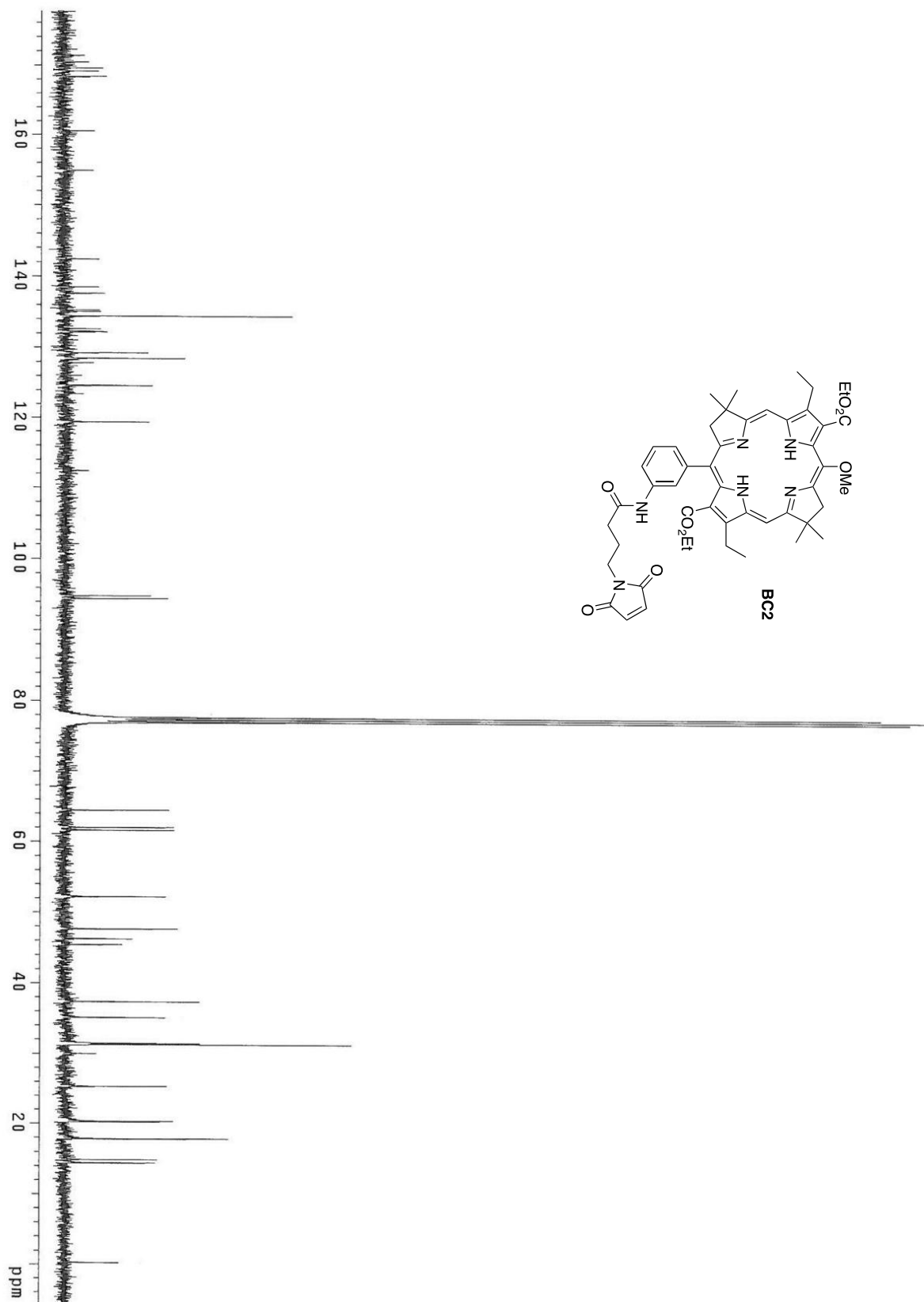


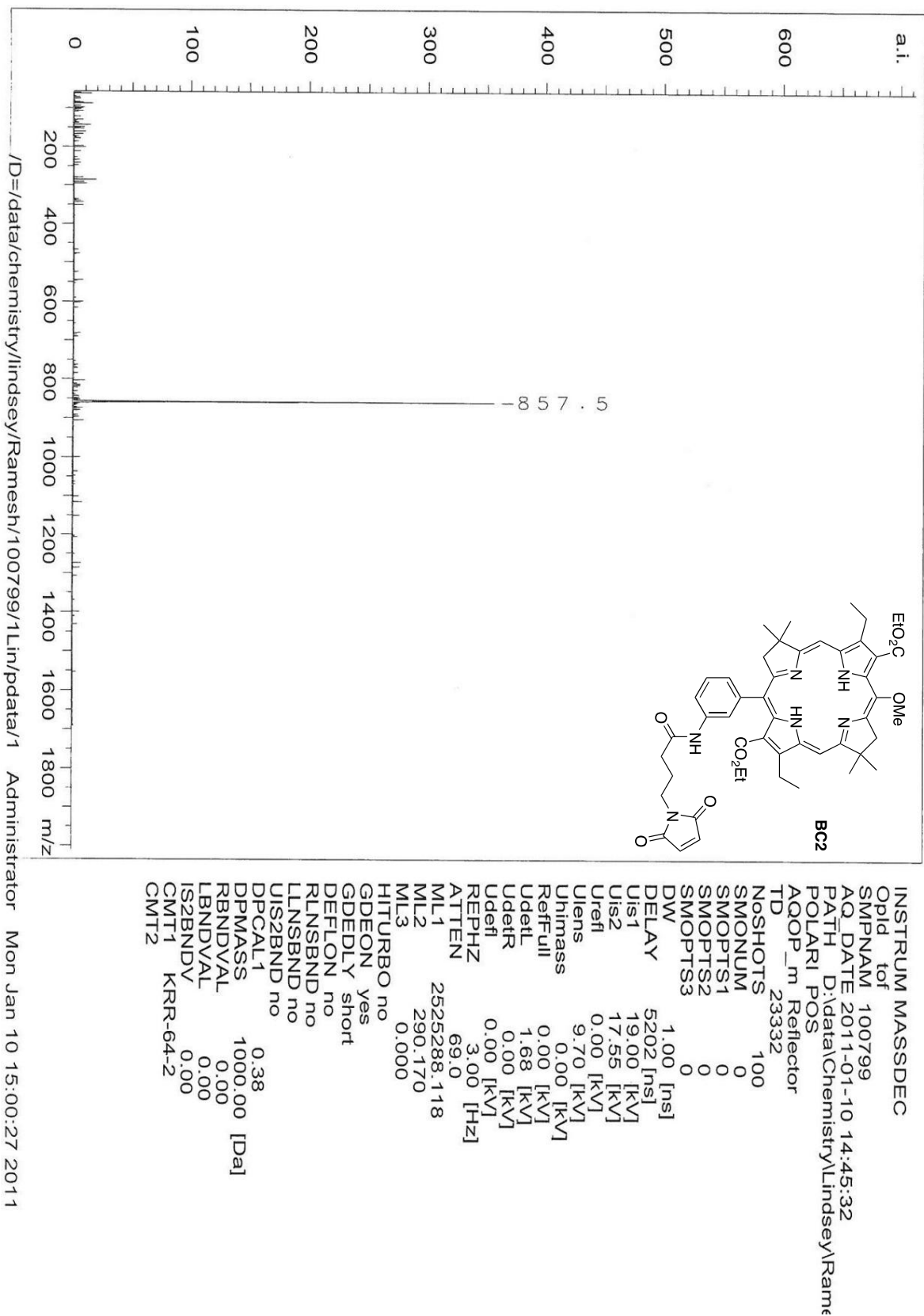


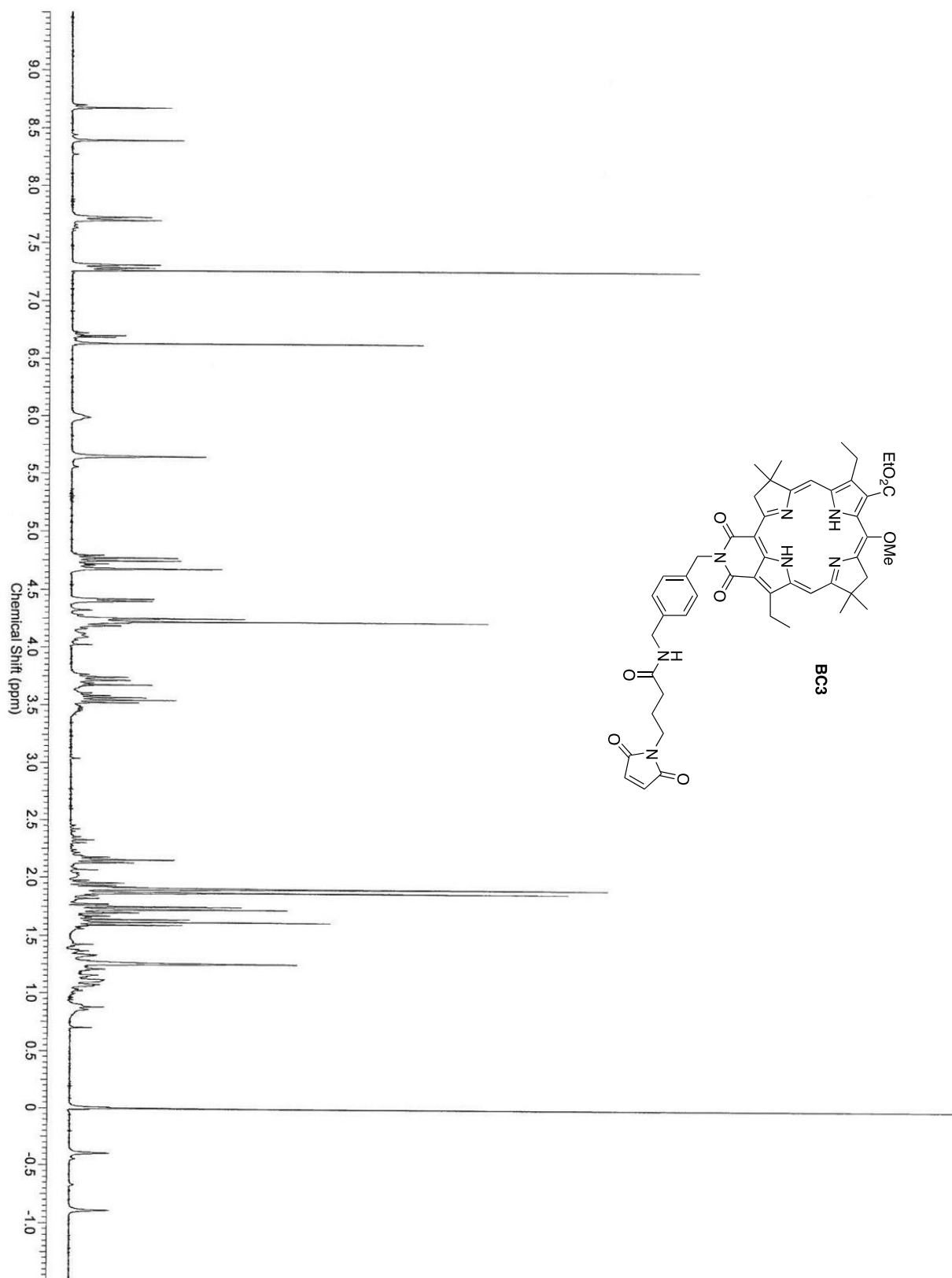
/D=/data/chemistry/lindsey/Ramesh/110693/1Lin/pdata/1 Administrator Wed Jul 27 10:13:53 2011

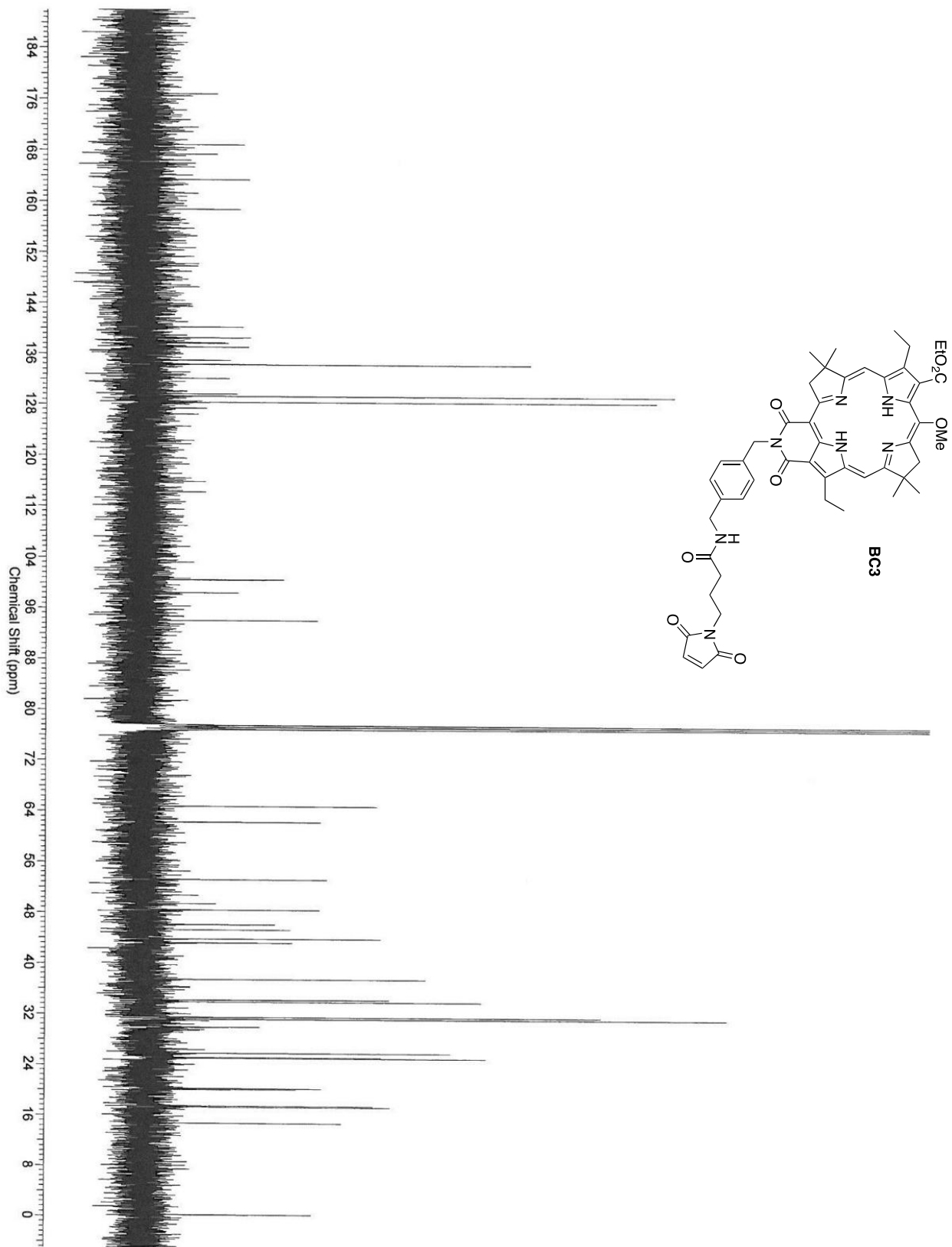
INSTRUM MASSDEC
 OpId tof
 SMPNAM 110693
 AQ_DATE 2011-07-27 10:07:41
 PATH D:/data/chemistry/lindsey/Rame:
 POLARI POS
 AAOPT_m Reflector
 TD 29673
 NOSHOT 100
 SMONUM 0
 SMOPTS1 0
 SMOPTS2 0
 SMOPTS3 0
 DW 1.00 [ns]
 DELAY 5184 [ns]
 Uis1 19.00 [kV]
 Uis2 17.50 [kV]
 Urefl 0.00 [kV]
 Urens 9.70 [kV]
 Uhimass 0.00 [kV]
 RefFull 0.00 [kV]
 UdetL 1.62 [kV]
 UdetR 0.00 [kV]
 Udefl 0.00 [kV]
 REPHZ 3.00 [Hz]
 ATTEN 86.0
 ML1 2521591.140
 ML2 297.203
 ML3 0.000
 HITURBO no
 GDEON yes
 GDEDLY short
 DEFLO no
 RLNSBND no
 LLNSBND no
 LIS2BND no
 DPCAL1 0.38
 DPMASS 1000.00 [Da]
 RBNDVAL 0.00
 LBNDVAL 0.00
 IS2BNDV 0.00
 CMT1 krr57
 CMT2

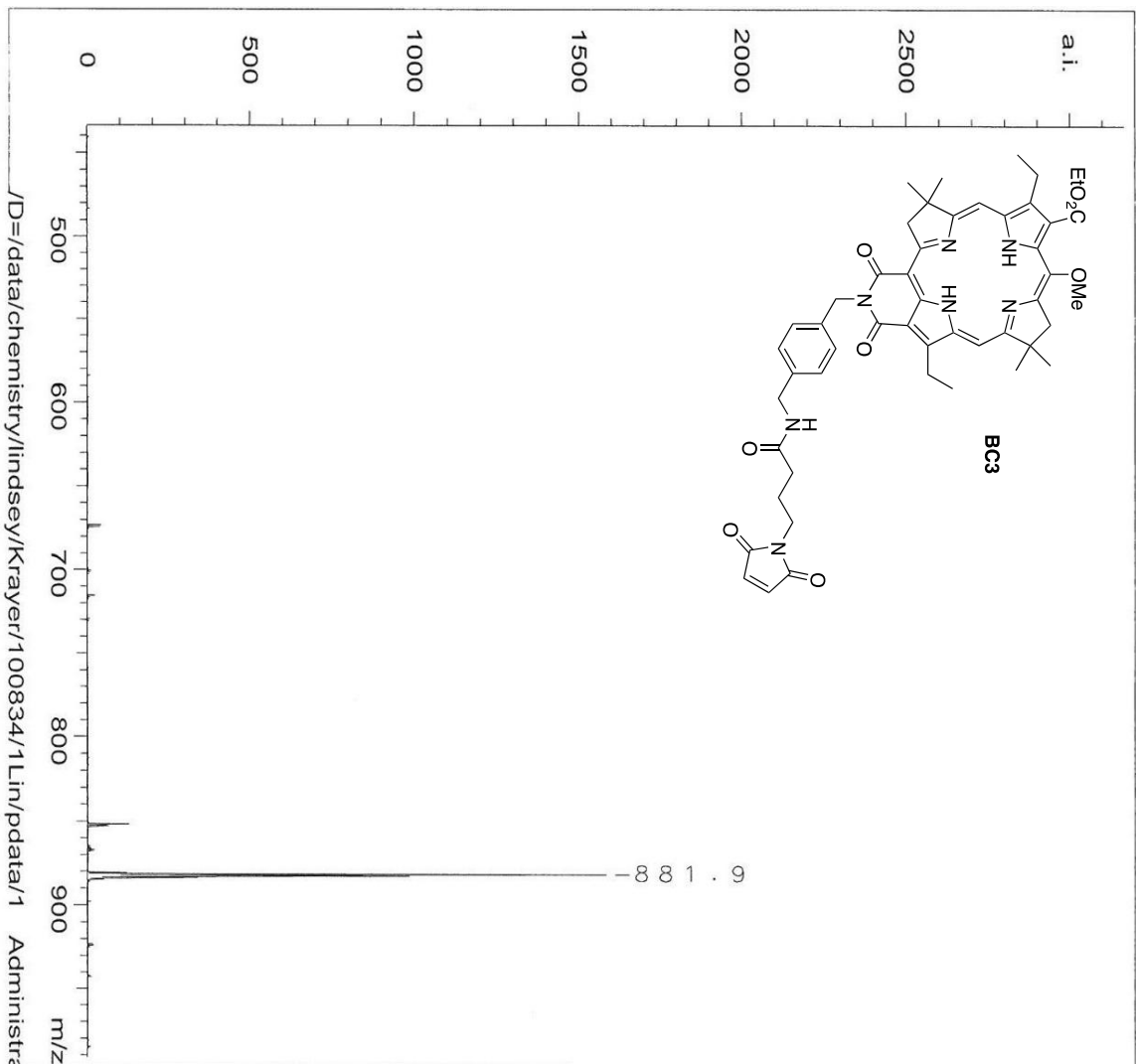








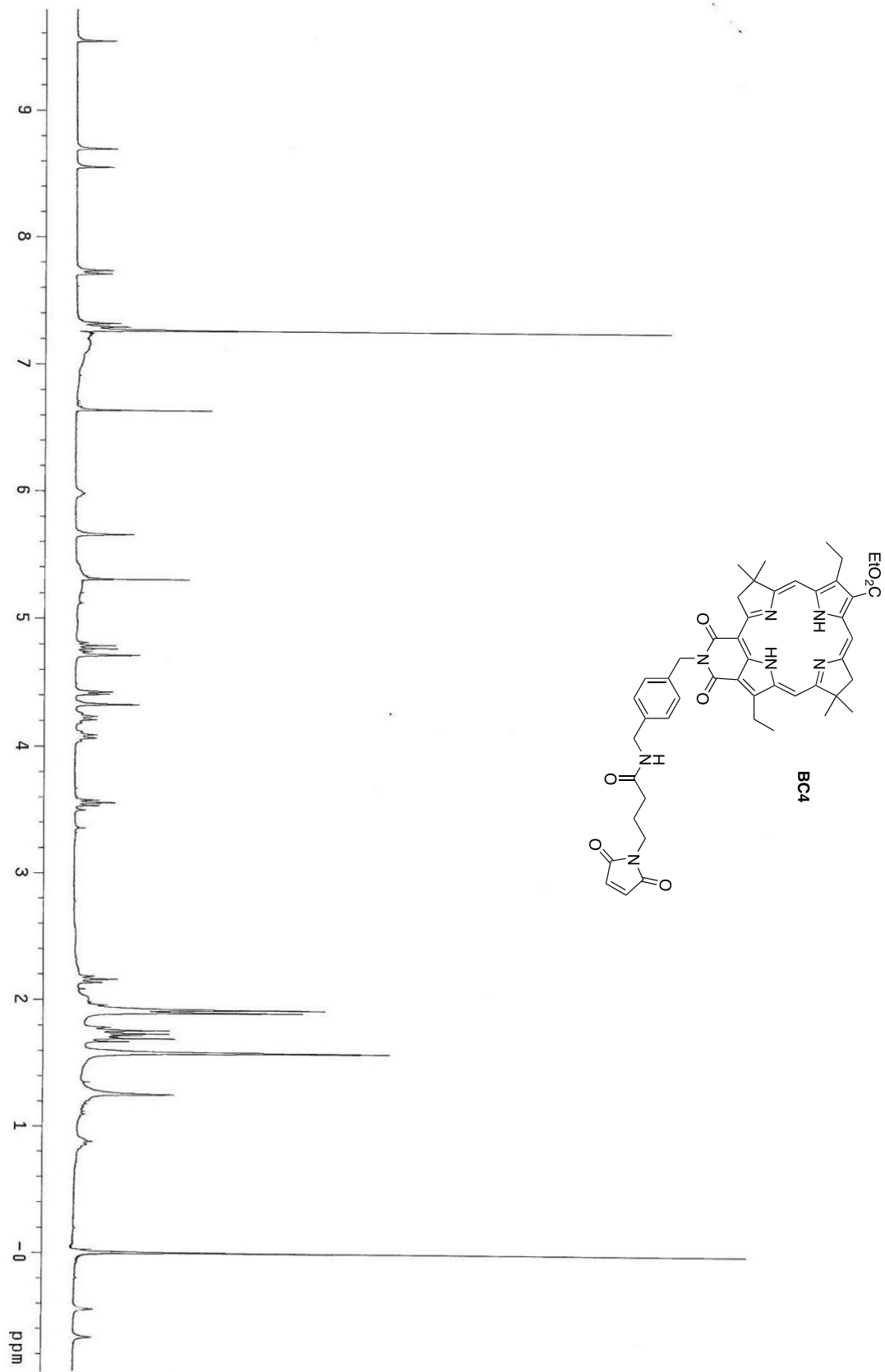


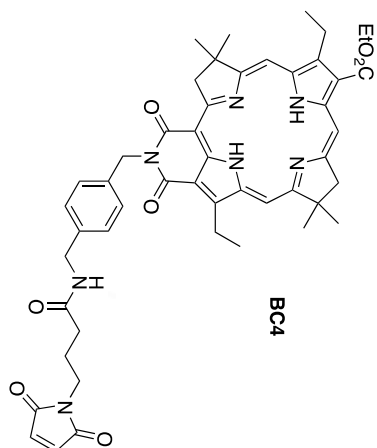
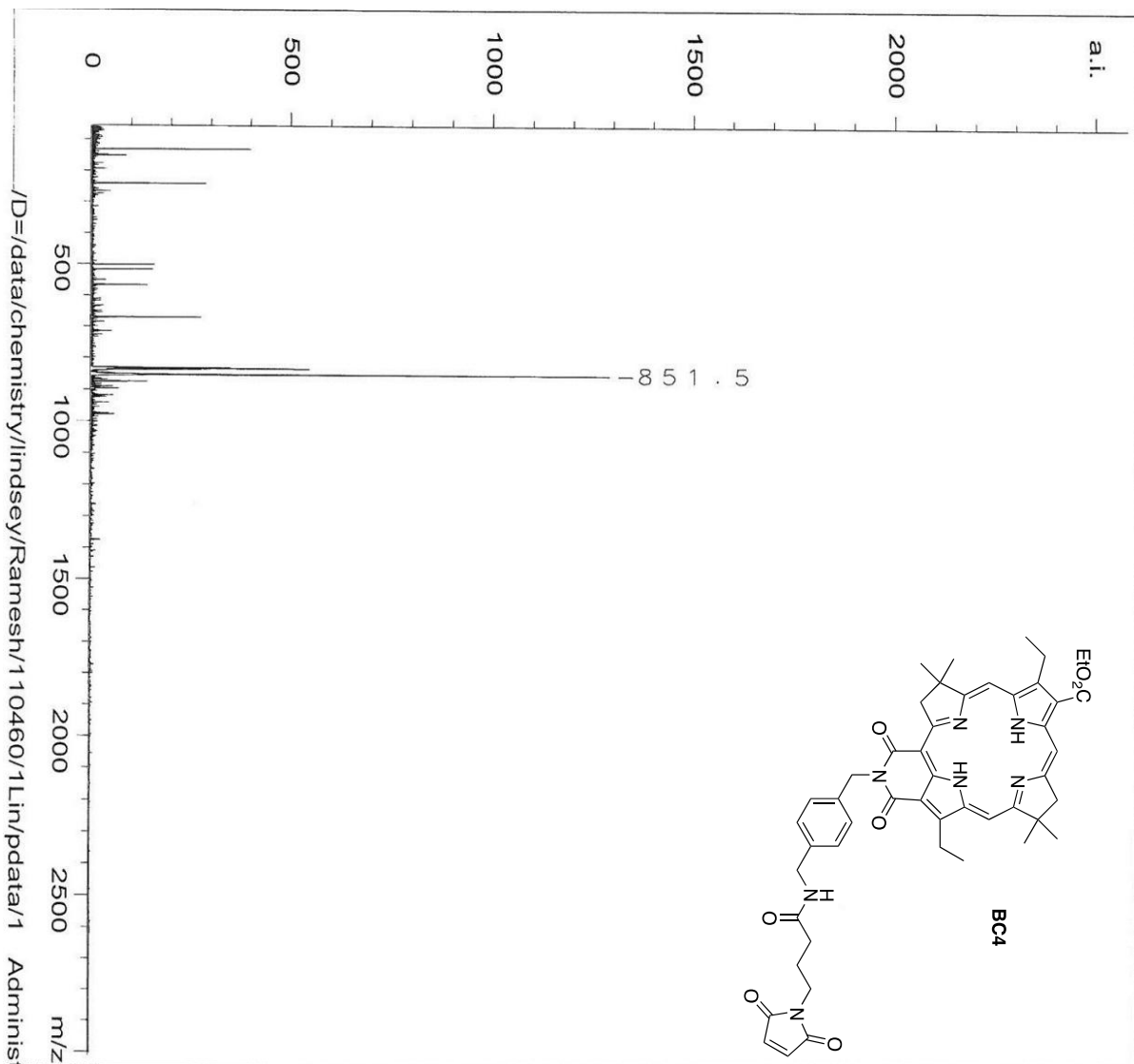


/D=/data/chemistry/lindsey/Krayer/100834/1Lin/pdata/1 Administrator Wed Jan 19 07:59:19 2011

```

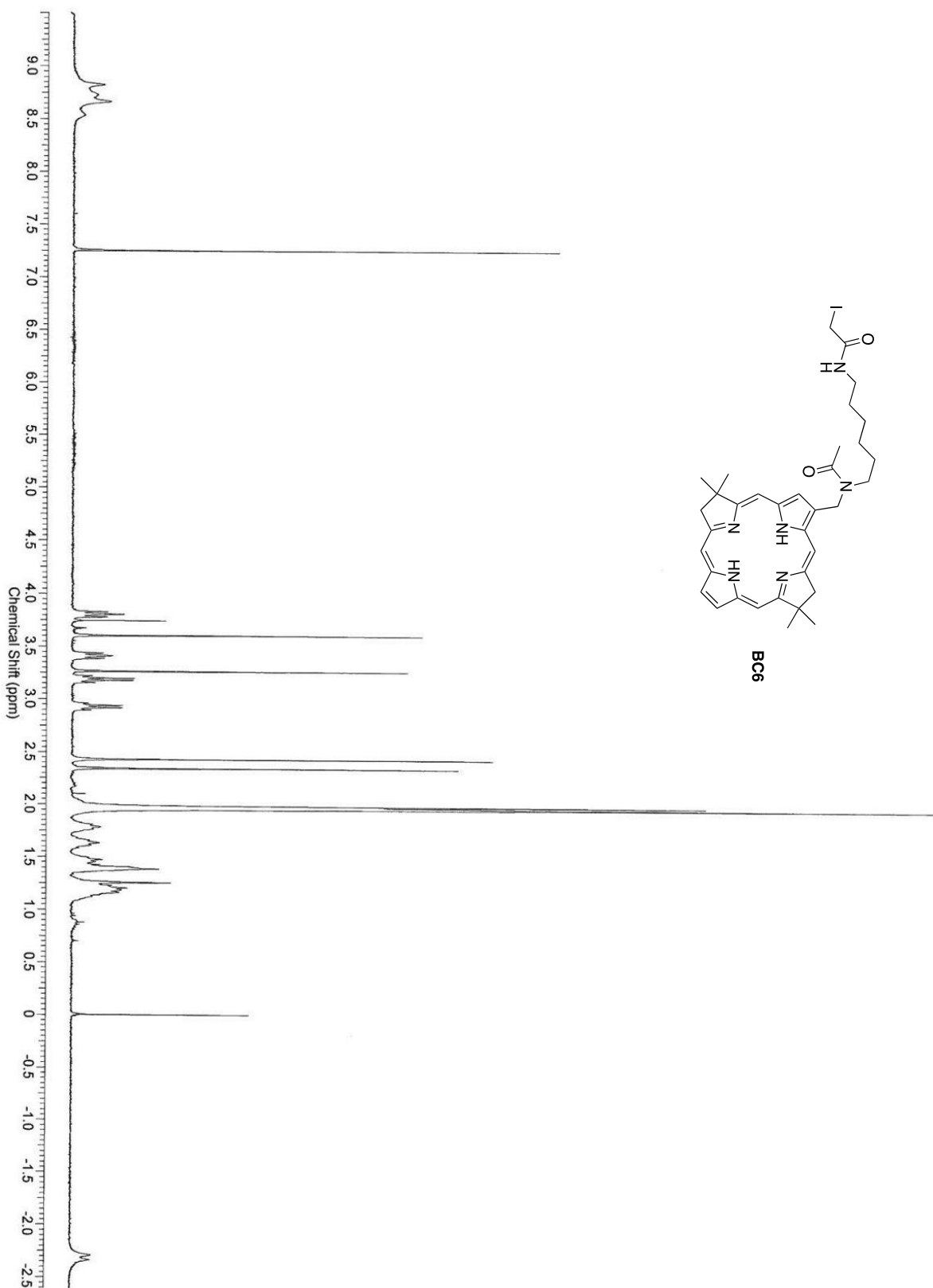
INSTRUM MASSDEC
OpId tof
SMPNAM 100834
AQ_DATE 2011-01-19 07:57:05
PATH D:/data/chemistry/Lindsey/Krayer
POLARI POS
AQOP_m Reflector
TD 29673
NOSHOTS 100
SMONUM 0
SMOPTS1 0
SMOPTS2 0
SMOPTS3 0
DW 1.00 [ns]
DELAY 5184 [ns]
Uis1 19.00 [kV]
Uis2 17.50 [kV]
Urefl 0.00 [kV]
Urefl 9.70 [kV]
Uhimass 0.00 [kV]
Reffull 0.00 [kV]
Udetl 1.62 [kV]
Udetr 0.00 [kV]
Udefl 0.00 [kV]
REPHZ 3.00 [Hz]
ATTEN 98.0
ML1 2531678.306
ML2 314.631
ML3 0.000
HITURBO no
GDEON yes
GDEDLY short
DEFLO no
RLNSBND no
LLNSBND no
UIS2BND no
DPCAL1 0.38
DPMASS 1000.00 [Da]
RBNVAL 0.00
LBNDVAL 0.00
IS2BNDV 0.00
CMT1
CMT2
    
```





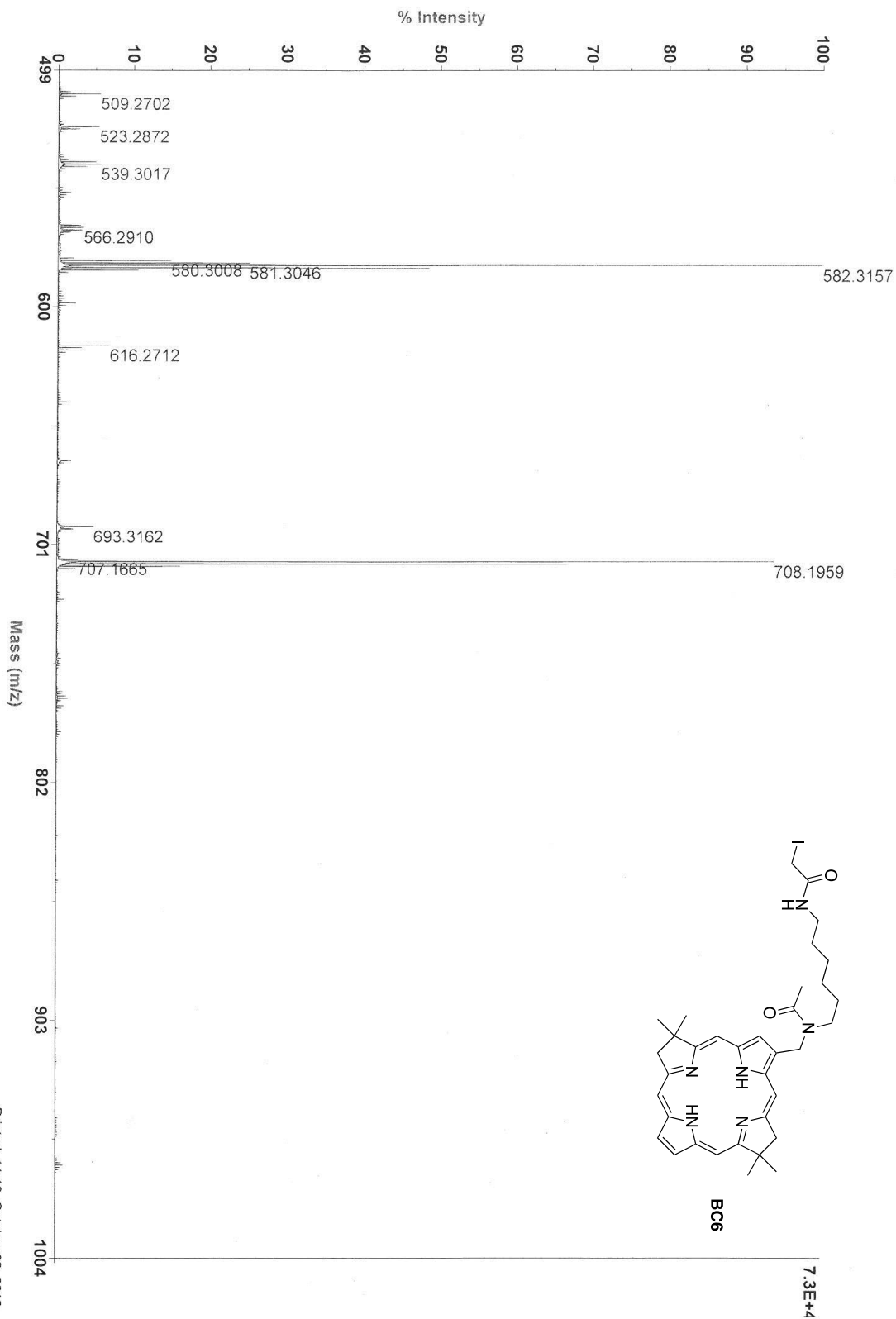
```

INSTRUM MASSDEC
OpId      tof
SMPNAM    110460
AQ_DATE   2011-06-13 11:20:57
PATH      D:/data/Chemistry/Lindsey/Rame
POLARI    POS
AQOP_m    Reflector
TD         29673
NoSHOTS   100
SMONUM    0
SMOPTS1   0
SMOPTS2   0
SMOPTS3   0
DW         1.00 [ns]
DELAY     5184 [ns]
Uis1      19.00 [kV]
Uis2      17.50 [kV]
Urefl     0.00 [kV]
Uens      9.70 [kV]
Uhimass   0.00 [kV]
Reffull   0.00 [kV]
Udetl     1.62 [kV]
Udetr     0.00 [kV]
Udefl     0.00 [kV]
REPHZ     3.00 [Hz]
ATTEN     63.0
ML1       2526496.701
ML2       315.251
ML3       0.000
HITURBO   no
GDEON     yes
GDEDLY    short
DEFLOX    no
RLNSBND   no
LLNSBND   no
UIS2BND   no
DPCAL1    0.38
DPMASS    1000.00 [Da]
RBNDVAL   0.00
LBNDVAL   0.00
IS2BNDV   0.00
CMT1      krr126 std
CMT2
    
```



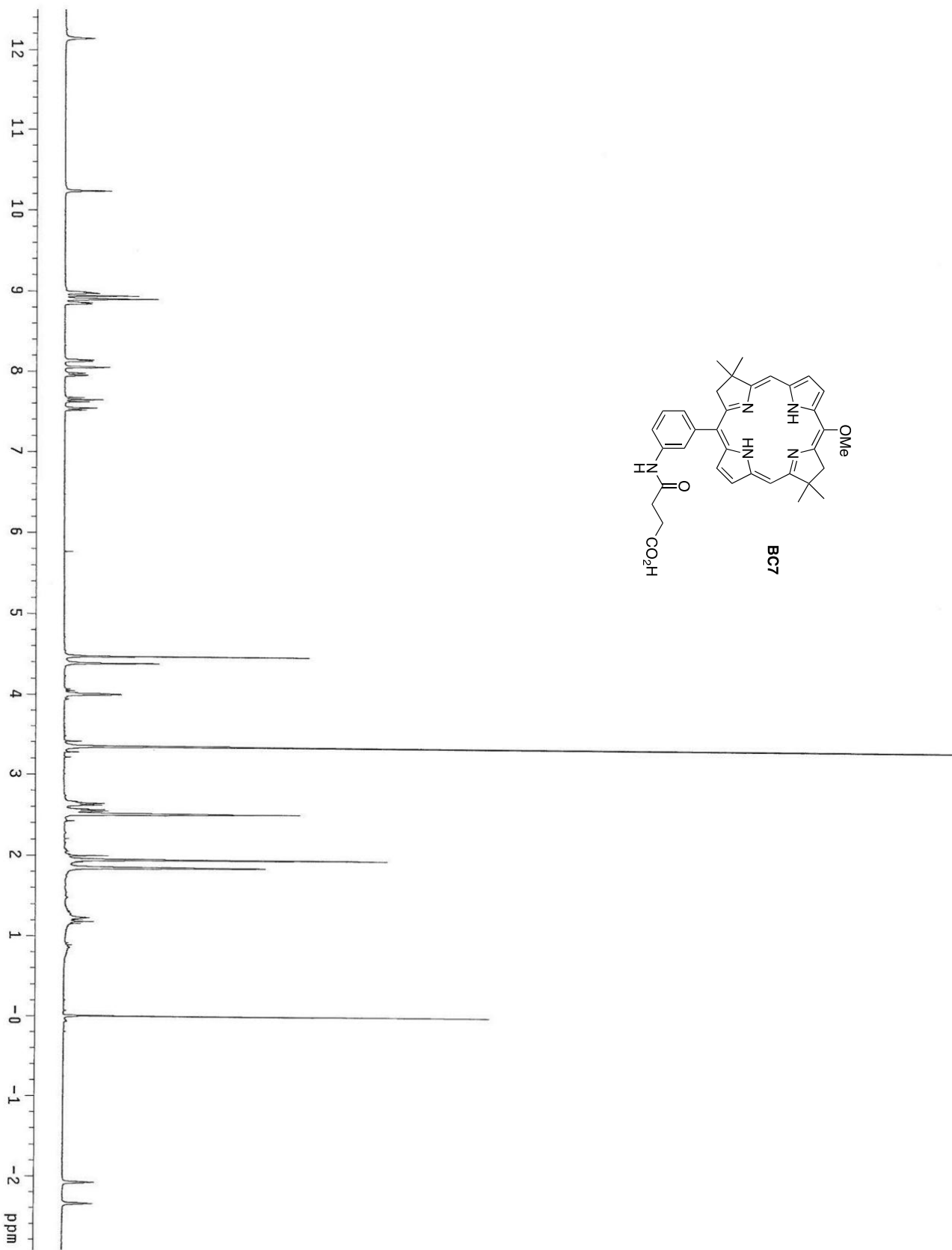
AB Sciex TOF/TOF™ Series Explorer™ 72098

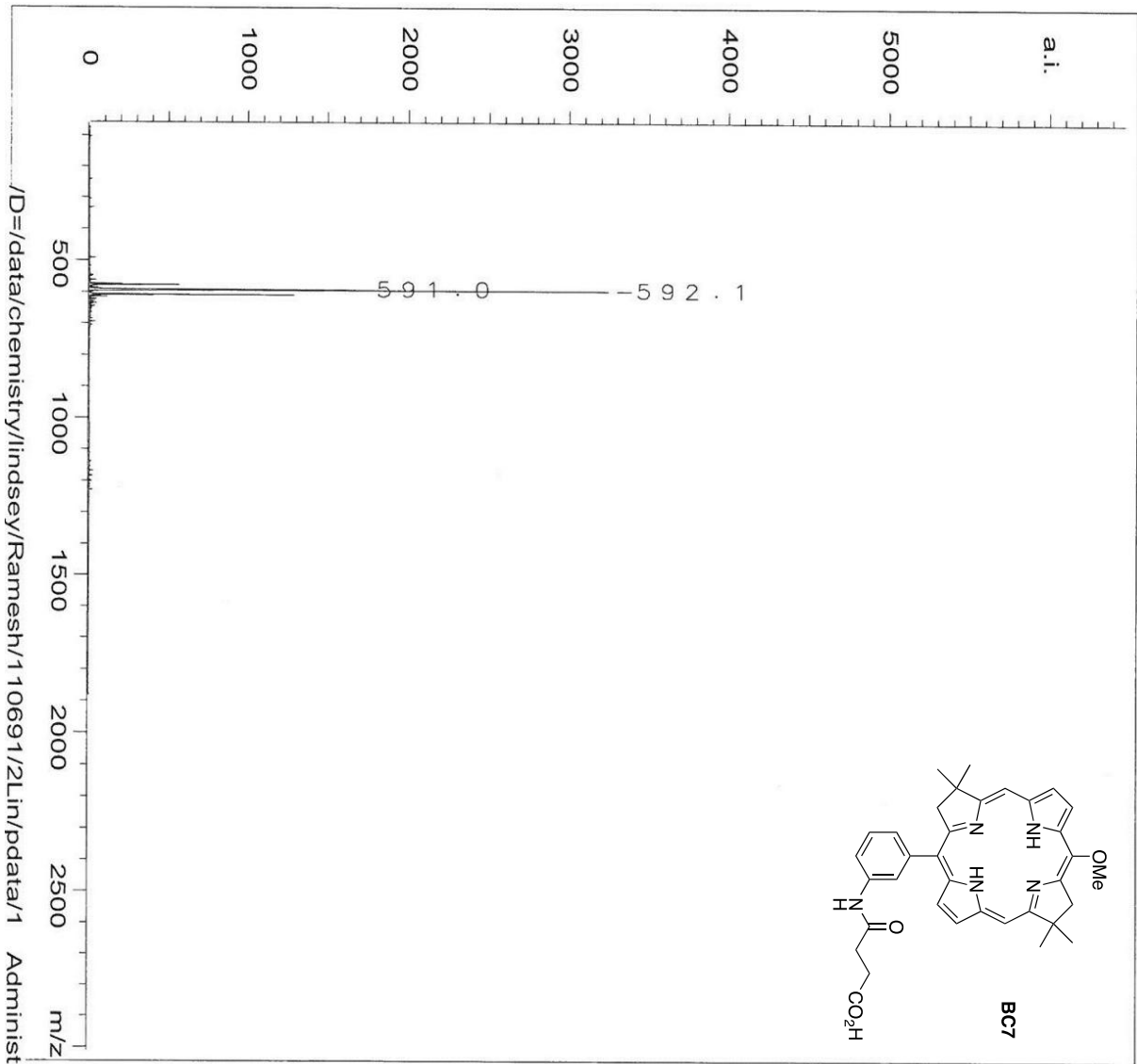
TOF/TOF™ Reflector Spec #1 MC[BP = 582.3, 73056]



C:\AB SCIEX\TOF\TOF Data\Export\2DU\user Project 1\Lindsey\10_02_12\E13_MS.r24

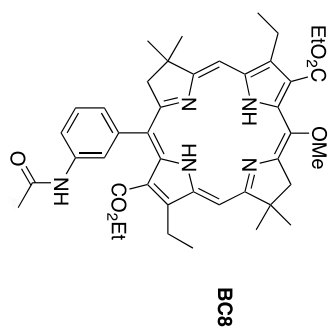
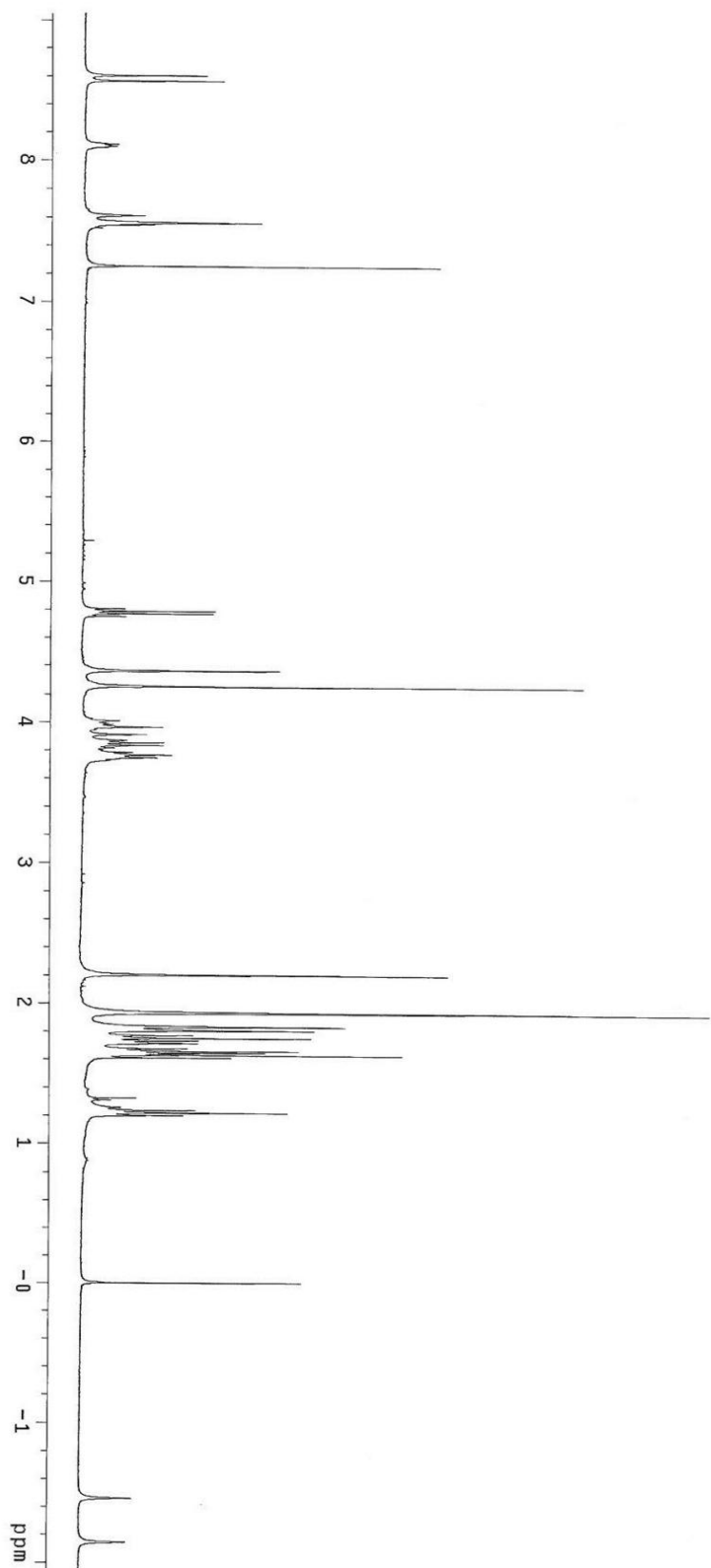
Printed: 11:19, October 02, 2012

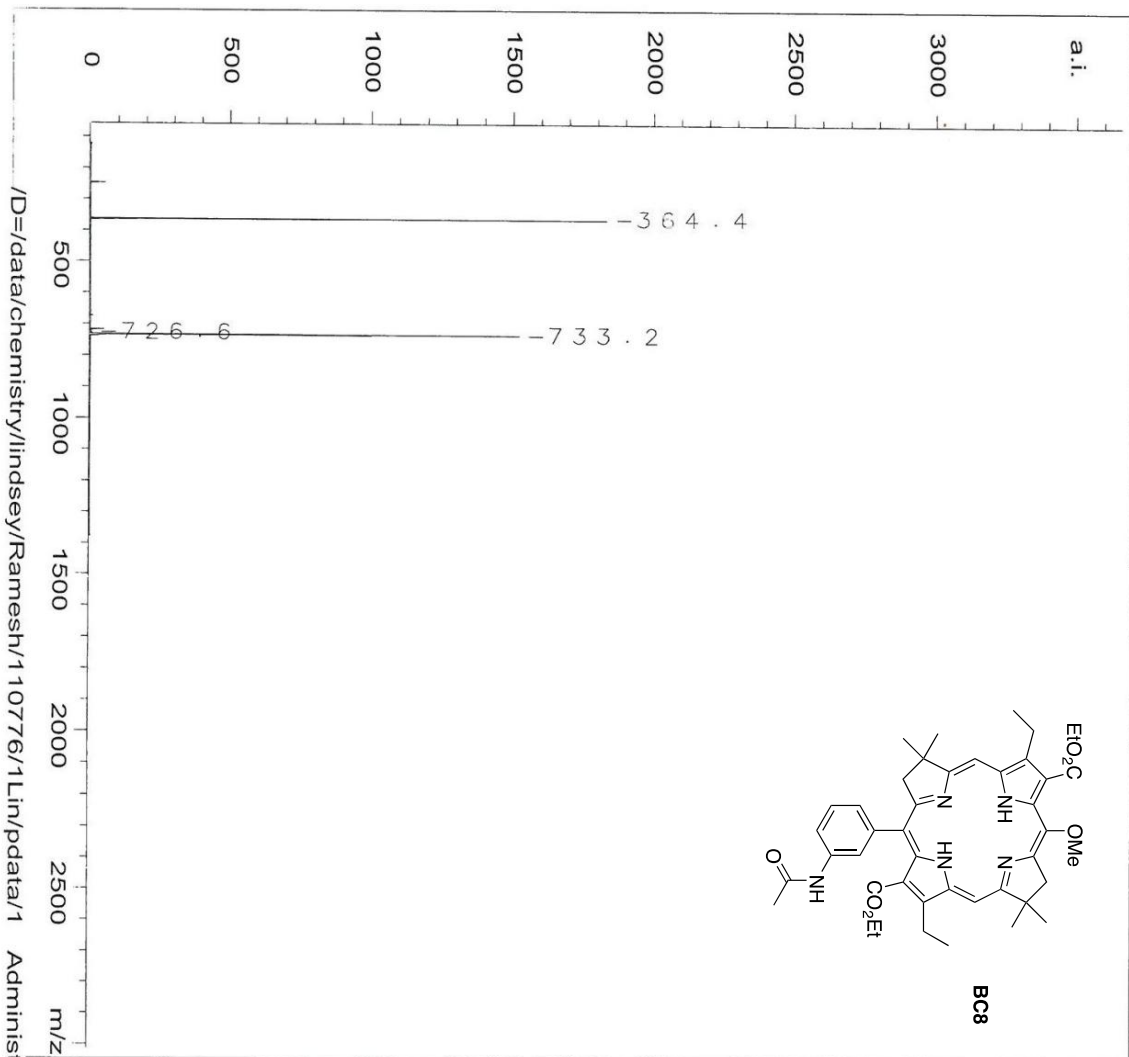




/D=/data/chemistry/lindsey/Ramesh/110691/2Lin/pdata/1 Administrator Wed Jul 27 10:12:44 2011

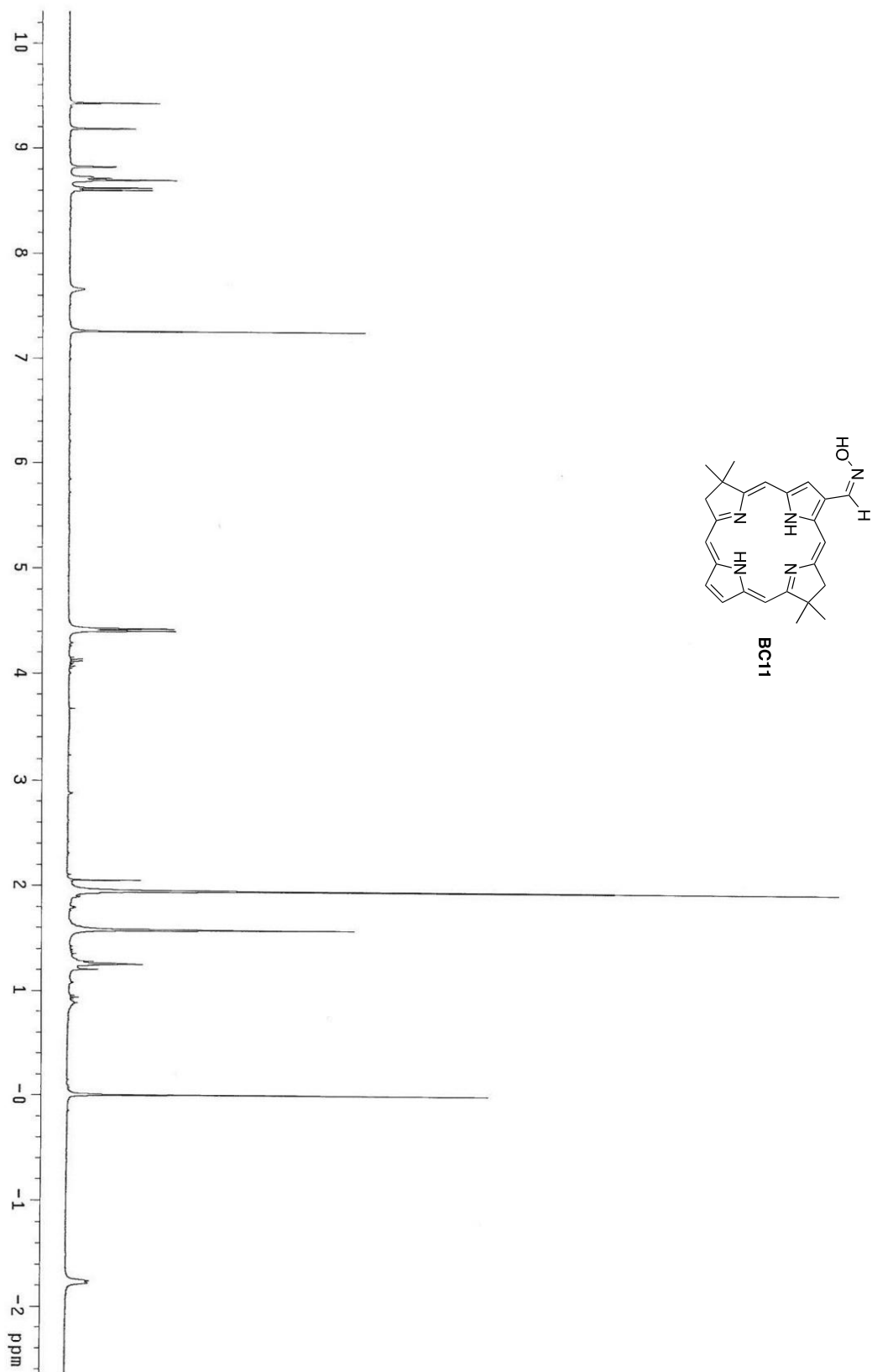
INSTRUM MASSDEC
 Opid tof
 SMPNAM 110691
 AQ_DATE 2011-07-27 10:06:50
 PATH D:/data/chemistry/lindsey/Rame
 POLARI POS
 AQOP_m Reflector
 TD 29673
 NoSHOTS 100
 SMO NUM 0
 SMOPTS1 0
 SMOPTS2 0
 SMOPTS3 0
 DW 1.00 [ns]
 DELAY 5184 [ns]
 Uis1 19.00 [kV]
 Uis2 17.50 [kV]
 Urefl 0.00 [kV]
 Uiens 9.70 [kV]
 Uhimass 0.00 [kV]
 RefFull 0.00 [kV]
 UdetL 1.62 [kV]
 UdetR 0.00 [kV]
 Udefl 0.00 [kV]
 REPHZ 3.00 [Hz]
 ATTEN 86.0
 ML1 2521591.140
 ML2 297.203
 ML3 0.000
 HITURBO no
 GDEON yes
 GDEDLY short
 DEFLO no
 RLNSBND no
 LLNSBND no
 UIS2BND no
 DPCAL1 0.38
 DPMASS 1000.00 [Da]
 RBNDVAL 0.00
 LBNDVAL 0.00
 IS2BNDV 0.00
 CMT1 krr57
 CMT2

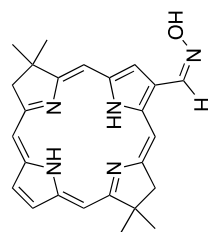
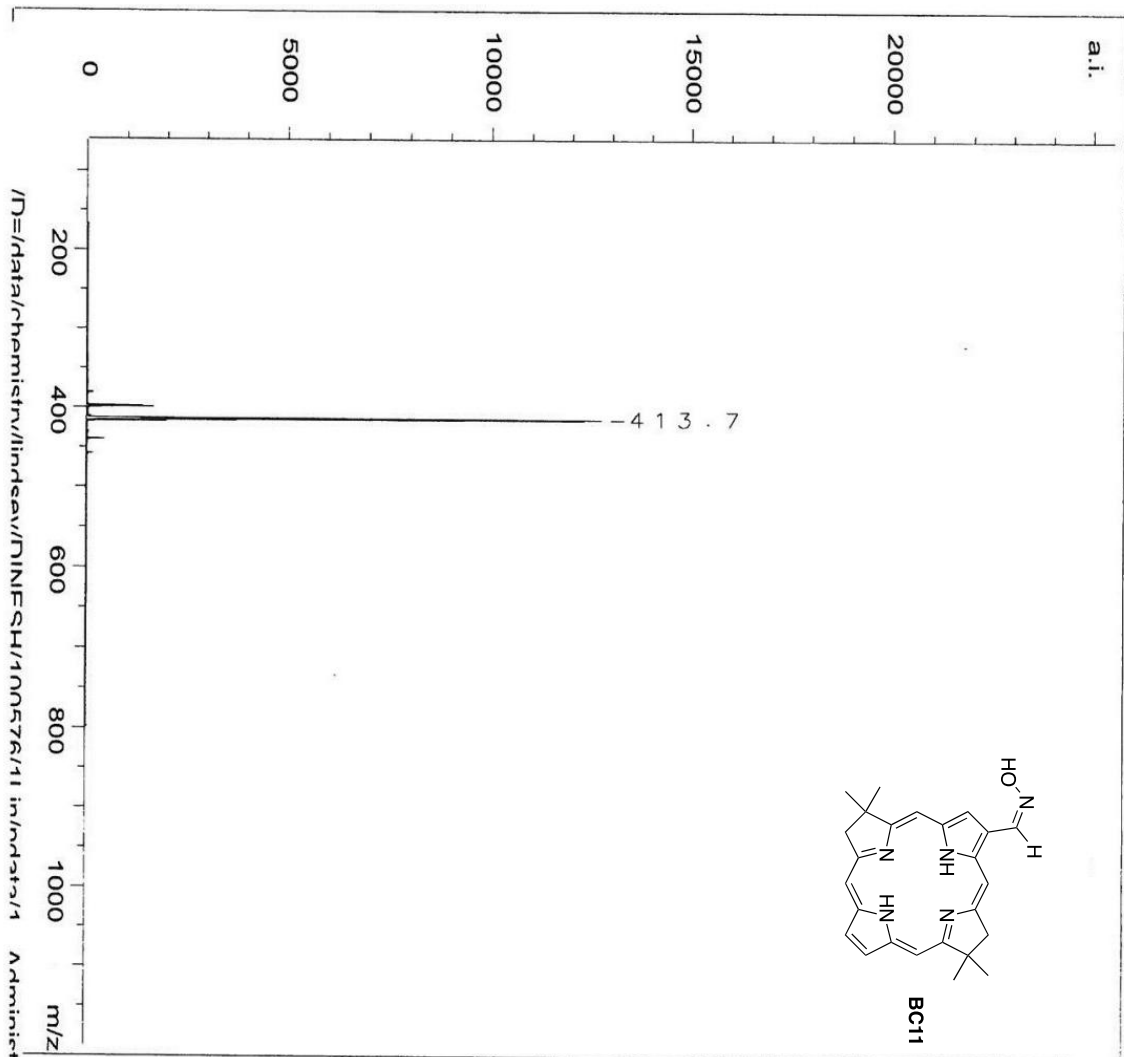




INSTRUM MASSDEC
 OpId tof
 SMPNAM 110776
 AQ_DATE 2011-08-16 16:49:05
 PATH D:\data\Chemistry\Lindsey\Ramesh
 POLARI POS
 AQOP_m Reflector
 TD 29673
 NoSHOTS 100
 SMONUM 0
 SMOPTS1 0
 SMOPTS2 0
 SMOPTS3 0
 DW 1.00 [ns]
 DELAY 5184 [ns]
 Uis1 19.00 [kV]
 Uis2 17.50 [kV]
 Urefl 0.00 [kV]
 Uilens 9.70 [kV]
 Uhimass 0.00 [kV]
 RefFull 0.00 [kV]
 UdetL 1.62 [kV]
 UdetR 0.00 [kV]
 Udefl 0.00 [kV]
 REPHZ 3.00 [Hz]
 ATTEN 79.0
 ML1 2526183.570
 ML2 311.198
 ML3 0.000
 HITURBO no
 GDEON yes
 GDEDLY short
 DEFLO no
 RLNSBND no
 LLNSBND no
 UIS2BND no
 DPCAL1 0.38
 DPMASS 1000.00 [Da]
 RBNDVAL 0.00
 LBNDVAL 0.00
 IS2BNDV 0.00
 CMT1 FLEXControl generated XMASS da
 CMT2 krr

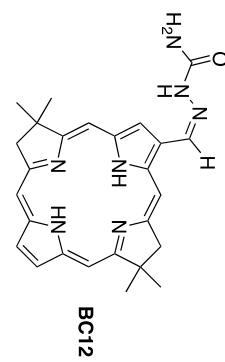
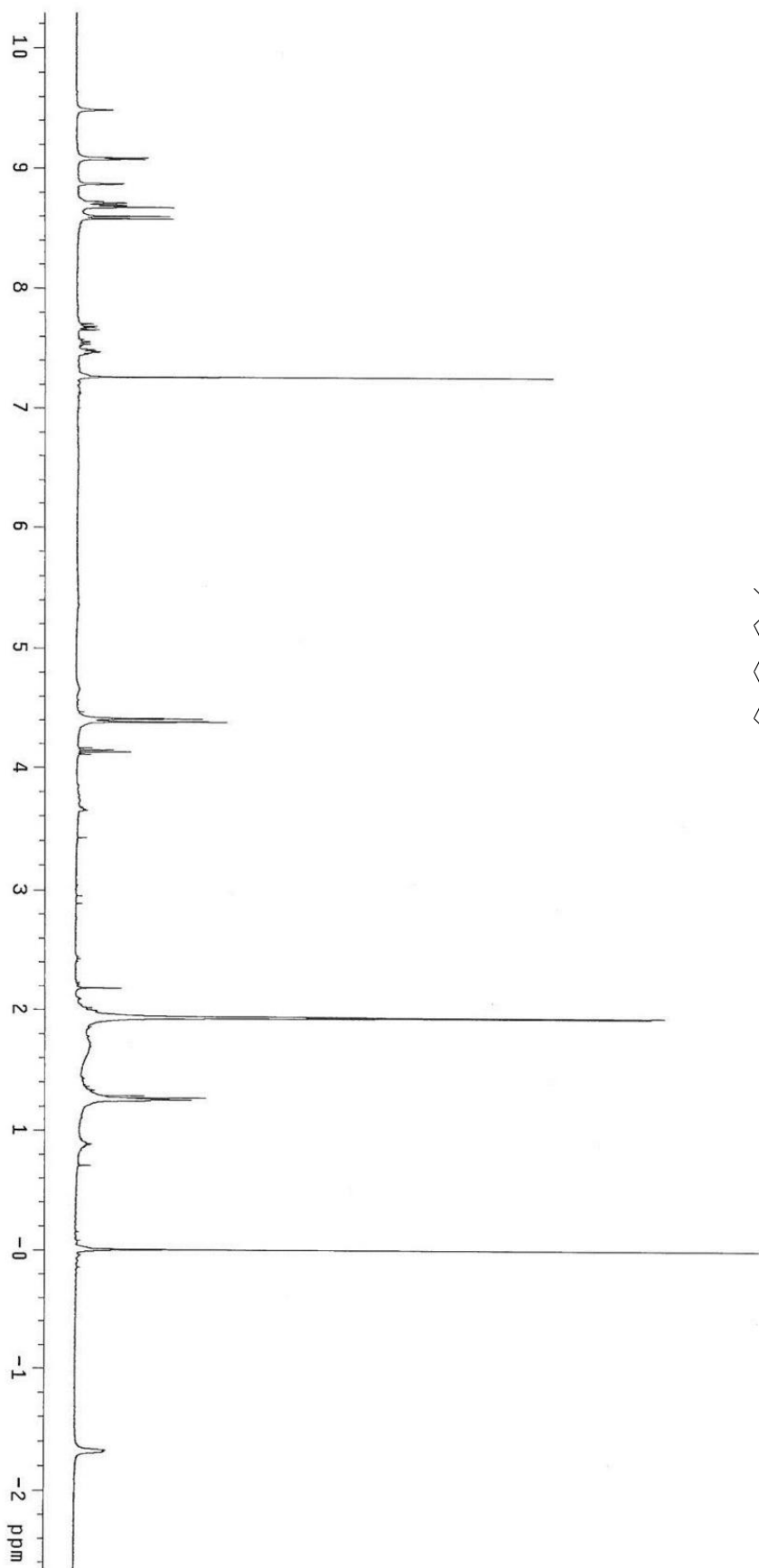
/D=/data/chemistry/lindsey/Ramesh/110776/1Lin/pdata/1 Administrator Tue Aug 16 16:53:12 2011

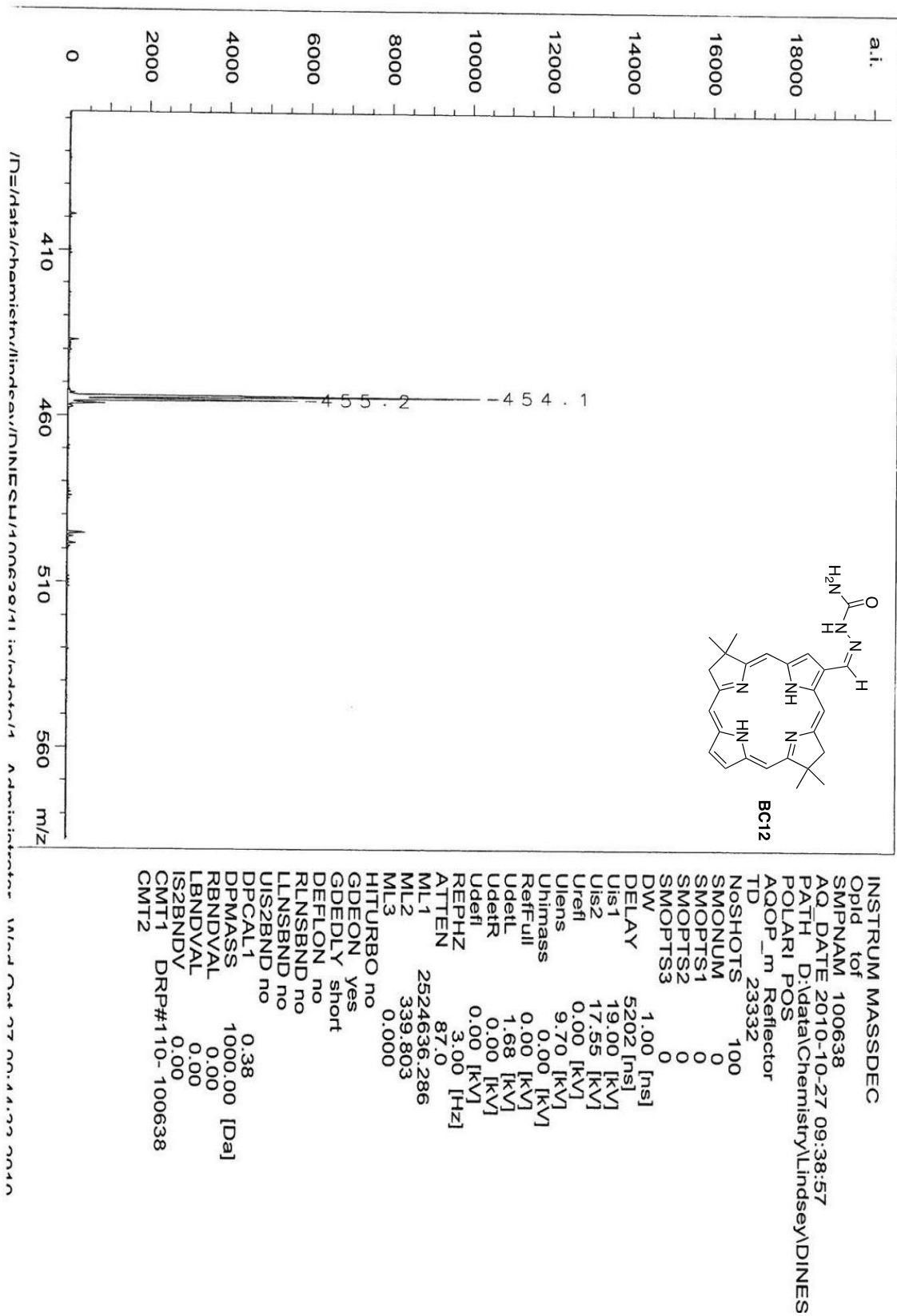


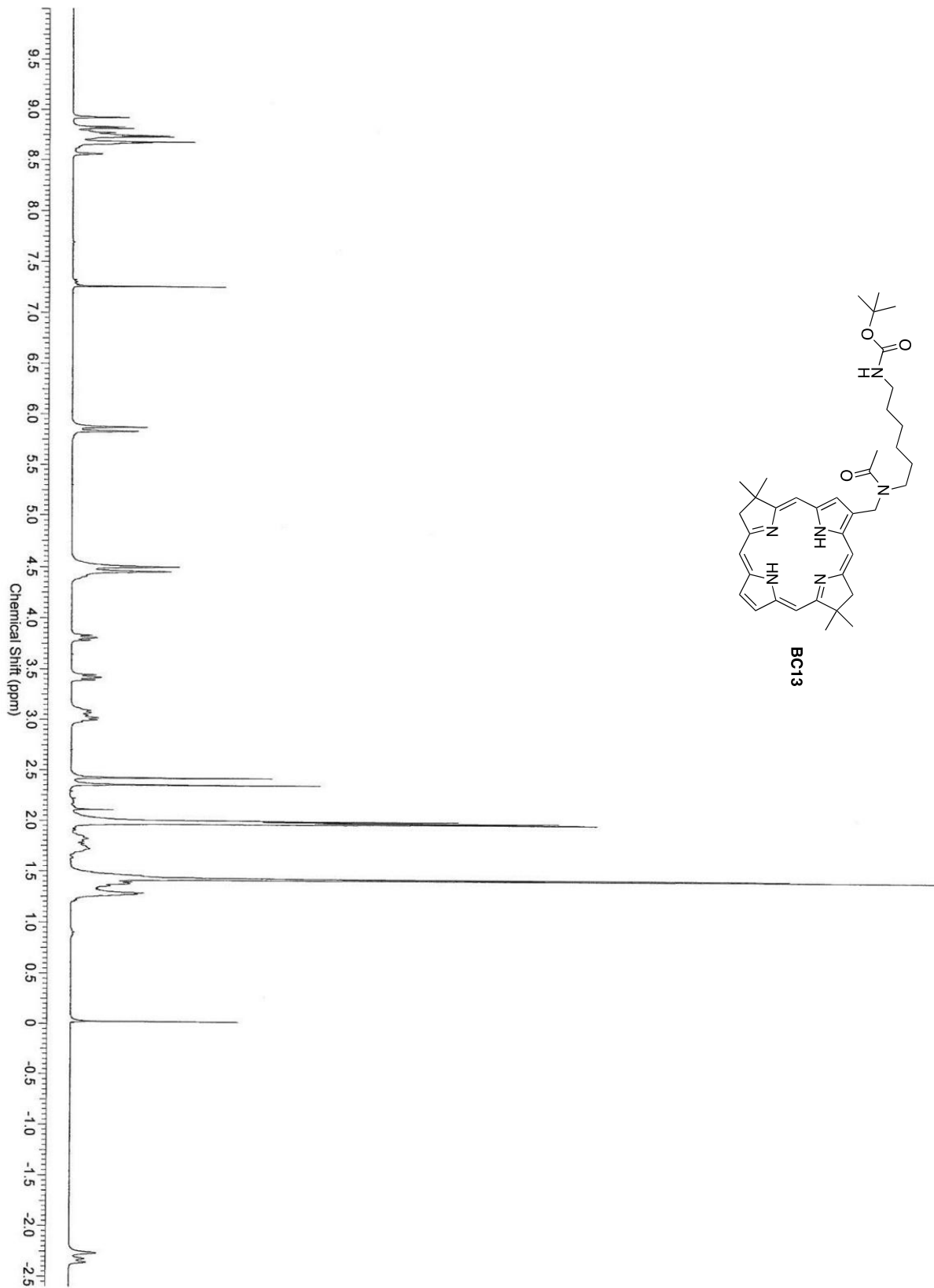


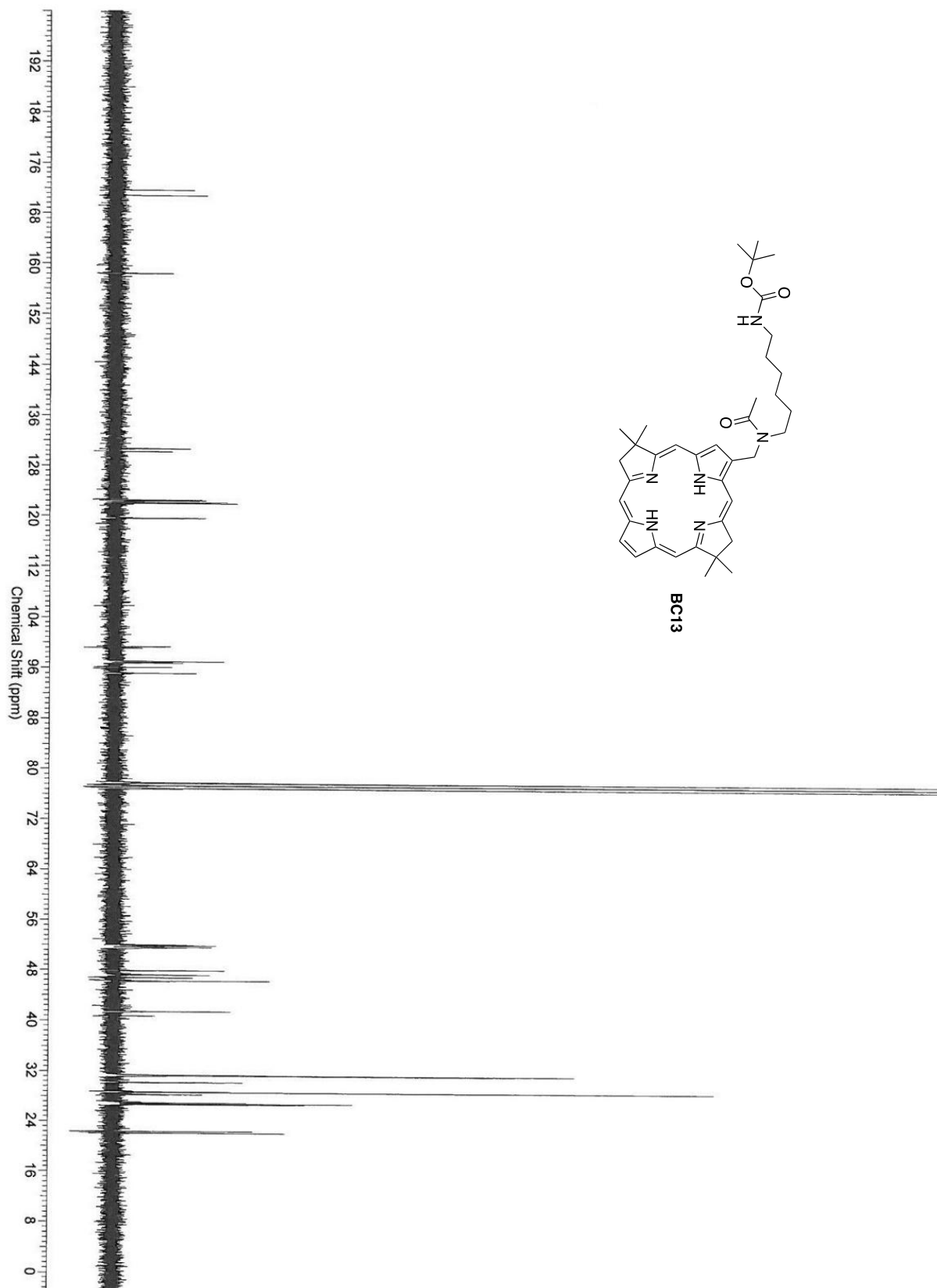
BC11

INSTRUM MASSDEC
 Opid tof
 SMPNAM 100576
 AQ_DATE 2010-09-28 09:57:58
 PATH D:\data\Chemistry\Lindsey\DINESH
 POLARI POS
 AQOP_m Reflector
 TD 23332
 NO SHOTS 100
 SMONUM 0
 SMOPTS1 0
 SMOPTS2 0
 SMOPTS3 0
 DW 1.00 [ns]
 DELAY 5202 [ns]
 Uis1 19.00 [kV]
 Uis2 17.55 [kV]
 Urefl 0.00 [kV]
 Urens 9.70 [kV]
 Uhimass 0.00 [kV]
 RefFull 0.00 [kV]
 UdeftL 1.68 [kV]
 UdeftR 0.00 [kV]
 UdeftI 0.00 [kV]
 REPHZ 3.00 [Hz]
 ATTEN 98.0
 ML1 2507860.985
 ML2 268.473
 ML3 0.000
 HITURBO no
 GDEON yes
 GDEDLY short
 DEFLO no
 RLNSBND no
 LNSBND no
 UIS2BND no
 DPCAL1 0.38
 DPMASS 1000.00 [Da]
 RBNDVAL 0.00
 LBNDVAL 0.00
 IS2BNDV 0.00
 CMT1 DRP#103-100576
 CMT2



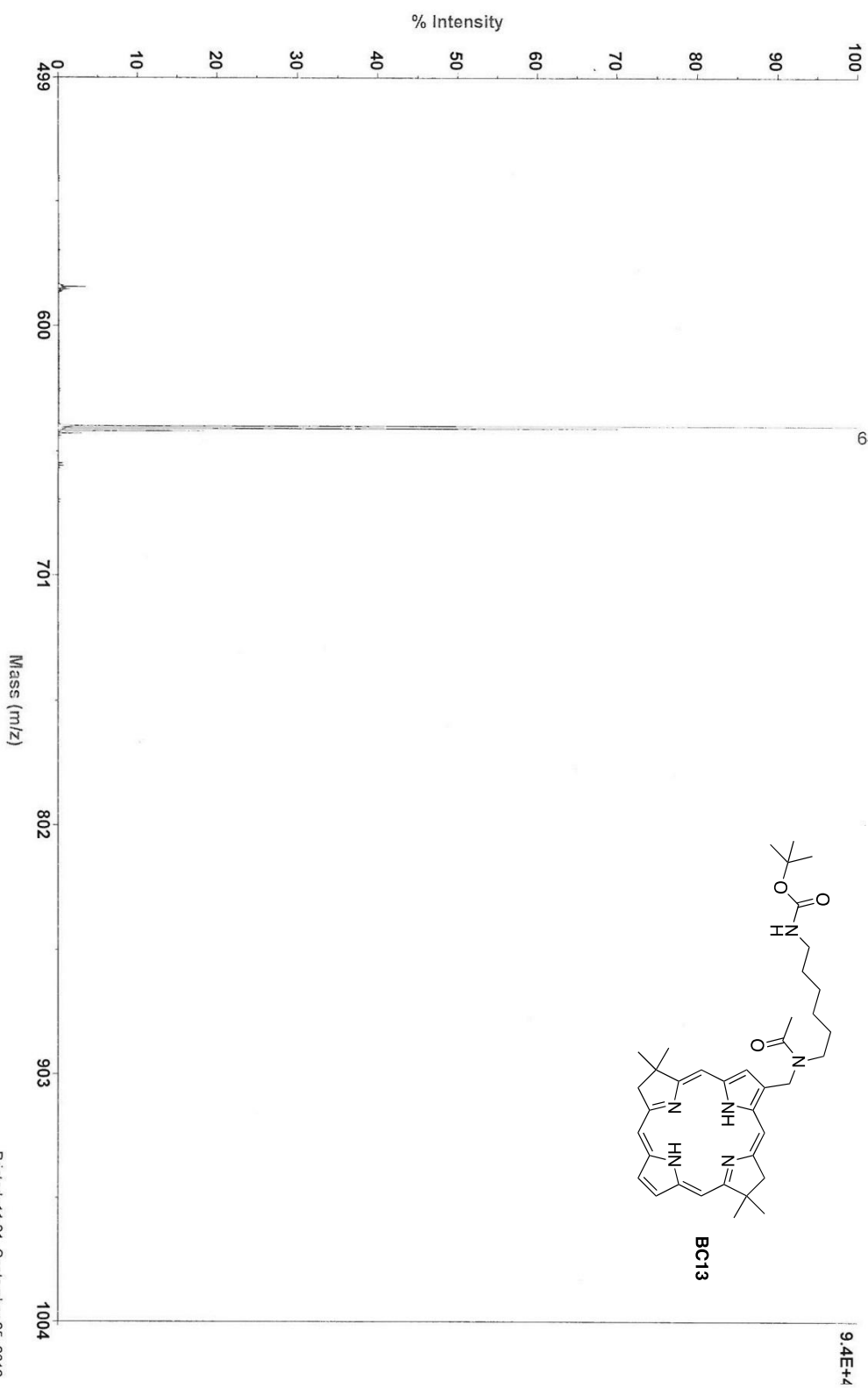






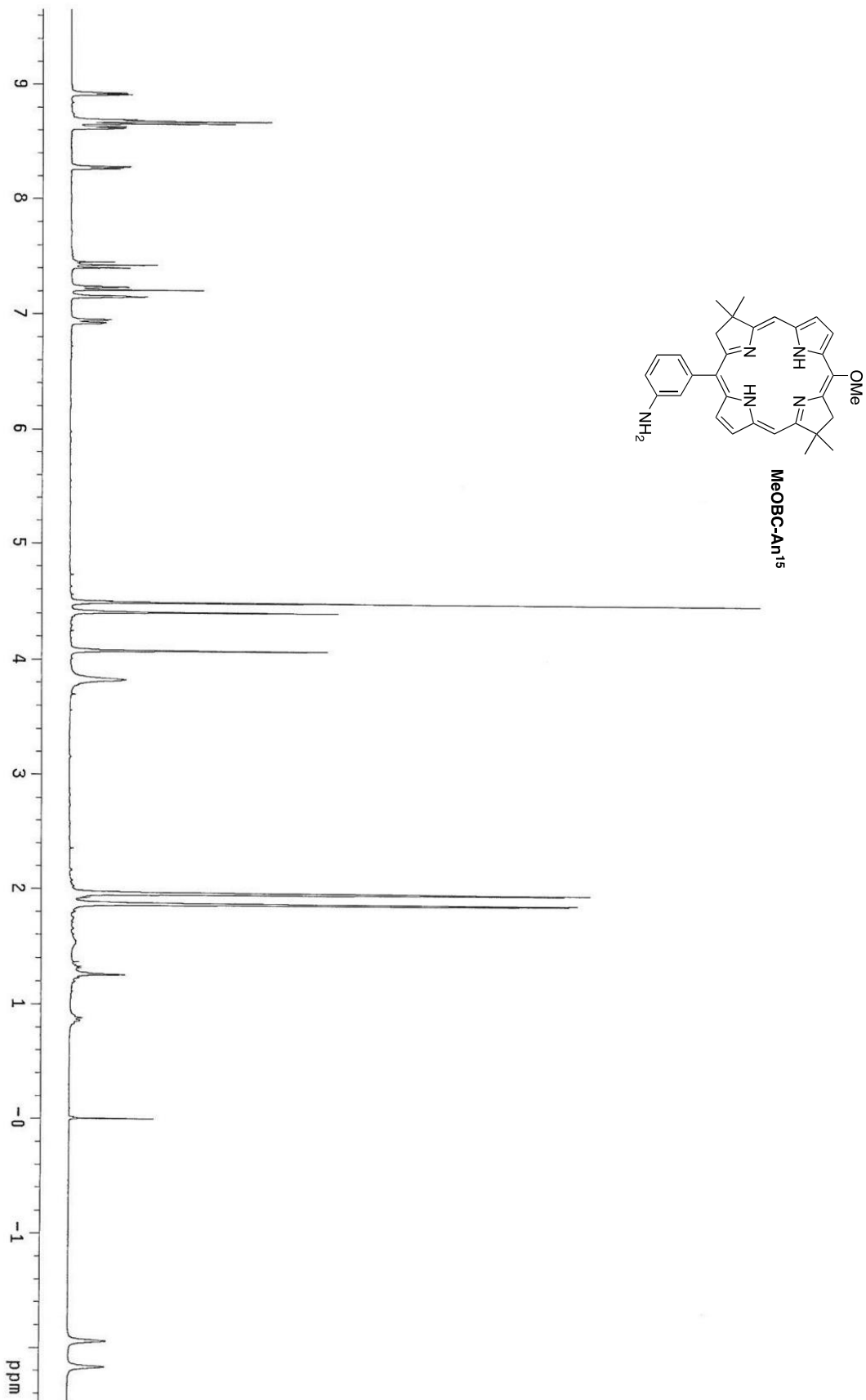
AB Sciex TOF/TOF™ Series Explorer™ 72098

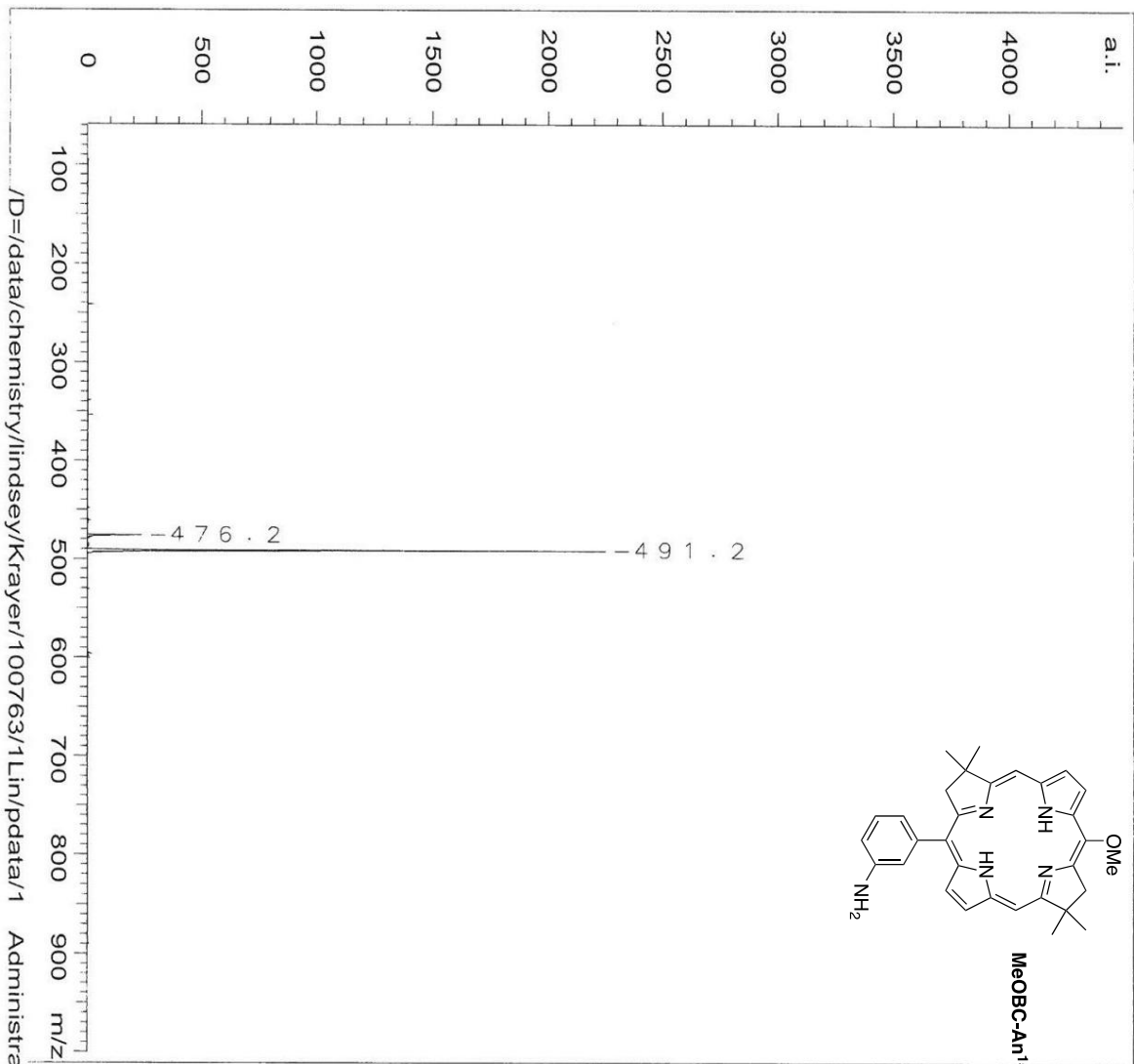
TOF/TOF™ Reflector Spec #1 MCIBP = 640.3, 94295]



C:\AB SCIEN\TOF\TOF Data\Export\T2D\User Project 1\Lindsey\09_25_12\F2_MS.L2d

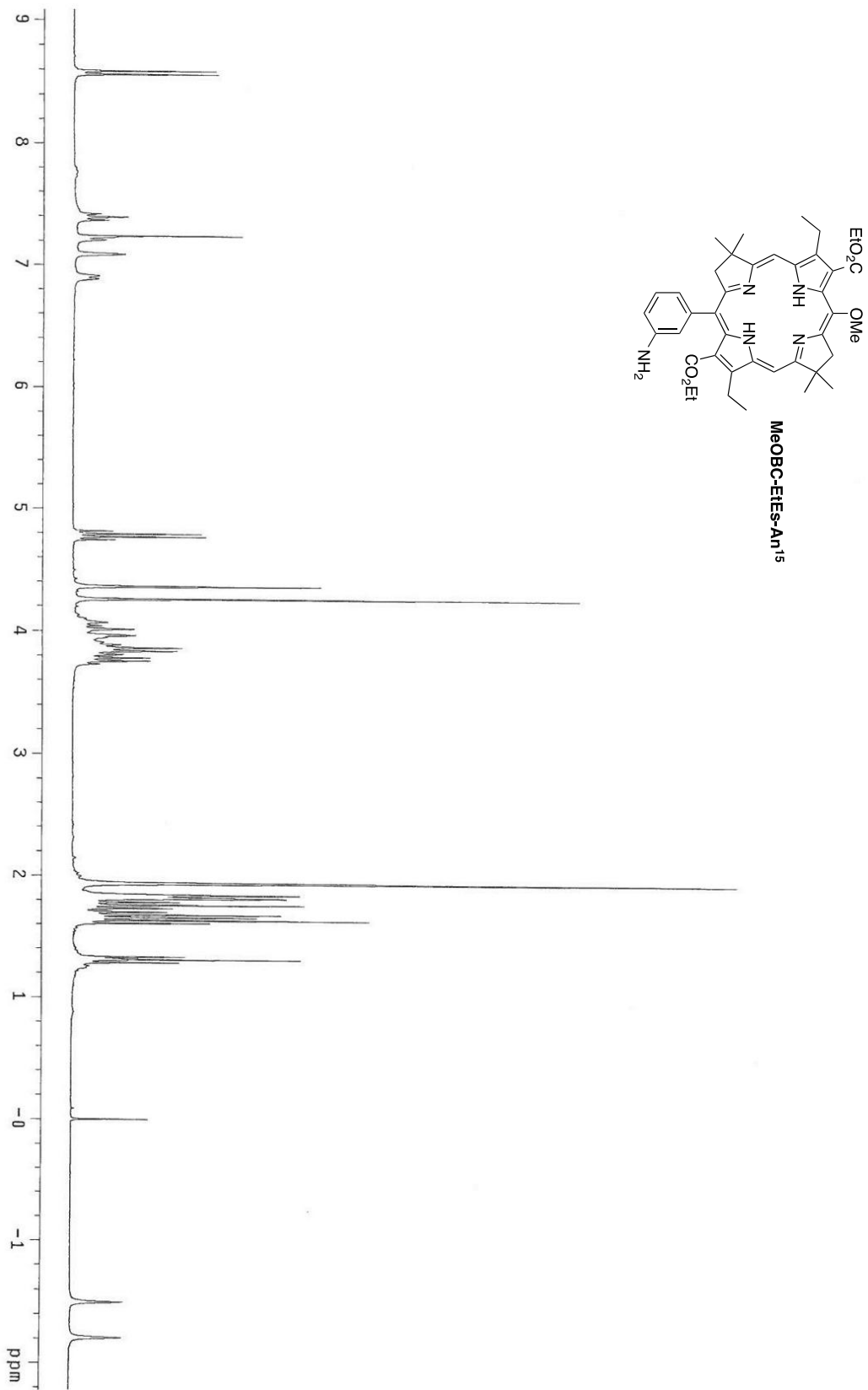
Printed: 11:21, September 25, 2012

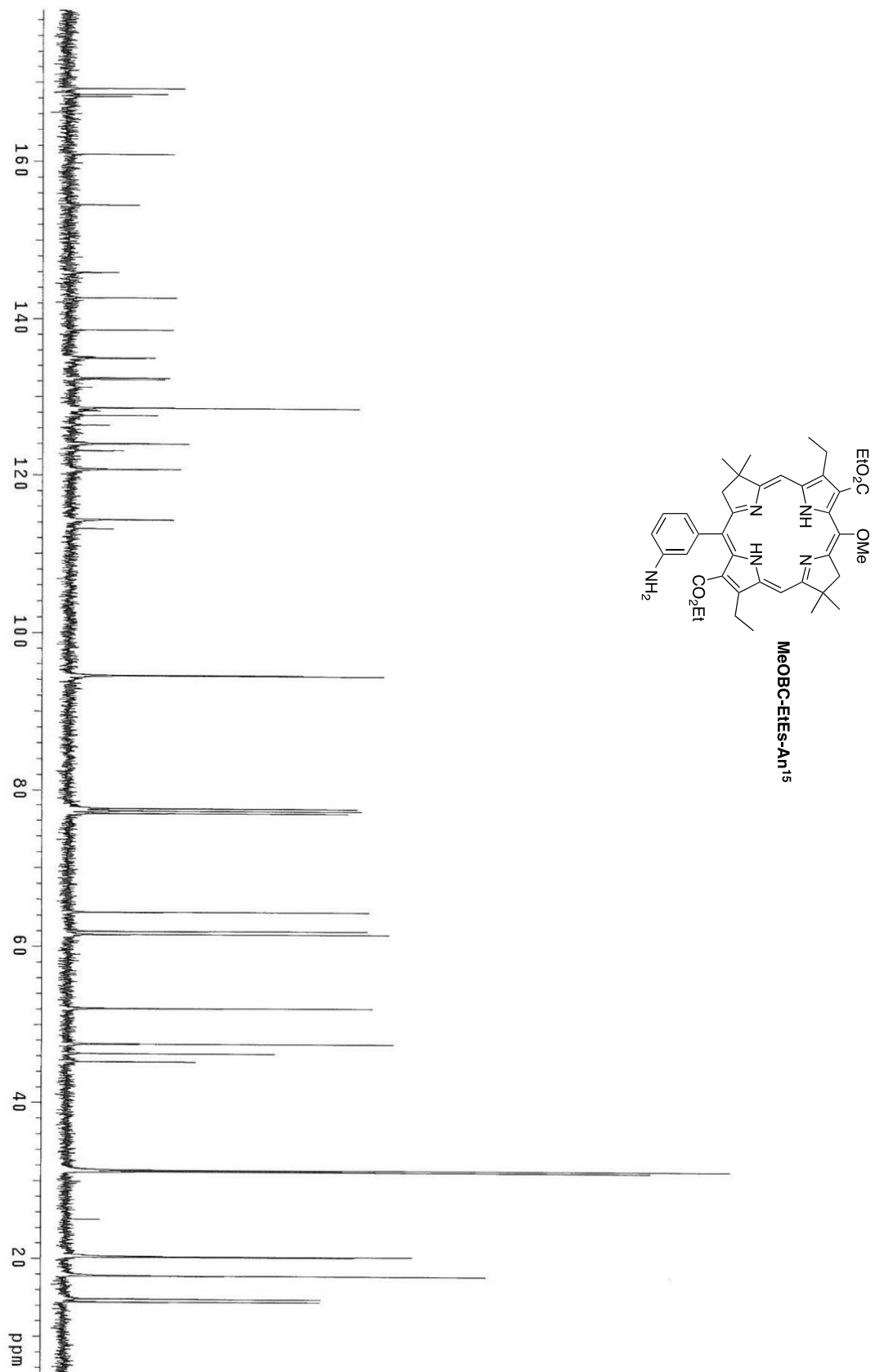




/D=/data/chemistry/lindsey/Krayer/100763/1Lin/pdata/1 Administrator Tue Nov 23 08:38:54 2010

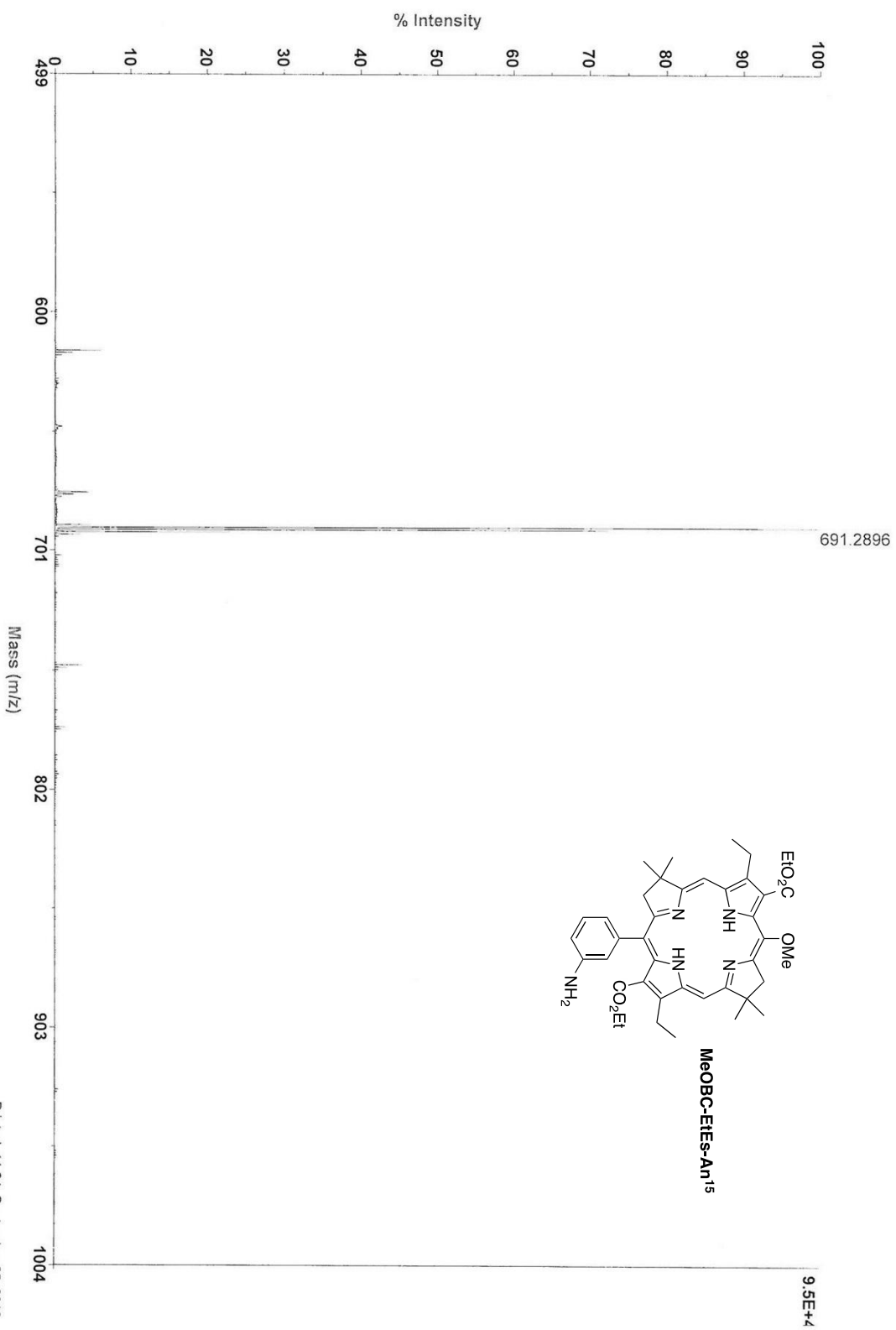
INSTRUM MASSDEC
 OpId tof
 SMPNAM 100763
 AQ_DATE 2010-11-23 08:34:27
 PATH D:/data/chemistry/Lindsey/Kray
 POLARI POS
 AQOP_m Reflector
 TD 29673
 NoSHOTS 100
 SMOPT3 0
 SMOPT2 0
 SMOPT1 0
 SMOPTS3 0
 DW 1.00 [ns]
 DELAY 5184 [ns]
 Uis1 19.00 [kV]
 Uis2 17.50 [kV]
 Urefl 0.00 [kV]
 Uliens 9.70 [kV]
 Uhimass 0.00 [kV]
 RefFull 0.00 [kV]
 UdetL 1.62 [kV]
 UdetR 0.00 [kV]
 Udefl 0.00 [kV]
 REPHZ 3.00 [Hz]
 ATTEN 99.0
 ML1 2520006.830
 ML2 312.082
 ML3 0.000
 HITURBO no
 GDEON yes
 GDEDLY short
 DEFLO no
 RLNSBND no
 LLNSBND no
 UIS2BND no
 DPCAL1 0.38
 DPMASS 1000.00 [Da]
 RBNDVAL 0.00
 LBNDVAL 0.00
 IS2BNDV 0.00
 CMT1 sdt
 CMT2





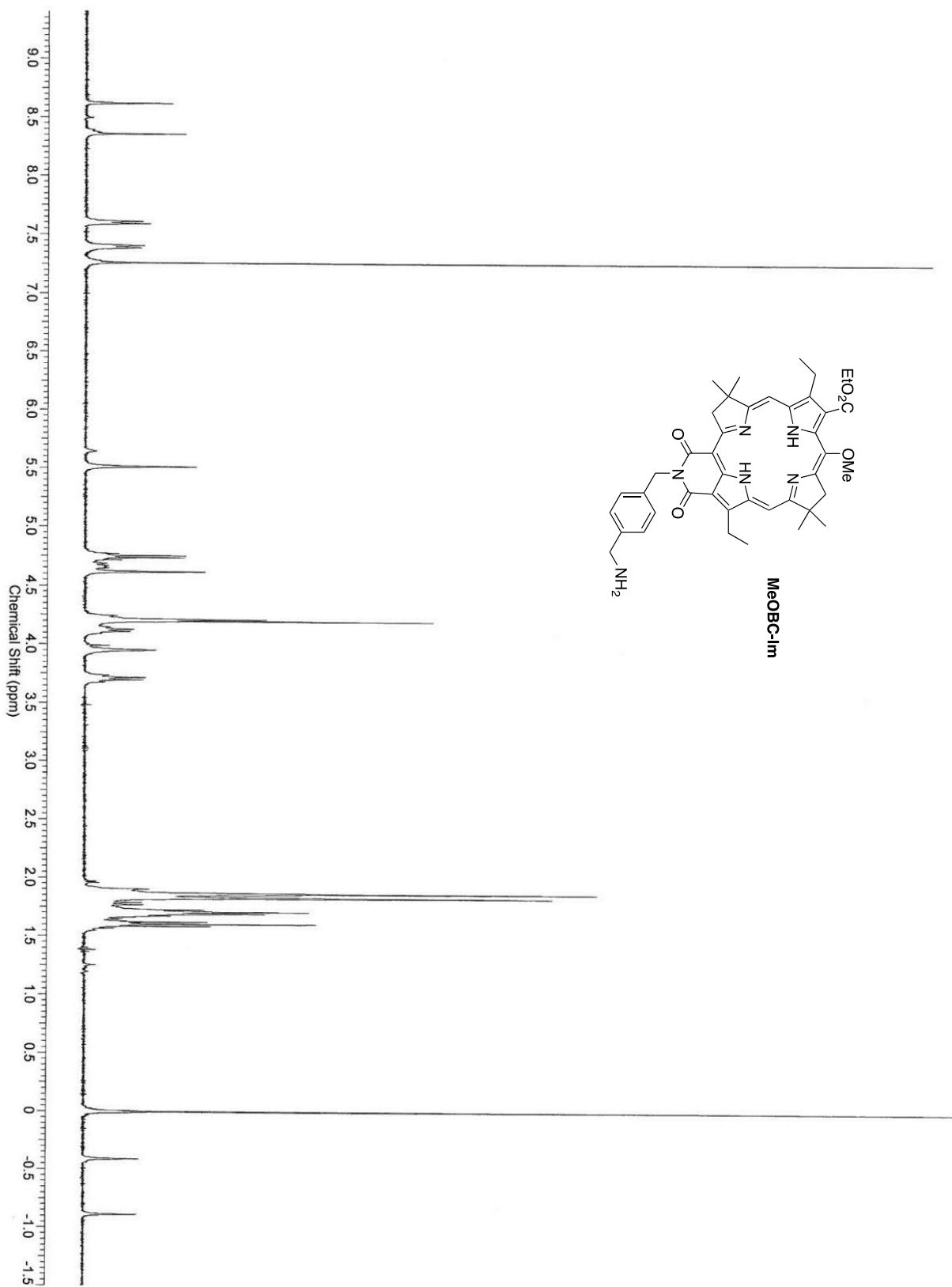
AB Sciex TOF/TOF™ Series Explorer™ 72098

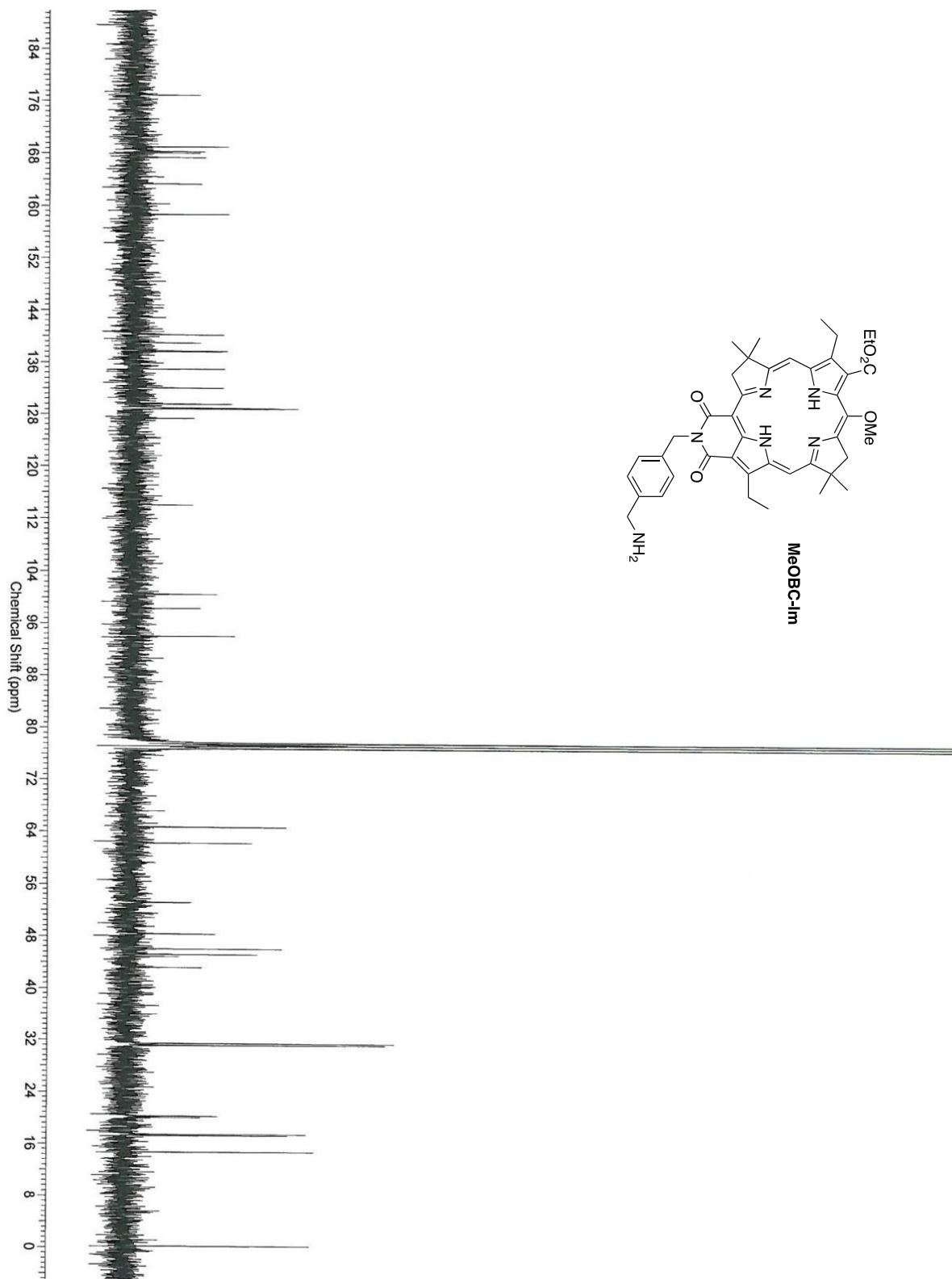
TOF/TOF™ Reflecter Spec #1 MClBP = 691.3; 95299]

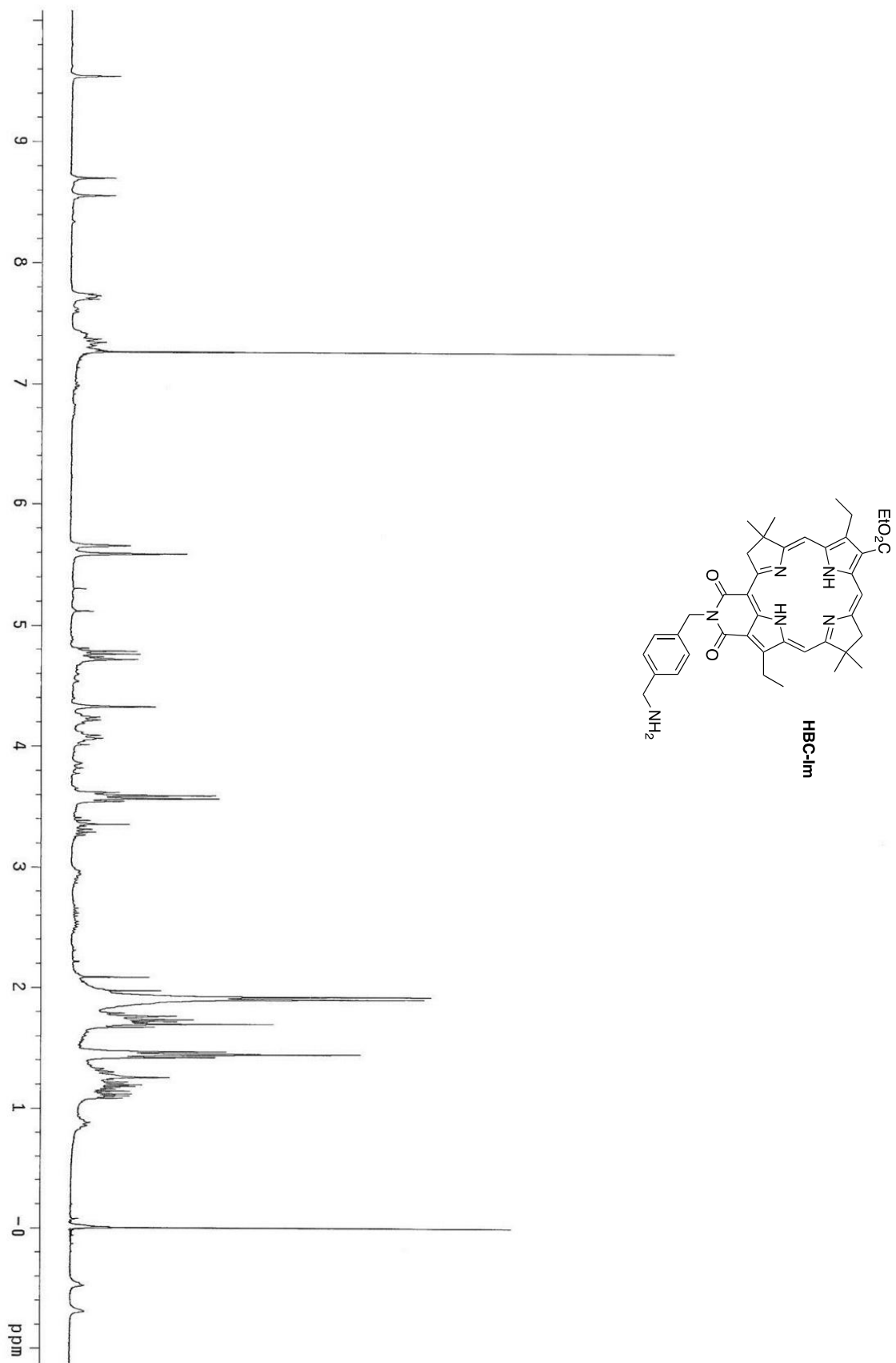


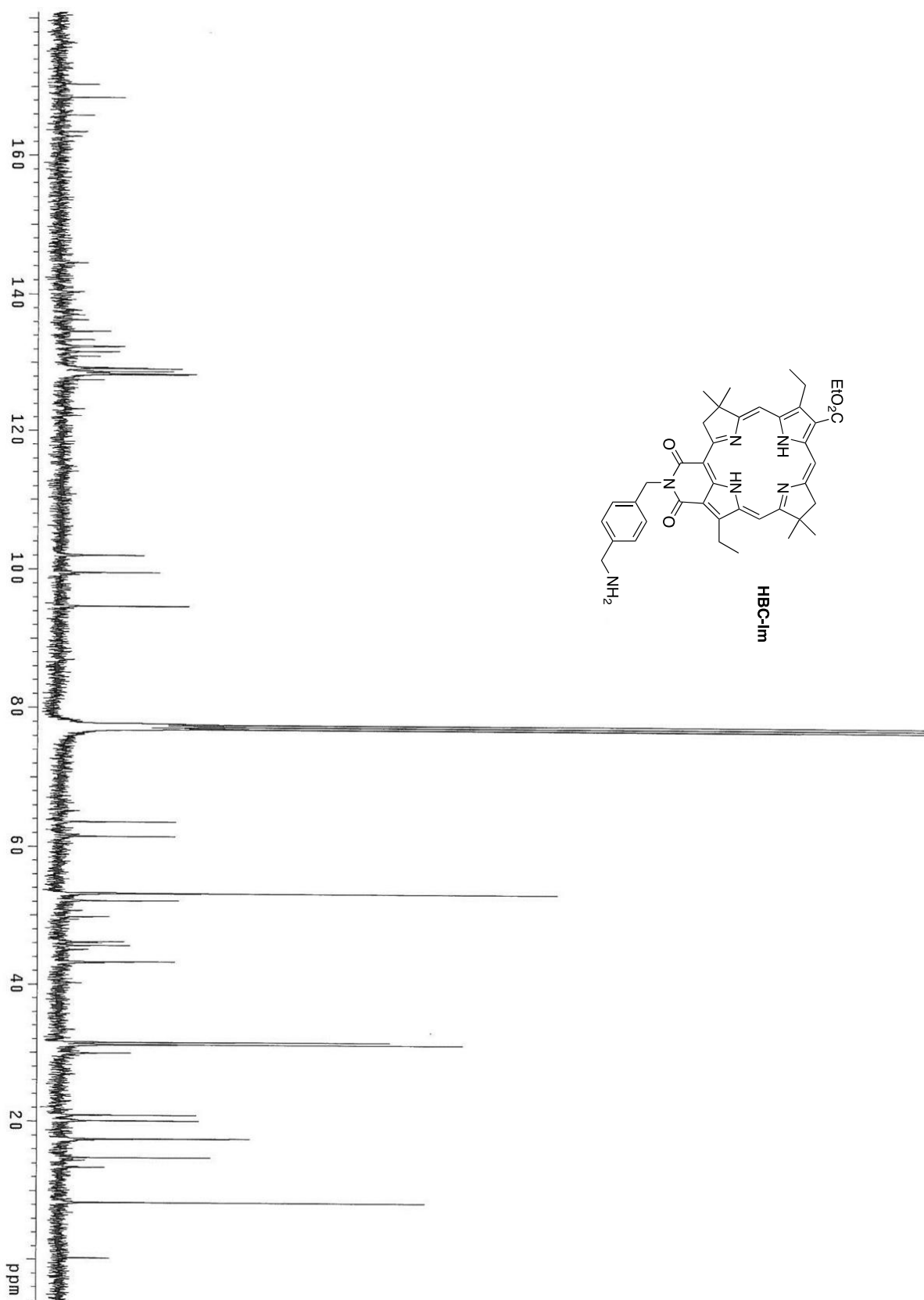
C:\AB SCIENX\TOF\TOF Data\Export\2D\User Project 1\Lindsey\09_25_12\F7_MS12d

Printed: 11:24, September 25, 2012



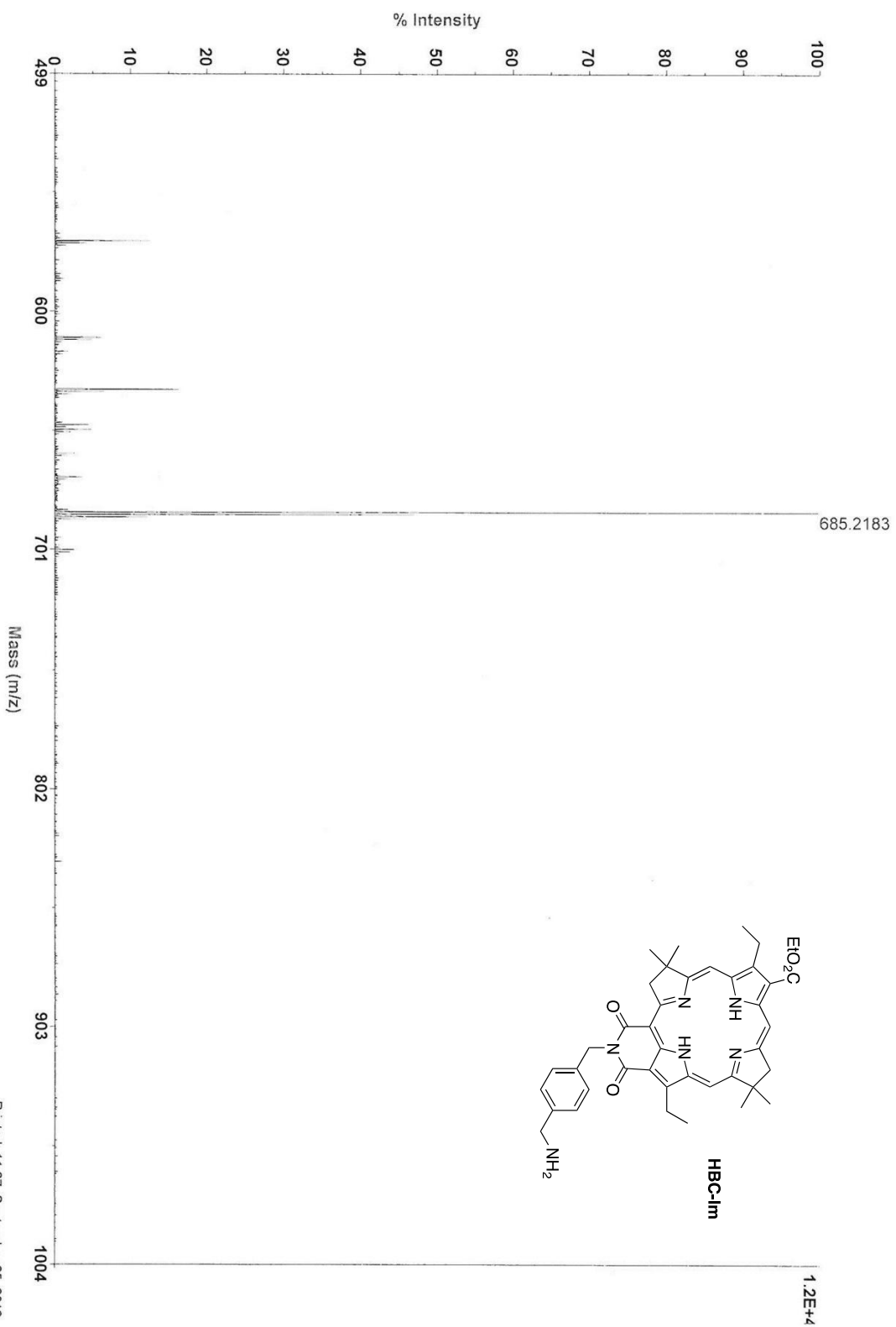






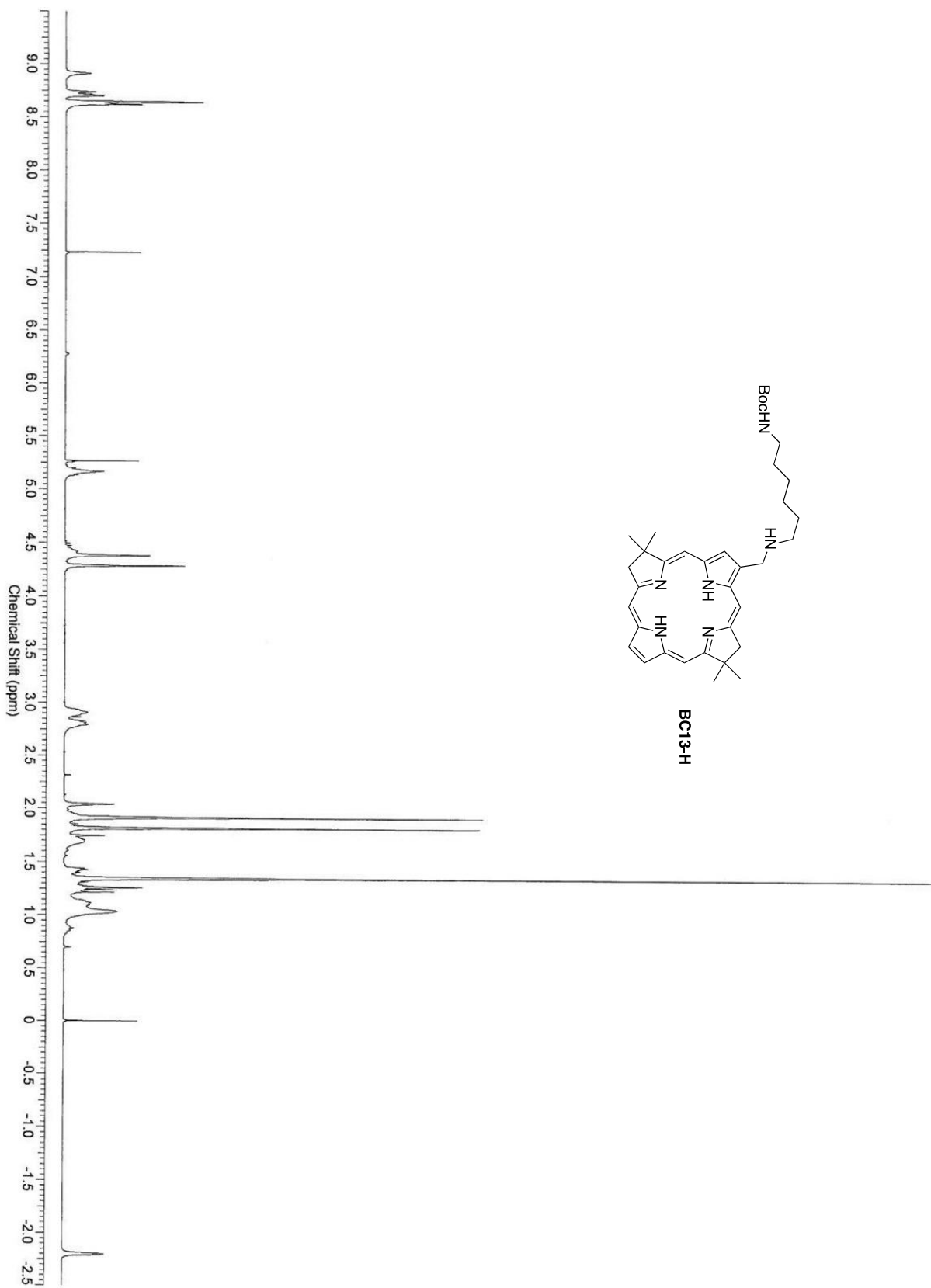
AB Sciex TOF/TOF™ Series Explorer™ 72098

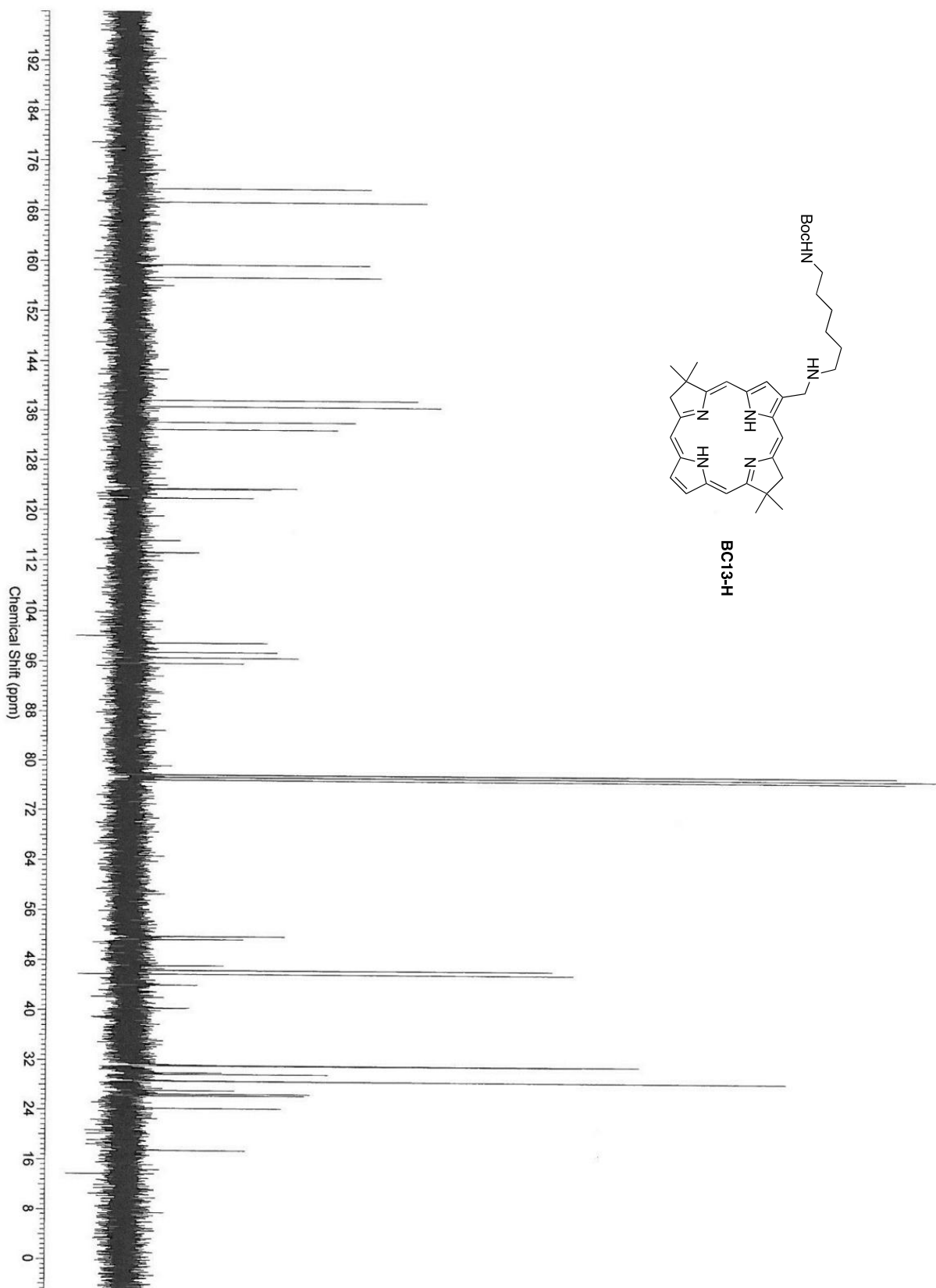
TOF/TOF™ Reflector Spec #1 MCI[BP = 685.2, 11915]

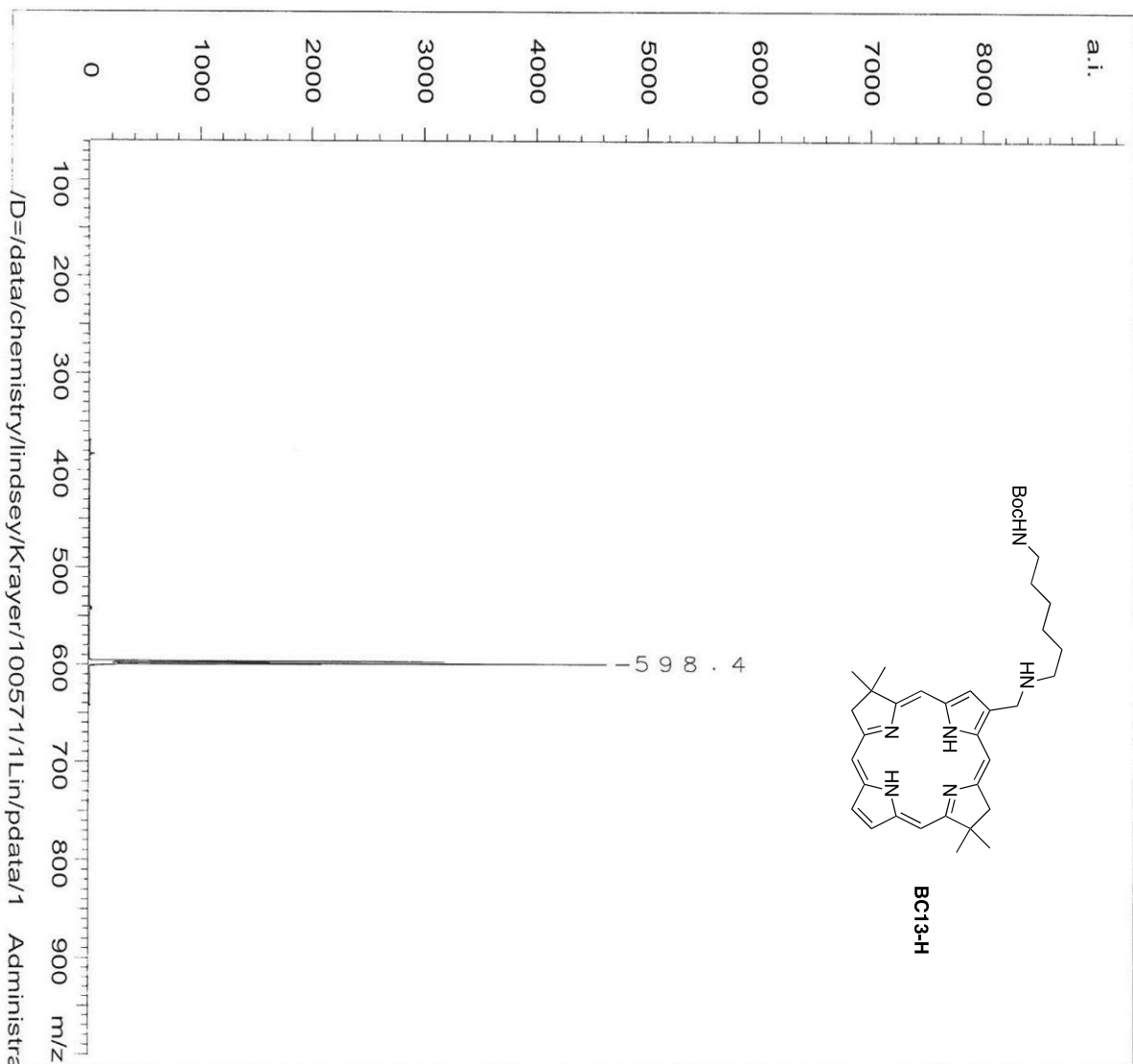


C:\AB SCIEN\TOF\TOF Data\Export\T2D\User Project 1\Lindsey\09_25_12\F11_MS12d

Printed: 11:27, September 25, 2012







INSTRUM MASSDEC
 OpId tof
 SMPNAM 100571
 AQ_DATE 2010-09-27 08:34:48
 PATH D:\data\Chemistry\Lindsey\Kraye
 POLARI POS
 AQOP_m Reflector
 TD 29673
 NoSHOTS 100
 SMOONUM 0
 SMOPTS1 0
 SMOPTS2 0
 SMOPTS3 0
 DW 1.00 [ns]
 DELAY 5184 [ns]
 Uis1 19.00 [kV]
 Uis2 17.50 [kV]
 Urefl 0.00 [kV]
 U lens 9.70 [kV]
 Uhimass 0.00 [kV]
 RefFull 0.00 [kV]
 Udetl 1.62 [kV]
 Udetr 0.00 [kV]
 Udefl 0.00 [kV]
 REPHZ 3.00 [Hz]
 ATTEN 97.0
 ML1 2520750.509
 ML2 313.984
 ML3 0.000
 HITURBO no
 GDEON yes
 GDEDLY short
 DEFLO no
 RLNSBND no
 LLNSBND no
 UIS2BND no
 DPCAL1 0.38
 DPMASS 1000.00 [Da]
 RBNDVAL 0.00
 LBNDVAL 0.00
 IS2BNDV 0.00
 CMT1
 CMT2